BELTCON 4

Belt Dynamics - An Alternative View

L Nordell

7 & 8 September 1987
Sandton Holiday Inn
Sandton

The S.A. Institute of Materials Handling
The S.A. Institution of Mechanical Engineers

The Theory and Practice of Belt Conveyor Dynamic Analysis

ABSTRACT:

Methods of calculating belt conveyor belt line forces are reviewed. These include the basic steady-state methods, and their effect on the dynamic analysis. Belt elastic-transient or dynamic analysis methods are presented, comparing a linear spring-mass model with more advanced forms and their differing influences on the predicted dynamics. Starting and stopping control theory is discussed, and supporting case study results are cited. The theory is applied to the mechanics of various types of soft-start control equipment and brake controls, comparing various methods. A brief discussion on the effect of digital versus analog feedback control (tachometers, PLC; microprocessors) on instrumentation is provided.

Lawrence K. Nordell, President
CONVEYOR DYNAMICS, INC.
369 East Calaveras Street
Altadena, California 91001, U. S. A.

INTRODUCTION:

In the last six years, methods of designing high capacity, long overland belt conveyor systems have undergone major changes. The ready availability of powerful and inexpensive computer systems has allowed designers to explore more sophisticated and more accurate methods of analysis. The physics of the belt conveyor as it responds to starting and stopping actions is a complex science, which this paper explores in brief detail. The focus of the paper is on the elastic transient behavior of the belt conveyor when subjected to conditions of plant operation. A number of case studies are presented, which provide insight into some of the differing design problems and their solutions. By studying many conveyors which exhibit bizarre and sometimes violent behavior, our understanding is expanded, allowing for better generalization on all design aspects. Better theory builds better practice, resulting in a safer and more economical design.

1. METHODS OF CALCULATING BELTLINE FORCES

Conveyor Dynamics, Inc. (CDI) uses two mathematical modelling techniques to predict the belt line forces. The techniques have been computerized and are tradenamed BELTSTAT and BELTFLEX. BELTSTAT was developed in 1977, and BELTFLEX in 1980.

BELTSTAT predicts the belt line forces and displacements from static principles, and includes methods of analyzing acceleration and stopping conditions, based on rigid body mechanics.

BELTFLEX predicts the belt line forces from elastic principles, which assumes the belt extends in length when subjected to a tensile force, and buckles when the nominal belt line force approaches a compression state of stress.

Both BELTSTAT and BELTFLEX require the belt to be divided into small finite sections that allow scrutiny of the component influences and their affect upon the belt line forces.

There are three main types of external forces acting along the belt's axis: gravity forces (vertical lift), friction forces, and driving or braking forces. The friction force (resistance to rolling) can be further divided into subcategories:

- idler drag losses (seal drag; bearing drag)
- idler indention losses (idler roll deforming into the belt cover)
- belt flexural losses (flexing of the belt's carcass)
- material trampling losses (material agitation when belt relaxes between idlers, and when material is accelerated vertically in idler trough zone)
- parasitic losses (pulley bearings and seals, skirtboards, scrapers and plows; material acceleration at load station)

Methods of determining steady-state operating tensions, developed along the belt's axis from the gravity and friction forces, are given in many industrial standards (references 1, 2, 3, and 4), as well as in various manufacturers' publications (for example, references 5, 6, 7, and 8) and research documents (references 9, 10, 11, 12, and 13). These recognized methods, unfortunately, are not in agreement with one another. Many of these approaches are oversimplified, or are not complete in their treatment with respect to actual operation. Since most designers are not standardized on one of the above recognized methods, it is difficult to generalize on the accuracy of resulting designs. Typically, the industrial standards will provide a reasonable and conservative level of accuracy. But, in the design of more complex overland and high lift systems, the simplified methods may lead to significant errors in design. Much of the more recent research and field measurements have shown that significant influence may be found from the many interactions of:

- belt construction materials and methods
- belt cover thickness and hardness
- belt speed
- idler trough shape
- idler roll diameter
- idler spacing
- idler bearing, seal and lubricant
- pressure and its distribution along idler roll and belt contact zone
- axial tensions
- ambient temperature
- material transported
- installation and manufacturing accuracy of idlers
- material buildup on idler and pulley surfaces

Some of the field data provided in this paper will demonstrate these influences empirically. This is particularly true for the dynamic behavior of the belt. Specifically, the drop or increase in axial belt tension and the respective increase or drop in belt line rolling resistance, during transient conditions, changes the fundamental dynamic behavior of the conveyor system and resulting forces along the belt's axis. Stated in another way, the variable rolling resistance can be substantially altered, in the dynamic phase of starting and stopping, by the conveyor's geometry and material position.

The evaluation method used by CDI in static (BELTSTAT) and dynamic (BELTFLEX) analysis incorporates variable rolling resistance as a function of both changing tensions along the belt's axis and many of the above noted basic influences.

BELTSTAT

A typical conveyor profile and static analysis (BELTSTAT V3.3I) is shown in Figures 1-2. The conveyor is divided into discrete belt line sections that represent changes in geometry and/or mechanical equipment.

Between sequential nodes, the changing belt tensions, due to the variances in geometry and equipment, are computed. The resulting "running" tension is the collection of forces developed from the node-to-node calculations, the effects of drive actions, and the take-up location and force. The "running" tensions are the only true known steady-state forces acting along the belt line. All belt tensions are computed from the take-up frame of reference location and force. The basic equation for the belt tension at any point around the circumference is simplified to:

$$T_x = T_{x-1} + f_1 (W_m) + f_2 (W_e) + W_l$$

where "x" is a point along the belt some distance from the last point, "x-1", with the associated belt, idlers, pulleys and material included between the point "x" and the previous point "x-1", in the direction of belt travel. For simplicity, no drives or brakes are assumed between the formulation of these sections.

The dynamic analysis for the same section at "x" is given as:

$$T_x^* = T_x + (a)\left(\sum_{T_{cwt}}^{T_x} \text{masses}\right) \; : \; \text{masses summed from } T_{cwt} \text{ to } T_x$$

where:

a	:	rate of acceleration
f_1	:	net rolling resistance coefficient acting from material weight
f_2	:	net rolling resistance coefficient acting from equipment weight, ambient temperature and operating conditions
W_e	:	weight of equipment per section length
W_l	:	weight of material lift per section length
W_m	:	weight of material per section length

T_x : belt tension at point "x" of the section under study, leading ahead of the belt flow along flite "x" and the prior section "x-1".

T_{x-1} : belt tension at point "x-1", just prior to section "x", between the take-up and point "x"

T_{cwt} : belt tension at the take-up, where the take-up is defined as $T_{cwt} = T_{x=0}$

T_x^* : acceleration tension at point "x"

BELTFLEX

The BELTFLEX model of elastic-transient response and drive control system interaction is based on a second order, non-linear, differential equation. The solution is obtained using numerical analysis techniques optimized for non-linear systems. This methodology allows the inclusion of strongly non-linear components in the equation, such as:

- o belt's elastic modulus (static and dynamic)
- o belt's internal hysteresis (visco-elastic damping)
- o internal rolling resistance f(speed, tension, material load; idler spacing)
- o belt sag, f(idler spacing; material load)

A presentation of this model is given in reference (reference 14), and in the following section of this text.

2. ELASTIC-TRANSIENT MODELLING METHODS

BELTFLEX is mathematically constructed with five basic rheological elements (Figures 3 and 4). It is claimed that these elements effectively model the many independent physical properties of the belt. The elements are identified as:

$C(x)$: external drag from idler seals (static friction), and influence function on belt friction` dependent on displacement

$G(F(t))$: influence on rolling resistance dependent by idler sag (belt tension and idler spacing -- i.e. geometric influence) function

$H(\dot{x}, x)$: belt hysteresis dependent on belt stretch and rate of strain

$K(\dot{x}, x)$: belt elastic modulus dependent on belt stretch and rate of strain

$V(\dot{x})$: visco-elastic element that models idler and belt rolling resistance that is dependent on velocity

From these basic rheological elements, a system of equations can be developed to express the distribution of forces, velocities, displacements, and rates of change. The individual rheological elements are then expressions of each lump mass node, or degree of freedom, that, as a group, combine to provide a unified description of the conveyor in matrix form. The development of forces is derived from the second order differential equation:

$$\mathbf{F}(t) = \mathbf{M}(\ddot{x}) + \mathbf{V}(\dot{x}) + \mathbf{K}(\dot{x}_t, x) + \mathbf{H}(\dot{x}, x) + \mathbf{C}(x) + \mathbf{G}(\mathbf{F}(t))$$

where the following matrices combined with the above rheological matrices denote:

F(t)	:	force for all nodes at time "t"
M	:	mass
$\ddot{x}$	:	acceleration
$\dot{x}; \dot{x}_t$	:	velocity ; time dependent (strain rate) velocity
x	:	displacement

When all of these elements work together, close agreement is achieved with the equivalent real world system. The following comparison will demonstrate the requirements for all of the model parameters.

CASE STUDY DEMONSTRATING MODEL ACCURACY

A conveyor, built in 1965, produced a violent and destructive reaction, at the gravity take-up, approximately 15 seconds after shutdown, when the belt was fully loaded. The engineer instrumented the belt around its circumference and at the take-up, in an effort to determine the magnitude and cause. The measured results are presented in Figures 5-9, together with the corresponding BELTFLEX predictions.

Figure 5 illustrates the belt's basic geometry and operating parameters.

Figures 6-8 illustrate the velocity wave response versus time, plotted at critical locations, that is propagated around the belt after shutdown, with a loaded conveyor.

Figure 9 illustrates the take-up force response by load cell measurement. A peak force of twice the normal running condition was measured 15 seconds after shutdown. When these measurements were made, a hydraulic retarder had been incorporated between the gravity counterweight and the take-up carriage in an attempt to reduce the structural damage. Thus, as the take-up displacement would change direction, an additional viscous and solid damping hysteresis drag would be induced between five and ten seconds into the shutdown phase. This can be seen in the irregular force plot over time. The hydraulic damper was installed to reduce the shock wave. The damper did alter the characteristics of the measured shock at the take-up, but did not dampen it. As more damping was applied the shock force increased toward the characteristics of a fixed take-up.

The CDI model shows close agreement with the field measured velocity and take-up tension values. Given that the widely spaced velocities and take-up force are in close agreement with the theory, it is inferred that the CDI generalized solution form is a reasonable predictor of all tension and velocity characteristics around the belt line, during the transient phase. Using the CDI model, four modelling methods are shown to demonstrate the respective model influences, which include:

1. Linear spring (no idler sag); fixed rolling resistance
2. Non-linear spring (idler sag included); fixed rolling resistance
3. Non-linear spring, variable rolling resistance, and no hysteresis
4. Non-linear spring, with fixed take-up; variable rolling resistance

The Linear Spring model results are illustrated in Figure 10. The major points of observation on the data shown are:

a) velocity and stress waves have greater undulation and are more periodic

b) velocity waves at tail and take-up show no major disturbance around 15 second time period

The linear vs. non-linear predictions are illustrated separately in Figure 11.

c) tension or stress waves go negative at the carryside above the drive, at the tail pulley, and into the primary drive

d) tension at the take-up shows no localized peak force around 15 seconds

The Non-Linear Spring model (idler sag included) results, with fixed rolling resistance, are illustrated in Figure 12. The major points of observation are:

a) all major attributes of field data are produced, but the magnitude and timing are slightly off

b) there are no negative tensions

c) peak take-up force reaches approximately 21 Kips (42 Kip counterweight force)

Non-Linear Spring model with variable rolling resistance and no hysteresis losses are illustrated in Figure 13. The major points are:

a) model accuracy is improved in timing and magnitude of stress wave

b) peak take-up force reached approximately 26 Kips (52 Kips counterweight force)

c) very clean response

The Fixed Take-up model results are illustrated in Figure 14. The major points of observation are.

a) velocity wave undulates with a natural period undamped spring

b) average tension increased, with respect to gravity take-up, during shutdown (i.e. no take-up travel), decreasing rolling resistance around the belt, prolonging coasting time (still moving after 25 seconds)

c) belt tension at take-up increased from 15 Kips to 89 Kips (approximately 6 times)

d) belt tension at tail pulley increased from about 20 Kips to 104.5 Kips, increasing beyond the maximum running tension at the drive during normal running

The model continues to be improved as more field information is collected and as belting manufacturers provide greater insight into the dynamic structural properties of their products.

3. STARTING AND STOPPING CONTROL THEORY

Starting and stopping control should be viewed from the perspective of what is required and why. The industry has provided guidelines and standards that are proven for a certain class of design. It is only when conveyor systems become more exotic, or complex, and/or when challenges are made on the established standards for economic reasons, that alternative design criteria need be reviewed. Some popular considerations now under review are:

- Reduced belt safety factor
- Improved splice efficiency
- Improved method of predicting splice structural properties
- Improved method of starting and stopping control

BELT SAFETY FACTOR

Belt safety factor has been defined in many ways. For this discussion, I will hold to the CDI interpretation of the DIN 22101 concept. The safety factor is divided into three categories:

	Multiple	SF
o Splice fatigue strength	(2.78)	1.00
o elongation allowances	(1.72)	2.78
o dynamic allowances	(1.40)	4.78
o running allowance	(1.00)	6.70

(See Figure 15)

The values following the categories indicate the operating margin of safety multiple allowed based on the previous category's safety multiple. (i.e., if fatigue safety factor = 2.78, then 2.78 x 1.72 = elongation safety requirement = 4.78:1 SF for splice fatigue and elongation allowance.) The dynamic starting and stopping allowance is given as about 140%, of the breaking strength above the splice and elongation allowance, for a steel cord belt with a manufacturing safety factor of 6.7:1. Reduction in the dynamic factor 1.40:1 to, say, 1.25:1 or less, is certainly possible, with modern starting and stopping controls. Improved splice designs and efficiencies have raised the splice fatigue factor, with certain manufacturers, to 2.50:1 (40% splice structural efficiency), from 2.78:1 (36%). The splice strength is also dependent on the number of steps and core rubber allowance about the cables. Prudent design control of the belt's alignment, transition zones, vertical curves, pulley arrangements, et al., which contribute to the elongation allowance, permit reduction of this allowance to 1.6:1 or less. Thus, the belt's safety factor may be reduced to a value closer to 5:1 (2.5 x 1.6 x 1.25)

3.1 STARTING AND STOPPING IDEAL CONTROL RAMP

Control of the belt's starting/stopping dynamic strength factor can be divided into two categories: (reference 15)

- o control of peak force (minimize acceleration rate)
- o control of peak rate of strain in splice (minimize jerk)

From the principles of designing for minimum acceleration (dv/dt) and for the minimum jerk (d^2v/dt^2) the following is proposed (v denotes velocity; t denotes time, and T denotes total time):

A. Minimum acceleration force (a = v/t) is obtained when the acceleration is constant for a given time period (Figure 16). But jerk is maximized (∞) at the onset of the velocity increase. If the belt splice is in the high tension zone of the drive assembly, potentially destructive strain rate loading may occur. Furthermore, the real-time control system will not be capable of providing the incremental starting force to meet the speed ramp. Undershoot will occur. More power will be requested by the control band error signal. The proportional-integral-derivative (PID) loop control will provide more power until the nominal ramp is reached, but also causing overshoot.

B. Minimum jerk ($4v/t^2$) is obtained when jerk is a constant as shown in Figures 16A-16B. This point of view differs from discussions offered by others on the subject (15).

When jerk is integrated, $\int_0^{T/2} \frac{4v}{t^2}\,dt$ and $\int_{T/2}^{T} \frac{4v}{t^2}\,dt$, an acceleration ramp configuration is generated as shown in Figure 16B.

Integration of the acceleration curve yields the velocity time ramp.

$$V(t) = V\left(\frac{2t^2}{T^2}\right);\ 0 \le t \le \frac{T}{2}$$

$$V(t) = V\left(-1 + \frac{4t}{T} - \frac{2}{T^2}t^2\right);\ \frac{T}{2} \le t < T$$

It is not presently known what jerk allowance value is tolerable. As the safety factors of a belt is reduced to the minimal practical limits, the strain rate properties in the belt splice may be of significant importance. It is a field in need of further study.

The control system selected for a given conveyor must strike a balance among many considerations:

1) It must be cost effective.
2) It must be reliable for long term use.
3) It must be easy to maintain and simple in concept.
4) It must have flexibility, allowing for a range of adjustment.
5) It must minimize excessive belt line stresses.
6) Ideally, it will be insensitive to belt velocity wave undulation.

Well conceived control systems and control philosophies can be rendered useless, or even detrimental, if the designer does not consider the integration of:

a) belt response mechanics
b) control logic
c) instrumentation performance

It has been our experience that the designer of the controls is usually not an expert in belt physics. As previously suggested, the starting ramp should ideally be of a non-linear form. The designer should have some awareness of the belt's response to changes in localized energy differentials, such as cut-off of motor power. By example, compare the response of an uphill and a downhill conveyor to power outage as illustrated in Figure 17A and Figure 17B respectively. In Figure 17A, the sudden loss of power retards the drive steady-state speed 35% in approximately 2.5 seconds. The instantaneous decay rate is dependent on the driving or braking tractive force and the drive assembly mass connected to the pulley under study. The high higher the driving power, or the smaller the drive mass, equates to greater initial response and subsequent stress wave amplification.

The same conditions apply for downhill conveyors with braking requirements.

Long overland conveyors with head and tail drives may require a more complex velocity ramp to idealize their integrated control. This concept is outside of this paper's presentation.

3.2 FEEDBACK VS. NON-FEEDBACK CONTROL

Starting and stopping control systems can be divided into specific categories:

a) speed feedback time loop - full action control
b) speed feedback time loop - one way action control
c) torque time loop with speed and/or torque feedback
d) torque passive control system without feedback

The speed feedback time loop with full action is the most conventional type utilized for large class conveyors. Typically, this concept uses a proportional band controller, as shown in Figure 18. The proportional control band can be modified to provide: velocity, differentiation, integration, torque limit and time control. The proportional control band can have tailored error offsets and band adjustments. The bands can be made parallel, convergent, divergent, or of more exotic configurations. The negative aspects of this control are: 1) it can be misapplied, resulting in excessive belt stress, and 2) it is more complex, which can result in lower reliability. Accurate integration regulation is possible, in particular with downhill conveyors where the low speed end of the proportional band may give unacceptable error.

Speed feedback loop control with one-way action is similar to speed feedback with full action, except the control action can never be reversed (i.e., once a control action has been invoked, it cannot be reversed, such as applying more torque during braking, increasing the oil fill level in a fluid coupling, et al.). The advantage of this system over a full action controller is that it is more stable, because it only controls on a part of the band width. Since it is a more stable control, the power modulation (stress wave impulsing) may be reduced, and there is less hunting of the control. Integration and differentiation can be implemented. Smoothing control algorithms can also be programmed. To make this control system effective, the designer must have a greater integrated knowledge of the specific conveyor's physical behavior.

Torque ramp control with ATL (automatic torque limit) with speed feedback applies torque at a preset rate until either the speed ramp is exceeded, or the torque limit is reached. Typically, these controls are utilized on fluid coupling systems with scoop controls. They could be considered one-way controllers as previously described. They are stable controllers and have been used on multiply driven pulleys. The disadvantage is that little after-installation monitoring is done. If the control goes out of adjustment, the operator has less instrument feedback diagnostics to effect proper settings. This is also true on initial installation. The fluid coupling characteristics are not linear. During starting, rates of acceleration can occur which would not be acceptable as good design practice, but go undetected until recurring breakdowns make the condition obvious.

Torque time control or passive torque control is typically used with wound rotor-resistor step timing or fluid couplings with fixed and delay fill chamber. There is no feedback signal in the control loop. Operating sensors are used to monitor and alarm or shutdown if control limits are exceeded. This type of control is of the KISS philosophy (Keep It Simple Stupid). It is the easiest concept for field operations. The cause and effect relationship is immediate and usually fairly obvious. The control is inherently more reliable and less prone to risky "what if" failures. The down sides are that the control is less flexible, and it is harder to initially set for optimum performance. Typically, this concept is utilized on the intermediate size conveyors that seem to be simplistic in design. Long overland and high horsepower, high lift systems are usually equipped with more sophisticated control. In later discussion I will show that the larger system can also utilize this concept.

General notes about the above controls: The controls can be very effective in meeting the designer's needs provided:

a) The belt response to control and the consequential control interaction with the belt are understood.

b) System instrumentation is compatible with the objectives - high modulus belts produce very fast response characteristics, often very non-linear, therefore the tracking and logic control tools must be capable of following (tracking) the response mechanics.

c) Failure analysis, failure detection, and system protection are integral to the design and specified control. It is not uncommon to find: 1) clients changing out a gravity take-up for a fixed take-up, followed by pulley replacement, structural modifications with a curse on the engineers, and ultimate loss of faith in belt conveyor technology; 2) moving the take-up in the hope of reducing observed hazards; 3) poor diagnostics which lead to guessing about cause and effects equals bad guesses on corrections and adjustments.

d) Assume the client is going to test the system to its limits. Provide data and documentation on the strength of each component and how the control will work or fault at higher than normal loading.

3.3 Wound Rotor Motor Control Concepts

There are many control systems for conveyor drives. The principle systems include:

1) wound rotor - resistor - timer
2) wound rotor - liquid rheostat
3) wound rotor - SCR slip recovery
4) fluid coupling - fixed fill with fixed oil reservoir
5) fluid coupling - delay fill with fixed oil reservoir
6) fluid coupling - refilling circuits - various scoop controls
7) eddy current couplings
8) eddy current brake
9) direct current SCR
10) hydroviscous clutch - various systems
11) centrifugal friction clutch
12) friction clutch, air or hydraulic
13) auto-transformer
14) saturable reactor
15) primary voltage SCR
16) inverters - variable frequency (variable voltage, current source, etc.)
17) cycloconverters - synchronous motors
18) flywheels

These controls, as well as others not listed, offer benefits and drawbacks. They have varying degrees of complexity and may require a designer to have a specialized technical expertise to be implemented effectively. I am selecting the often used wound rotor motor with resistor timing control for technical review. I am not advocating the wound rotor over other systems, but believe since it is universally used with varying degrees of success, a more detailed discussion on one widely used control could be useful. Following is CDI's approach to the wound rotor resistor selection process, and considerations associated with the process relevant to belt dynamic behavior.

Wound rotor resistor step selections vary. For the purposes of this presentation, I will be selective and discuss the use of a binary sequential controller. The binary control sequence refers to a series of resistors connected on each phase of the induction motor rotor circuit. The resistors can individually be placed in the circuit by switching the respective contactor on or off, hence "binary" name. (See Figure 19.) The objective is to select the minimum series of binary combinations from among the many that are available (7 resistors = 2^7 - 1 or 127 steps, or 8 resistors = 2^8 - 1 = 255 steps available). The conveyor designers and wound rotor manufacturers have developed differing methods of selection. Given that a binary sequential control is to be used, there is one best method for selecting the following:

a) the number of resistors per phase
b) the starting step or initial torque jump
c) the intermediate steps or torque jumps
d) the last permanent slip step (multiple-pulley drives)

From the above, it can be shown that the wound rotor resistor step design criteria can be directly specified for a given conveyor design. The design boundary conditions must be given for the following:

a) lowest allowable torque step for first resistor position
b) lowest allowable final motor electrical slip
c) least belt acceleration rate to maintain material stability on incline or decline belt
d) least torque spike acceptable between steps
e) least peak belt stress to meet the belt factor of safety
f) number of restarts in succession and per hour at full load

In addition to these boundary conditions, a) the number of resistor closures should be minimized to maximize contactor life, b) the heat load on each resistor must be evaluated to eliminate hot spots, and c) load sharing (electrical slip allowance) among multiple-driven pulleys must be accounted for to minimize power loss due to slip.

Once power conditions are set, a mathematical geometric progression series can be implemented that defines the step-wise impedance of each resistor, the number of resistors required, and the best suited binary combinatorial selection which yields the total number of steps.

Two additional comments are offered when designing for multiple-pulley drives. The relative and absolute electrical slip should be minimized. It is not uncommon practice to specify a 5-6% permanent electrical slip. I believe this rather large slip loss corrects for design, manufacturing and/or operating deficiencies. To provide good load sharing the following conditions should be considered:

a) drive pulley diameters (steel rim and lagging) should be matched with great care
b) drive pulley eccentric tolerance should be minimized
c) potential for material buildup or abrasion wear should be minimized
d) lagging hardness, thickness and abrasion resistance should be researched
e) only drive from the belt's clean side to provide common neutral axis of belt to pulley and to minimize problems associated with dirty side contact with pulleys

These conditions are all linked to the pulley specifications. The following example illustrates the point. Assume the drive pulley to be 1500 mm in diameter, motor slip between drives is given to be 1% at full load, the drives are specified to load share within 5% of each other, then what is the pulley diameter tolerance allowed between drives? (gearbox matching elongation of belt, belt cover and pulley cover compression are ignored for this analogy.)

a) 1500 mm diameter x .01 drive slip difference = 15 mm delta
(i.e., 15 mm diameter differential = 100% motor slip)
b) 15 mm delta x .05 (5% load sharing allowance) = .75 mm
$\therefore$ pulley diameters must be matched to $\pm$.375 mm to control load sharing within $\pm$5%

The economic incentive to meet this goal can be understood by evaluating the cost of power. Assume the following:

a) plant operating hours at capacity = 6000 hours/year
b) power cost at $.05/kw hr
c) value of money per year is 8% (cash flow)
d) 20 year operating life

What is the net present value, in percentage of motor nameplate, of each 1% motor slip loss? The answer is 9.8%. For large drives, this will amount to a substantial cost or cost savings. I studied this condition on a large mine installation which is proposing to use over twenty motors requiring load sharing, and where the electrical slip was specified to be 6%. Conservatively, 4% would be lost x 9.8% per motor x 20 motors = 784%. Thus, the loss equals the value of eight motors.

3.4 DIGITAL VS. ANALOG CONTROL

CDI recommends utilizing digital logic controllers in place of analog drive and/or system controllers. Analog devices are more versatile, can perform certain operations faster, and can be adapted to resolve certain types of complex control requirements. But, for belt conveyor systems they can be very risky and provide no significant benefit over digital control.

A brief list of major advantageous attributes offered by digital control over analog are:

- o can communicate logical influence and response between drives and to central processor for general monitoring of performance
- o major operating parameters are software setable
- o highly immune to noise, and if noise is problematical, software filters can easily be implemented
- o control logic can be standardized for various control functions
- o alternative hardware can be made available increasing sources of supply
- o offers greater reliability through mass use
- o control functions can be more complex
- o control choice is more flexible
- o can derive multiple uses gaining greater utility
- o provides greater safety in separation of control logic from hardware functions
- o allows for easy expansion
- o system diagnostics and operator interactions are enhanced

Conveyor driver controls, braking system and take-up controls, together with their instrumentation, are capable of being digitally controlled. Failure of diodes, transistors, op-amps, etc. cause electrical function failure, but they do not alter the system's program logic. If components fail in the digital system, the failure status is predictable, which is not necessarily true of analog systems (circuit may fail open or fail closed).

4. CASE STUDIES ON STARTING AND STOPPING CONTROL

4.1 GENERAL

The following case studies were selected from CDI projects to illustrate some of the common problems with large conveyor design. Model accuracy is shown, and some of the solutions developed using dynamic analysis techniques are presented. No client names are given.

4.2 STUDY NO. 1 - Shock Loads at Shutdown with Fixed Take-up

The study illustrates shock wave impulses with fixed take-up and shows agreement between theory and practice.

Figure 19 shows the conveyor profile and operating parameters. The conveyor is driven by four 2000 horsepower motors near its head end. The conveyor is equipped with a fixed take-up (TU). In late 1984, the conveyor take-up carriage was dislodged into the surrounding structure during a loaded stop. The conveyor was rebuilt. Field measurements were taken after the accident to determine the possible cause of the failure. CDI was requested to study and report on the design. Field data was obtained on the load cell connected to the take-up and power readings were studied. Figures 20-22 illustrate the results of the study. Figure 20 is a tension vs. time plot and shows the CDI prediction of the belt's general tension pattern at shutdown with a fully loaded belt. The following points of interest are noted:

1) The 7100 HP (5300 kw) drive energy collapsed in less than one second.

2) The drive pulley speed retardation (30% in 1 second) produces a very large compression wave which acts into the carry strand, and its reflected tensile force increase into the secondary drive and on into the return strand. The belt return strand tensile impulse rises from 66,000 lbs. (294 kn) to 208,000 lbs. (925 kn) in 3.5 seconds.

3) The tail pulley is hit by the return strand tensile stress wave 1.5 seconds after shutdown. This is equal to a wave velocity of 5700 FPS (1740 m/s). The stress wave reaches a peak value of 118,000 lbs. (525 kn). The impulse increase at the tail is equal to 42% of the collapsed drive energy. About half went into the carry side and half into the return. The tail pulley's initial belt tension was approximately 10,000 lbs. (44.5 kn). The tail pulley force rises higher than the initial shock wave impulse of the differential energy collapse shown (145,000 lbs-66,000 lbs = 79,000 lbs. + initial tail tension of 10,000 lbs. = 89,000 lb. increase = 118,000 lbs.). This is due to the increased mass resistance of the carryside at the tail, which increases the rate of deceleration of the shockwave. The pulley stress increase at the tail is approximately twelve times greater than the nominal operating tension.

4) The concave curve zone, on the carry strand, has a sharp drop in tension due to the drive's compression wave. The wave appears to travel at approximately 4560 FPS (1390 m/s). The low tension zone is maintained for about 3.5 seconds. This low tension is not transmitted back to the tail loading zone.

Figure 21 is a velocity plot. The belt appears to be whipped violently in the concave curve zone.

Figure 22 is an expanded scale version of the same take-up force shown in Figure 20. Three plots are shown. The solid line is the field measured force. The broken line is replotted from Figure 20. The dotted line is the take-up subjected to an aborted-start when maximum drive energy is released. The field value is somewhat out of phase with the predicted values. This is partially due to the take-up being put in motion by the take-up controller. In general, the phase characteristics are relatively close, and the magnitude of force predictions is within 3%.

4.3 STUDY NO. 2 - Shock Loads at Shutdown with Gravity Take-up

This study illustrates the characteristic differences between fixed and gravity take-up, and the influence of mass tuning the drive to minimize undesirable shock waves. This conveyor was commissioned at the end of 1984. Just prior to commissioning CDI was requested to review the design for potential shock damage. The conveyor is powered by two 2000 HP wound rotor motors. The conveyor design capacity was given to be 4000 STPH.

Figures 23-30 show the study results. With the gravity take-up at the head drive zone, during shutdown, the return strand tensile stress wave is absorbed by the take-up. The carry strand compression wave impacts the tail loading station, dropping the belt tensions close to zero. Spillage, idler damage at the tail station, and possible belt damage could result from this action. Figures 24-25 illustrate the shutdown cycle with the proposed engineer's design, at 3000 TPH. The figure shows:

1) 2000 HP collapses into a stress wave in approximately .40 seconds

2) Reverse motion at the tail pulley shows the belt's potential energy resolved into a tensile stress wave that travels from the tail up the carry strand to the head pulley. Note, the impulse of the tail and head are similar in magnitude and form.

3) The holdback is shown engaging at four seconds in Figure 25.

4) The holdback impulse is beyond the motor's running torque by 157%.

5) Significant belt motion reversal is shown at the take-up. This is not harmful. At 7.5 seconds, a sudden shock wave hits the take-up coming from the tail station, which may be damaging depending on take-up design.

Figures 26-27 show the shutdown with the design load of 4000 STPH (3636 t/h)/ The same characteristics are exhibited as shown with 3000 STPH, except the forces are proportionately larger. The tail pulley is impacted with a force 3.5 times its running condition. The holdback momentary peak force is 169% greater than the running motor torque. The take-up is impulsed at 7.7 seconds with an additional 76% load.

Figures 28-29 show the system shutdown under an aborted-stop with 5000 STPH. The significant comments are:

1) The drive energy (4000 HP) again collapses in less than .50 seconds.

2) The holdback force is momentarily 165% of the motor's drawing torque.

3) The tail pulley force exceeds 3.2 times the running tension.

4) The belt festoons between the idlers for 6 seconds and then is hammered with a high tension impulse of approximately 100,000 lbs. (444 kn) in about .10 seconds.

5) The belt motion at the tail reverses up to 200 FPM.

6) The head pulley stops in 2 seconds.

Figures 30-31 show the resulting analysis using the CDI recommended fix. A moderate size flywheel was added to the high speed shaft of the gear reducer opposite the motor. As shown in Figure 30, the conveyor does not exhibit any of the prior violent actions. There is a tolerable momentary low tail station tension. The holdback load is approximately equal to the motor's running torque. The fix was implemented prior to start-up. The conveyor has been loaded beyond this value and has had many loaded stops. The conveyor has been running since without event.

4.4 STUDY NO. 3 - Overland Starting with Wound Rotor Control

CDI was commissioned in 1986 to design a series of high capacity conveyors for a large copper producer in the U.S.A. There are five conveyors connected in series which transport the ore over 5.5 miles at 10,000 STPH. Part of the scope of work included development of the starting and stopping control logic. One conveyor is reviewed herein.

The conveyor is approximately 17,500 ft. (5347 m) long, with a slight downhill grade. The belt is powered by three 1500 HP (1119 kw) motors at its head and one 1500 HP motor at its tail. The conveyor is equipped with a head and tail brake.

The drive component manufacturer proposed to use a binary system of seven resistor steps. This is shown in Figure 32. Note, the first step is given to be 60% of motor nameplate, and the full load running resistance is with 6% electrical slip. The contract proposed the following:

a) Acceleration to be controlled by a dv/dt ramp signal for all drives. All drives to have same dv/dt ramp.

b) All drives to be activated simultaneously

c) No integration control included

d) No drive staggering or delayed sequencing included

The concept was modelled using BELTFLEX. The results are shown in Figures 33-35. Points of interest are:

1) Figure 33 shows the tension out of the tail drive to drop to an unacceptable level. As can be seen, the drive traction ratio (T1/T2), at the tail, exceeds 10:1. The drives do not load share.

2) Figure 34 shows the programmed velocity ramp, and the resultant proposed control response. When the brakes are released, at the head and tail, the belt starts in motion in the normal direction due to the applied force from the last stop. The first resistor steps aid this action, causing the resistors to be held in until the initial energy is dissipated into an acceleration force and slows the belt below the ramp. Note the overspeed at the tail, indicating an uneven application of torque to belt.

3) Figure 35 shows the motor torque output, the timing, and the sequence of resistor steps being engaged. Note, the secondary and tail drives hog all power during the last third of the acceleration cycle.

The concept was not acceptable. Another proposal was offered by the manufacturer, but it did not improve the condition.

CDI offered the concept of fixed-timed resistor engagement with a different selection of resistor combinations and ohmic values. The distribution of resistor combinations is shown in Figure 36. The figure shows a starting torque of 38% and a full load slip level of 1.5%. The torque spikes are reduced and the full load electrical slip will not unduly waste electrical operating costs. The final slip value was recommended to be increased to 2.5%.

Figure 37 shows the velocity startup ramp. The resistors are engaged at fixed time intervals. All resistor engagements are staggered between drives.

Figure 38 shows the tension profiles at all drives and take-up.

Figure 39 shows the drive traction ratio T1/T2 and equal distribution.

Figure 40 shows the motor torque versus time. Note the uniform load sharing of all drives. Also, note the delayed engagement between steps.

Figure 41 shows the calm take-up response to this starting cycle.

References

1. Conveyor Equipment Manufacturers Association (U.S.A.), "Belt Conveyors for Bulk Materials", Second Edition, 1979.

2. DIN 22101, "Belt Conveyors for Bulk Materials", 1982.

3. International Standard ISO 5048, "Continuous Mechanical Handling Equipment", First Edition (1979).

4. JIS - Japanese Industrial Standard

5. Goodyear Tire & Rubber Co., "Handbook of Conveyor and Elevator Belting", 1975.

6. Continental Gummi - standard manufacturer's handbook

7. Clouth - standard manufacturer's handbook

8. Dunlop BTR - standard manufacturer's handbook

9. Behrends, U., "Untersuchungen zum Walkwiderstand schwerer Förderbandanlagen", Dissertation, Technical University Hannover, 1967.

10. Schwarz, F., "Untersuchungen zum Eindruckrollwiderstand zwischen Fördergut und Tragrolle", Dissertation, Technical University Hannover, 1966.

11. Spaan, C., "The Indention Resistance of Belt Conveyors", Delft Technical University, Dept. of Mech. Eng. WTHD Nr. 103, Jan. 1978.

    Spaan, C., "The Flexure Resistance of Belt Conveyors", Delft Technical University, Dept. of Mech. Eng. WTHD Nr. 117, Sept. 1979.

12. Jonkers, C., "The Indention Rolling Resistance of Belt Conveyors", Fördern und Heben, Vol. 30, (1980) pp. 312-318.

13. Könneker, F., "Untersuchung zur Bestimmung des Leistungsbedarfs von Gurtförderanlagen", Dissertation, Technical University Hannover, 1984.

14. Nordell, L. and Ciozda, Z. P., "Transient Belt Stresses During Starting and Stopping: Elastic Response Stimulated by Finite Element Methods", Bulk Solids Handling, Vol. 4, Nr 1, March 1984.

15. Harrison, A., "Specific Design Considerations for Achieving High Speed Operation of Long Conveyor Belts", Proceedings, Chapter 5, International Materials Handling Conference, Johannesburg, Sept. 12, 1985.

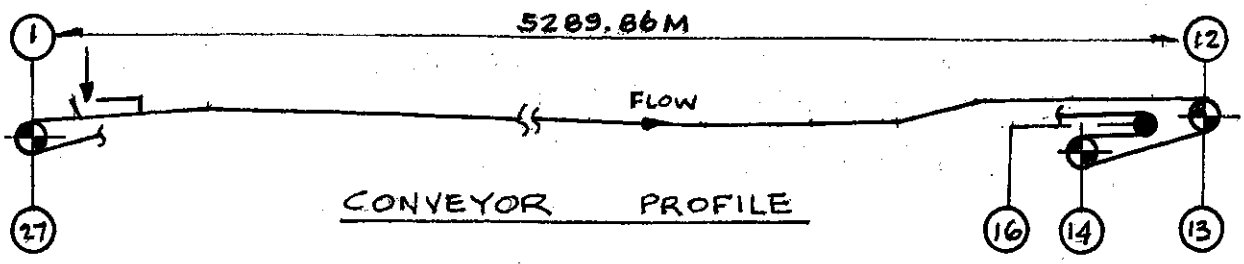


```
                                        ****************************************************
     CLIENT  :  STUDY                   *  C O N V E Y O R   D Y N A M I C S ,  I N C .  *  PAGE NO:  1
   JOB NUMBER :  EXAMPLE                *   369 E. CALAVERAS ST.   ALTADENA, CA 91001   *     DATE: 08-26-1987
 CONVEYOR NO. :  1                      *    BELTSTAT V3.3I : CONVEYOR DESIGN PROGRAM    *   RUN NO:  1.1WF
*****************************************************************************************************************
 REMARKS:  WINTER / FULLY LOADED / 3x1500HP DRV AT HEAD : 1x1500HP AT TAIL / 2:1 TAIL TO HD BRK RATIO
*****************************************************************************************************************

MATERIAL SPECIFICATIONS
-----------------------
 1. MATERIAL CONVEYED ..................  CRUSHED COPPER ORE
 2. DESIGN TONNAGE .....................  9071.85  T/H
 3. BULK DENSITY .......................  1601.85  KG /CU M
 4. SURCHARGE ANGLE ....................    15.00  DEG
 5. LUMP SIZE AND PERCENTAGE ...........   381.00  MM X      5.00 PCT
 6. LUMP SHAPE FACTOR ..................     1.00
 7. CHUTE DROP DISTANCE ................     3.66  M
 8. ABRASIVE INDEX .....................  EXTREME
    ENVIRONMENTAL CONDITION .(CEMA INDEX) DIRTY
    MAINTENANCE CONDITION ...(CEMA INDEX) POOR
11. HOURS IN SERVICE PER DAY............    24.00  HRS
12. TEMPERATURE RANGE .................   -17.78  TO  37.78 DEG C

BELT SPECIFICATIONS
-------------------
 1. WIDTH ..............................  1828.800 MM ( 578.9 /LUMPS)
 2. SPEED ..............................     4.572 M/S
 3. TYPE OF BELT CARCASS ...............  STEEL
 4. BREAKING STRENGTH ..................  3520.050 N/MM
 5. TENSION UTILIZATION RUNNING ........    94.191 PERCENT OF RATED
                    ACCEL/DECEL .....    110.818 PERCENT OF RATED
 6. WEIGHT .............................    86.790 KG /M
 7. COVER THICKNESS ....................    15.748 X  6.350 MM
 8. ELASTICITY .....................365110.031 N  X1000
 9. SAG ALLOWABLE ON CARRY SIDE, PCT ....     1.000 PCT
10. EDGE DISTANCE / BED DEPTH...........   138.672 MM /   340.346 MM
11. X-SECTIONAL AREA AVAIL (100% OF CEMA)     0.359 SQ M
12. X-SECTIONAL AREA AVAIL (NO EDGE DIST)     0.494 SQ M
13. X-SECTIONAL AREA UTILIZED      (CEMA)     0.344 SQ M
14. X-SECTIONAL LOADING PERCENTAGE (CEMA)    95.720 PCT
15. IMPACT FORCE FROM LUMPS ...........  1663.839 N-M
16. TAPE LENGTH (NOT INCL SPLICE LENGTH) 10626.027 M

IDLER AND ANCILLARY SPECIFICATIONS
----------------------------------
                                          CARRY        RETURN
 1. IDLER SERIES .....................    BALL BRG     BALL BRG
   A. IDLER ANGLE ....................    35.00 DEG    15.00
   B. DIAMETER .......................   177.80 MM     177.80
   C. LOAD RATING ....................  8896.44 N     6672.33
   D. ADJUSTED LOAD CAPACITY .........  5511.49 N     4822.54
   E. APPLIED LOAD AT MAX SPACING ....  7627.64 N     5188.41
   F. ROTATING WEIGHT ................    65.18 KG      47.72
   G. SEAL DRAG (Ai) .................     6.67 N        4.45
   H. NUMBER OF IDLERS (APPROX) ......     4508.         1504.
 2. (KY) TROUGH SHAPE MULTIPLIER .....     1.000         1.030
 3. (KY/KX) CORRECTION (REGENERATION) ...     1.000
 4. BREAKAWAY FRICTION MULTIPLIER .....     1.250
 5. (KT) TEMPERATURE ADJUSTMENT (KY/KX)     1.350
 6. IDLER SEAL CORRECTION (REGENERATION)    1.000
 7. SKIRTBOARD FRICTION FACTOR ........     0.060
             WIDTH ....................  1219.200 MM
             MAXIMUM MATERIAL HEIGHT ..   136.137 MM

MOTOR / REDUCER / BRAKE SPECIFICATIONS
--------------------------------------
 1. LOCATION OF DRIVE / BRAKE UNITS .....      12        14        27         0
 2. MOTOR NAMEPLATE KILOWATTS  ..........    2237.1    1118.5    1118.5      0.0
        RUNNING  KILOWATTS  .............    2164.4    1082.2    1082.2      0.0
 3. POWER RATIO .........................     0.500     0.250     0.250     0.000
 4. MOTOR SYNCHRONOUS RPM ...............    1200.0    1200.0    1200.0      0.0
        RUNNING  RPM .....................    1177.4    1177.4    1177.4      0.0
 5. BREAKAWAY TORQUE (PCT FULL-LOAD-TORQUE) 102.516   102.516   102.516     0.000
 6. STARTING TORQUE LIMIT  (PCT FULL-LD-TQ) 117.385   117.385   117.385     0.000
 7. DRIVE INERTIA AT MOTOR .....(KG-M-SQ)     179.0      89.5      89.5      0.0
 8. DRIVE EFFICIENCY ....................     0.950     0.950     0.950     0.000
 9. DRIVE WRAP ANGLE ..........(DEGREES)   160.000   180.000   180.000     0.000
10. DRIVE FRICTION FACTOR, RUNNING .....     0.350     0.350     0.350     0.000
                    ACEL/DEC .....       0.400     0.400     0.400     0.000
11. GEARBOX RATIO ......................    18.666    18.666    18.666     0.000
12. BRAKE TORQUE LOW-SPEED ..........(N-M) 49053.5       0.0   98107.0      0.0
13. BRAKE ENERGY ABSORBED .....(KW-SECS)    2916.2       0.0    5832.4      0.0
14. ACCELERATION ..... TIME  90.000 SEC    TRAVEL:   205.74 M
15. DRIFT ............ TIME  22.151 SEC    TRAVEL:    50.64 M
16. BRAKING .......... TIME  18.000 SEC    TRAVEL:    41.15 M
```

FIG. 1

CONVEYOR DYNAMICS, INC. * PAGE NO: 2
369 E. CALAVERAS ST. ALTADENA, CA 91001 * DATE: 08-26-1987
BELTSTAT V3.3I : CONVEYOR DESIGN PROGRAM * RUN NO: 1.1WF

REMARKS: WINTER / FULLY LOADED / 3x1500HP DRV AT HEAD : 1x1500HP AT TAIL / 2:1 TAIL TO HD BRK RATIO

FLITE NO		LENGTH (M)	HEIGHT (M)	IDLER SPG (M)	SAG TEN (N)	KY	KX	WM (N/M)	WT (N/M)	MASSES (KG)	LOADING (PCT)
1	CARRY	2.44	0.00	1.22	12971.0	0.0160	0.4410	0.00	851.12	342.	0.0
2		8.23	0.00	0.46	35754.6	0.0160	1.3671	5405.15	6256.27	6418.	100.0
3		4.27	0.00	1.22	95345.5	0.0268	0.7002	5405.15	6256.27	2948.	100.0
4		24.07	-0.59	0.61	95345.5	0.0183	1.1004	5405.15	6256.27	17920.	100.0
5		34.71	-1.00	1.22	95345.5	0.0268	0.7002	5405.15	6256.27	23990.	100.0
6		4894.48	-17.40	1.22	95345.5	0.0212	0.7002	5405.15	6256.27	3381452.	100.0
7		61.83	1.76	1.22	95345.5	0.0192	0.7002	5405.15	6256.27	42733.	100.0
8		61.83	4.11	1.22	95345.5	0.0192	0.7002	5405.15	6256.27	42810.	100.0
9		84.02	6.15	0.61	95345.5	0.0160	1.1004	5405.15	6256.27	62701.	100.0
10		84.02	2.10	0.61	47672.7	0.0160	1.1004	5405.15	6256.27	62551.	100.0
11		29.97	0.00	1.22	95345.5	0.0190	0.7002	5405.15	6256.27	20706.	100.0
12	RETURN	1.83	-1.52	0.00	95345.5	0.0154	0.0000	0.00	851.12	133036.	0.0
13		-31.47	-2.13	6.10	33354.0	0.0154	0.0945	0.00	851.12	2982.	0.0
14		-1.83	1.52	0.00	33354.0	0.0154	0.0000	0.00	851.12	67230.	0.0
15		19.51	1.52	6.10	33354.0	0.0154	0.0945	0.00	851.12	1850.	0.0
16		-16.94	0.00	3.66	33354.0	0.0154	0.1303	0.00	851.12	2453.	0.0
17		-84.02	-2.10	1.83	12007.5	0.0154	0.2198	0.00	851.12	9479.	0.0
18		-84.02	-6.15	1.83	4864.1	0.0154	0.2198	0.00	851.12	9502.	0.0
19		-61.83	-4.11	3.66	12007.5	0.0154	0.1303	0.00	851.12	6181.	0.0
20		-61.83	-1.76	3.66	12007.5	0.0154	0.1303	0.00	851.12	6170.	0.0
21		-4894.48	17.40	3.66	12007.5	0.0154	0.1303	0.00	851.12	488254.	0.0
22		-34.71	1.00	3.66	12007.5	0.0154	0.1303	0.00	851.12	3464.	0.0
23		-24.07	0.59	1.83	12007.5	0.0154	0.2198	0.00	851.12	2716.	0.0
24		-4.27	0.00	3.66	12007.5	0.0154	0.1303	0.00	851.12	426.	0.0
25		-8.23	0.00	3.66	12007.5	0.0154	0.1303	0.00	851.12	821.	0.0
26		-2.44	-0.91	3.66	12007.5	0.0154	0.1303	0.00	851.12	260.	0.0
27		-1.83	1.52	0.00	12007.5	0.0154	0.0000	0.00	851.12	66987.	0.0

STATION PT.	ITEM	TENSION SPECIFICATIONS RUNNING (N)	EMPTY (N)	ACCEL. (N)	BRAKE (N)	DRIFT (N)	CONC. WEIGHT (N)	MISC. DRAG (N)	CURVE RADIUS (M)	PULLEY DIAMETER (MM)	ESTIMATED SHAFT X BRG (MM)
1	TAIL	126137.	285594.	99732.	346782.	233444.	0.	0.0	0.	0.0	0.00 X 0.00
2	LOAD/SKT	126203.	285660.	99816.	346761.	233440.	0.	5760.3	0.	0.0	0.00 X 0.00
3		133048.	285991.	106987.	351976.	238960.	0.	1134.6	0.	0.0	0.00 X 0.00
4	CONVEX R	134993.	287241.	109081.	353171.	240296.	0.	0.0	471.	0.0	0.00 X 0.00
5		134678.	287577.	109676.	348304.	236283.	0.	0.0	0.	0.0	0.00 X 0.00
6	CONCAV R	134998.	287666.	111215.	342531.	231651.	0.	0.0	423.	0.0	0.00 X 0.00
7	CONCAV R	773912.	405357.	921907.	122556.	172644.	0.	0.0	1219.	0.0	0.00 X 0.00
8	CONCAV R	793571.	408529.	943737.	131361.	183483.	0.	0.0	1219.	0.0	0.00 X 0.00
9		827922.	413703.	980262.	154838.	208998.	0.	0.0	0.	0.0	0.00 X 0.00
10	CONVEX R	877084.	421886.	1032610.	188075.	245219.	0.	0.0	1714.	0.0	0.00 X 0.00
11	CONVEX R	900859.	426611.	1059563.	195962.	256084.	0.	0.0	1783.	0.0	0.00 X 0.00
12	HEAD DR1	905002.	427422.	1064758.	194846.	255953.	26901.	0.0	0.	1384.3	400.31 X368.30
13	CONCAV R	456566.	297370.	509630.	244409.	240979.	0.	960.8	792.	0.0	0.00 X 0.00
14	DRIVE 2	456329.	297134.	509545.	243415.	240127.	19419.	0.0	0.	1384.3	311.74 X292.10
15	CONVEX R	234075.	234075.	233981.	234545.	234457.	0.	0.0	630.	0.0	0.00 X 0.00
16	TAKE-UP	235756.	235756.	235756.	235756.	235756.	7494.	991.2	0.	939.8	274.58 X215.90
17	CONVEX R	237091.	237091.	237216.	236468.	236585.	0.	0.0	666.	0.0	0.00 X 0.00
18	CONVEX R	237160.	237160.	237766.	234129.	234697.	0.	0.0	667.	0.0	0.00 X 0.00
19		233782.	233782.	234871.	228338.	229358.	0.	0.0	0.	0.0	0.00 X 0.00
20	CONCAV R	231544.	231544.	232947.	224530.	225844.	0.	0.0	288.	0.0	0.00 X 0.00
21	CONCAV R	231304.	231304.	233021.	222723.	224331.	0.	0.0	288.	0.0	0.00 X 0.00
22	CONCAV R	345570.	345569.	372089.	212971.	237822.	0.	0.0	459.	0.0	0.00 X 0.00
23		347126.	347126.	373822.	213648.	238664.	0.	0.0	0.	0.0	0.00 X 0.00
24	CONVEX R	348164.	348164.	374997.	213996.	239141.	0.	0.0	208.	0.0	0.00 X 0.00
25		348250.	348250.	375105.	213974.	239139.	0.	0.0	0.	0.0	0.00 X 0.00
26	CONVEX R	348417.	348417.	375314.	213933.	239137.	0.	0.0	208.	0.0	0.00 X 0.00
27	TAIL DR3	347692.	347692.	374602.	213142.	238358.	17035.	960.8	0.	1384.3	280.81 X279.40

SUMMARY					
(TE1)	447182.	128797.	553873.	-50819.	13720.
(TE2)	223594.	64398.	276903.	10210.	7009.
(TE3)	223855.	64398.	277170.	-131340.	7214.
WR FACTR (1)	2.657	2.657	3.056	3.056	
T1/T2 (DR 1)	1.982	1.437	2.089	1.254	1.062
WR FACTR (2)	3.003	3.003	3.514	3.514	
T1/T2 (DR 2)	1.950	1.269	2.178	1.038	1.024
WR FACTR (3)	3.003	3.003	3.514	3.514	
T1/T2 (DR 3)	2.756	1.217	3.756	1.627	1.021

DRIVE PULLEY DRAG	DRIVE 1	AISI 1045 STEEL 2559.	N
	DRIVE 2	1277.	N
	DRIVE 3	1016.	N
LIFT FORCE		-26360.	N
FRICTION FORCE		911183.	N
TOTAL MISCELLANEOUS DRAG		9808.	N

COUNTERWEIGHT SPECIFICATIONS (DIMENSIONS IN METERS):

LENGTH OF SPLICE	2.49		THERMAL TRAVEL	3.45	
PERM. ELONGATION	7.97	(0.15 %)	TAKEUP DISPL.	16.8	
TENSION TRAVEL	1.413	0.567	1.993	-0.954	-1.053
TAKEUP TYPE	GRAVITY		INPUT DISPL.	0.000	

TAKEUP TENSION	235756.	N	
TAKEUP TENSION DIFFERENTIAL ..	9622.	N	
GOVERNED BY DRIVE NO. 3,	ACCELERATION CASE		
INPUT TAKEUP TENSION	235756.	N	

HORIZONTAL LENGTH	5289.86	M	
TOTAL ELEVATION	-4.88	M	
MATERIAL LIFT	-4.88	M	
SUM OF FLITE HEIGHTS	0.00	M	
TOTAL MASS	4466382.	KG	
DIN FACTOR	0.02231		

FIG. 2

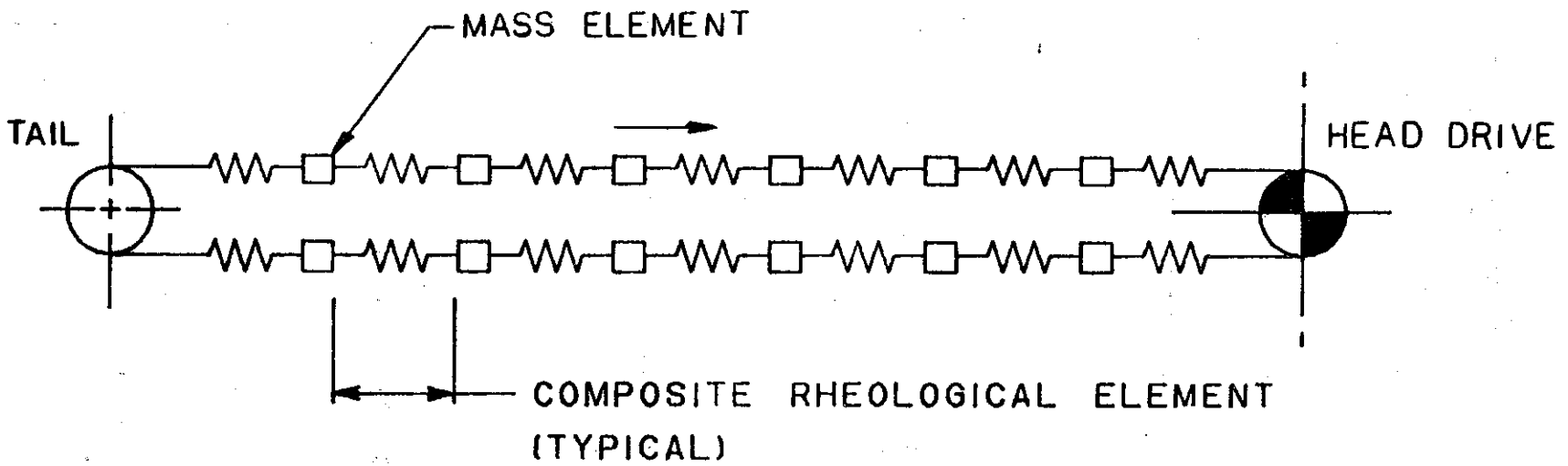

FIG. 3 LUMP-MASS SPRING-DAMPENED FINITE ELEMENT MODEL

FIGURE 4-1

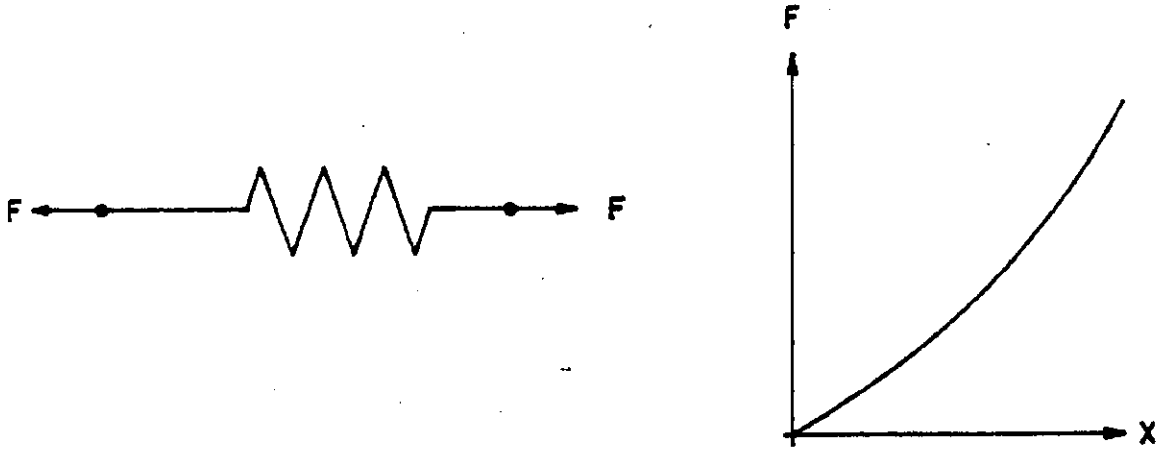

FIG. A HOOKEAN ELEMENT (K_1)

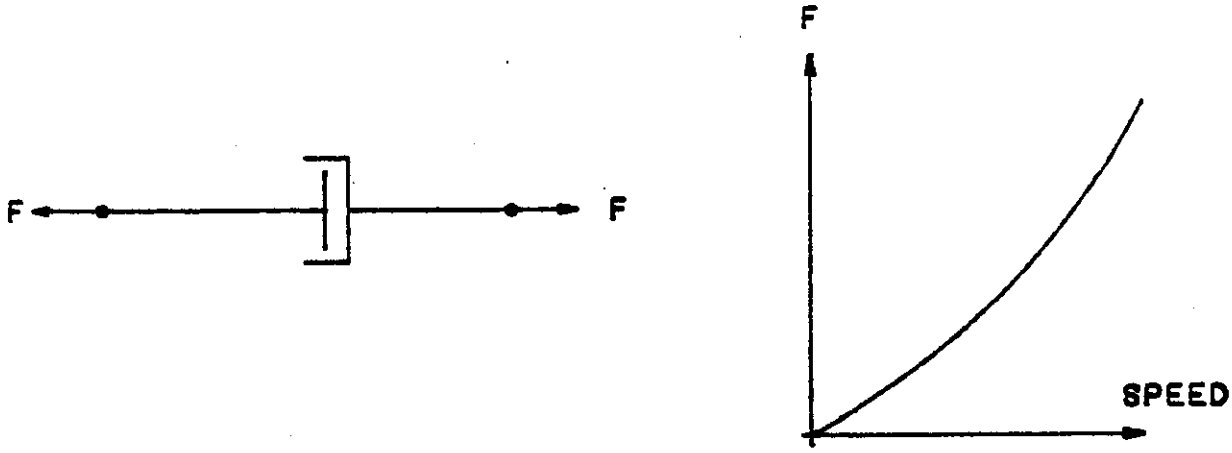

FIG. B NEWTONIAN ELEMENT (V)

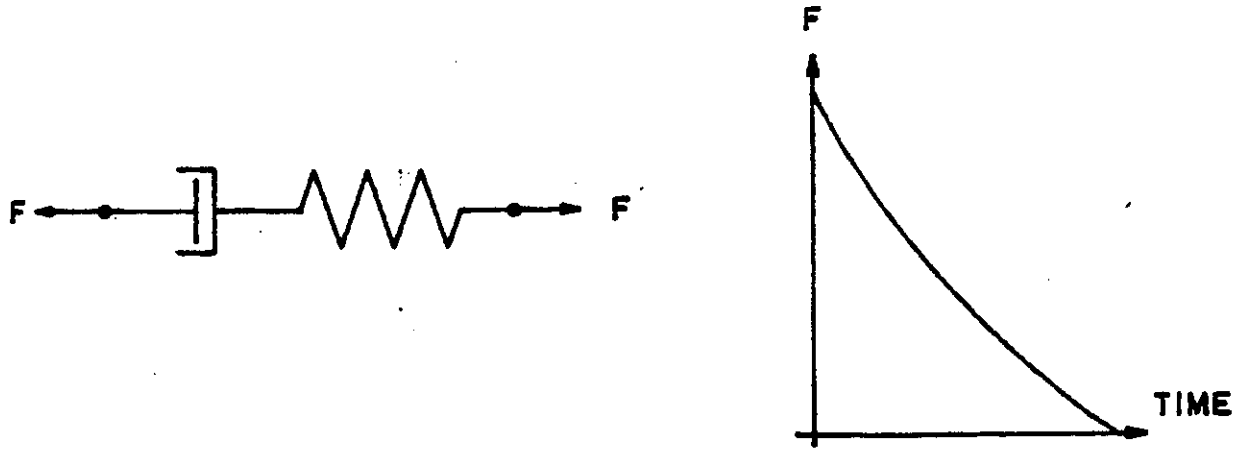

FIG. C MAXWELL ELEMENT (H)

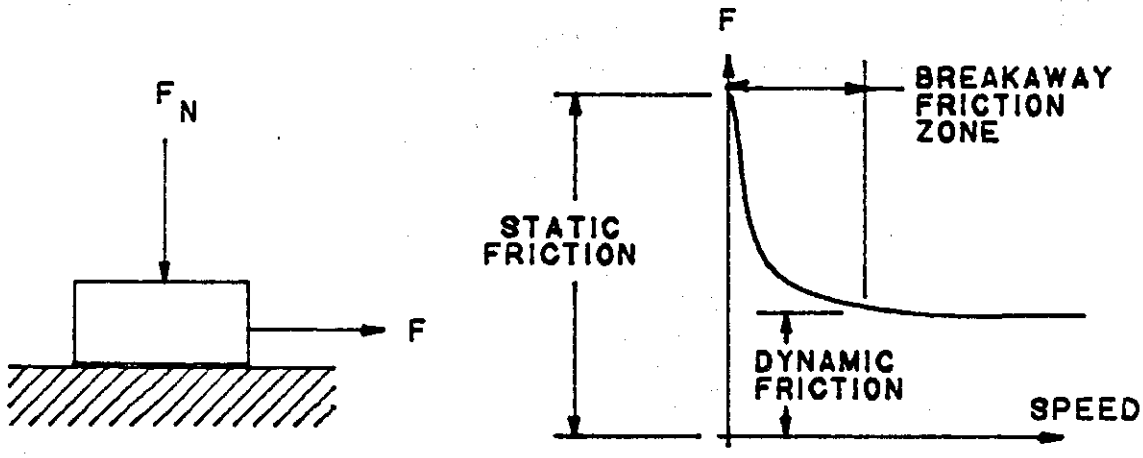

FIG. D ST. VENANT ELEMENT (C)

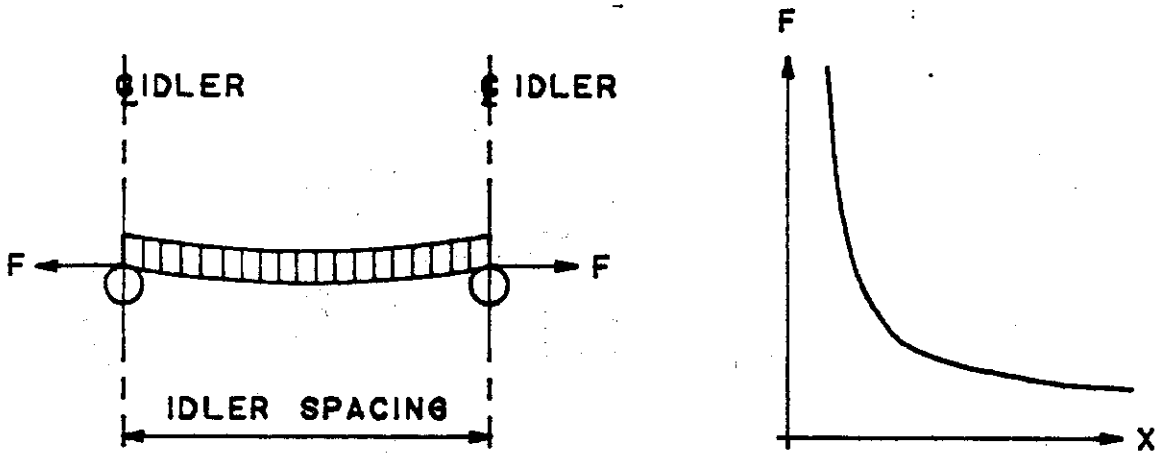

FIG. E CDI GEOMETRIC BEAM ELEMENT (G)

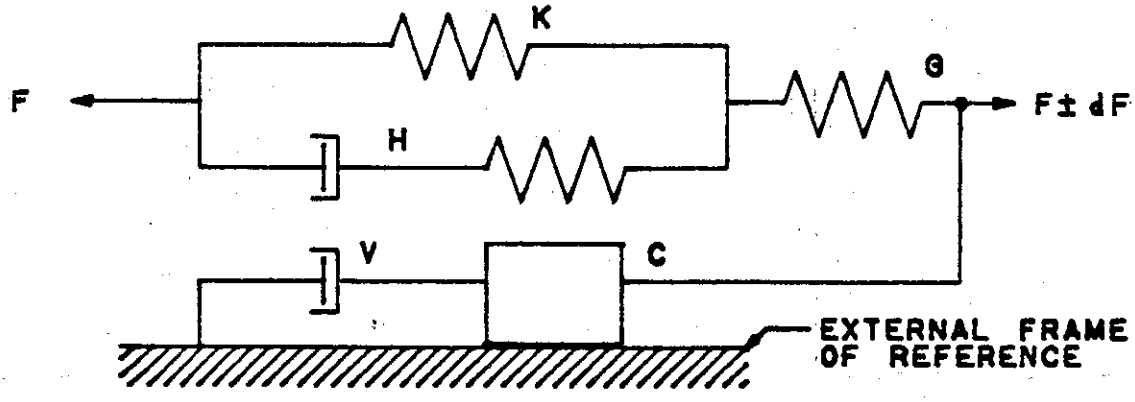

FIG. F CDI FIVE-ELEMENT COMPOSITE MODEL

FIGURE 4-2

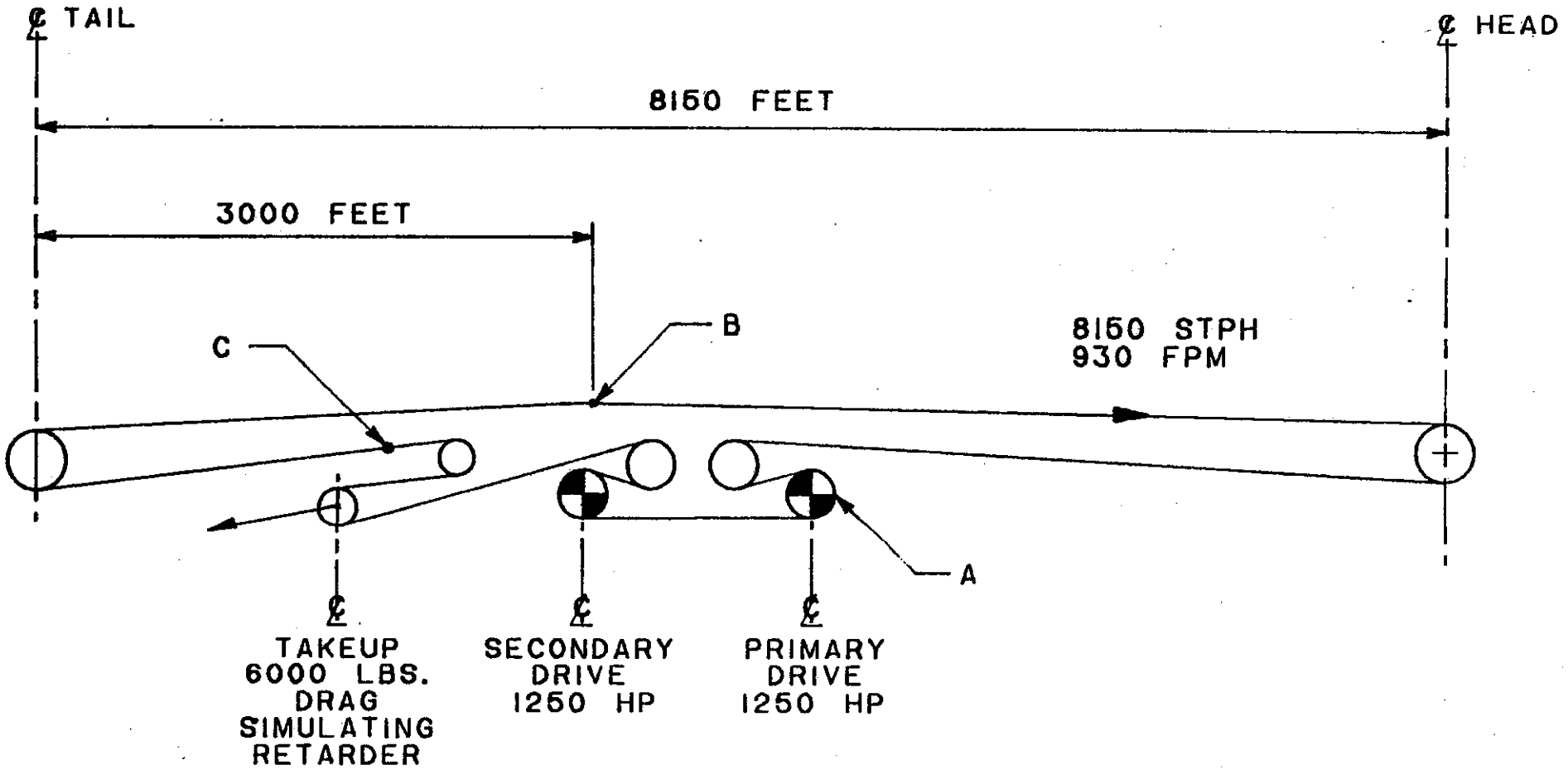

FIG. 5 GEOMETRIC PROFILE OF STUDY

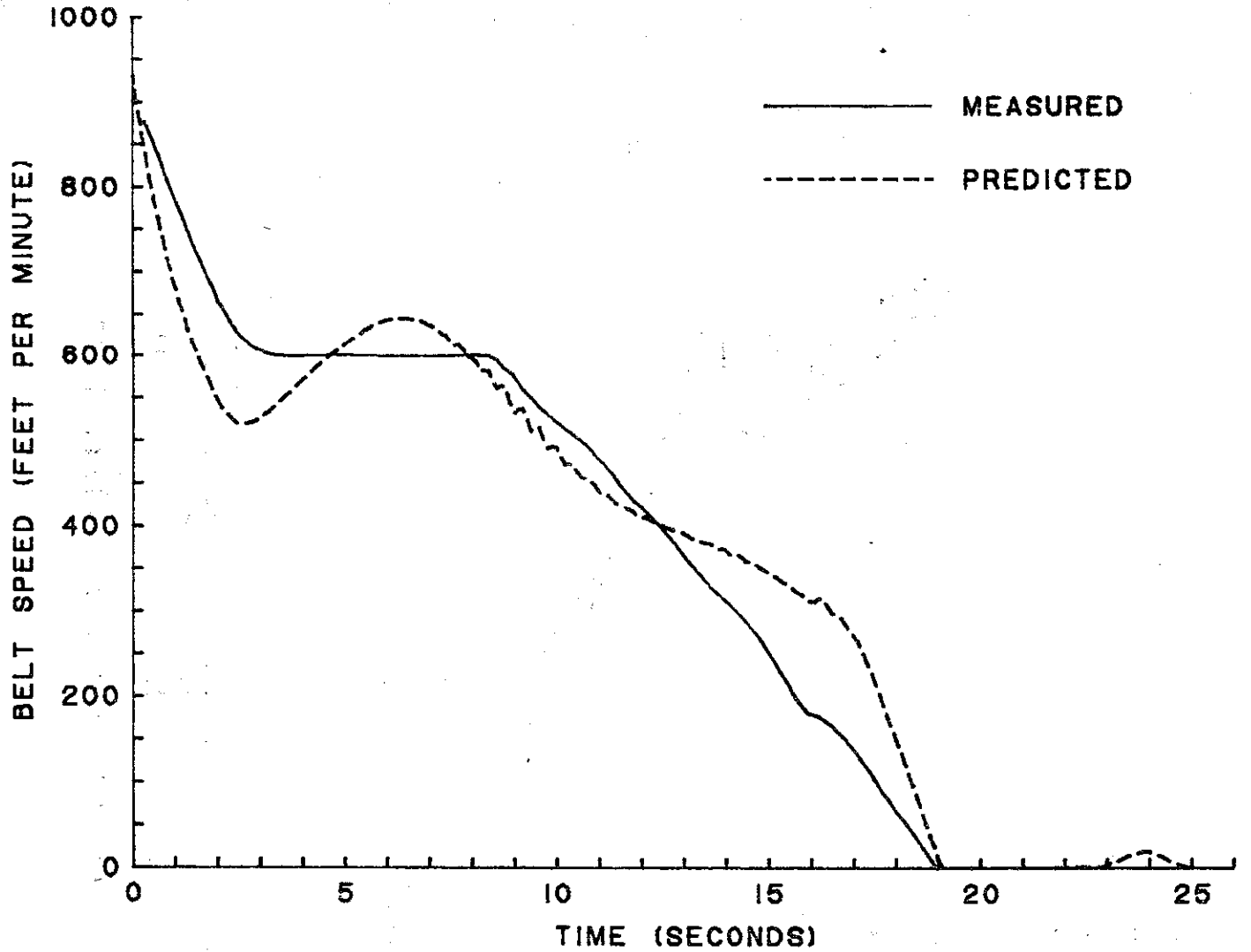

FIGURE 6 VELOCITY VS. TIME AT SHUTDOWN - POINT A

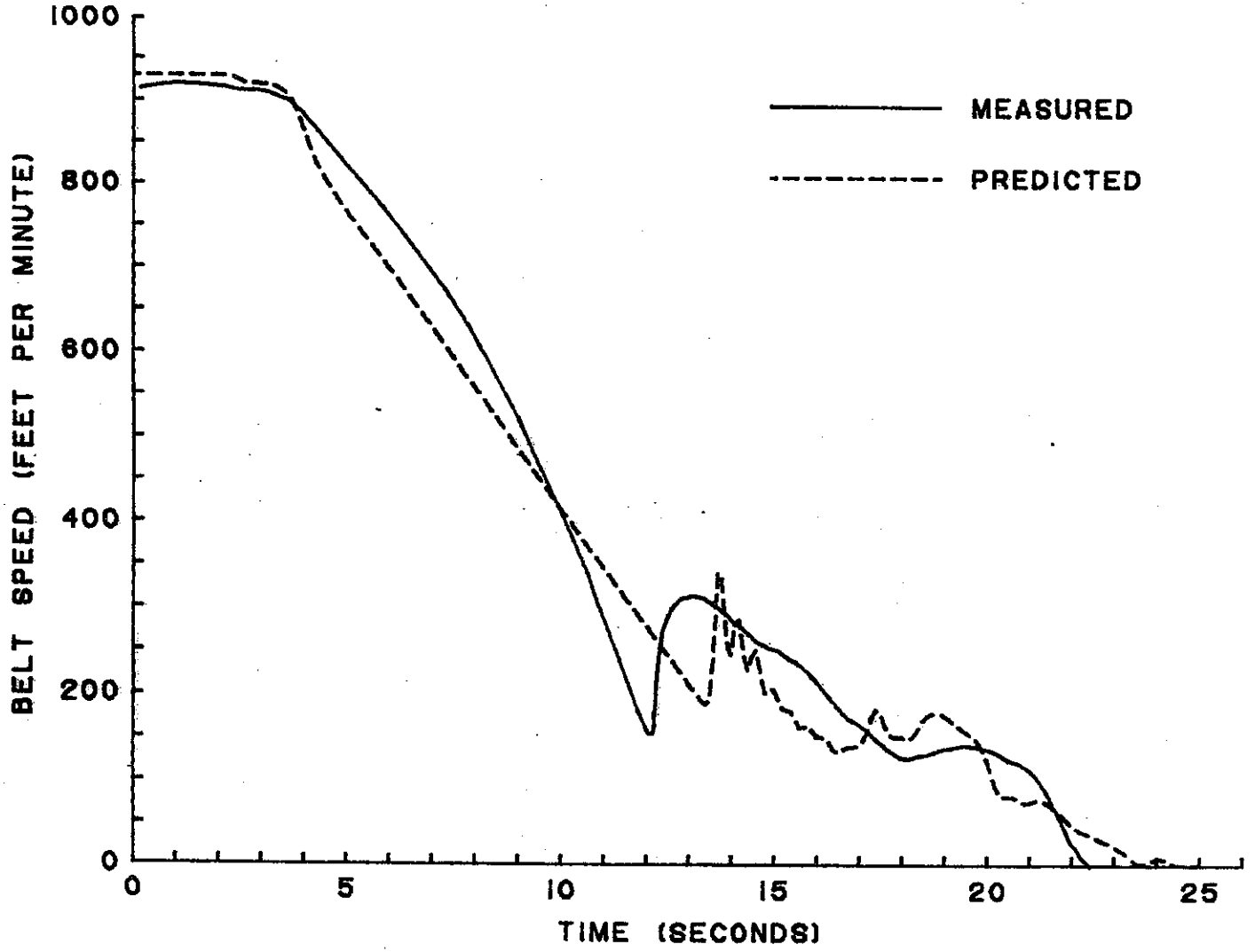

FIGURE 7 VELOCITY VS. TIME AT SHUTDOWN - POINT B

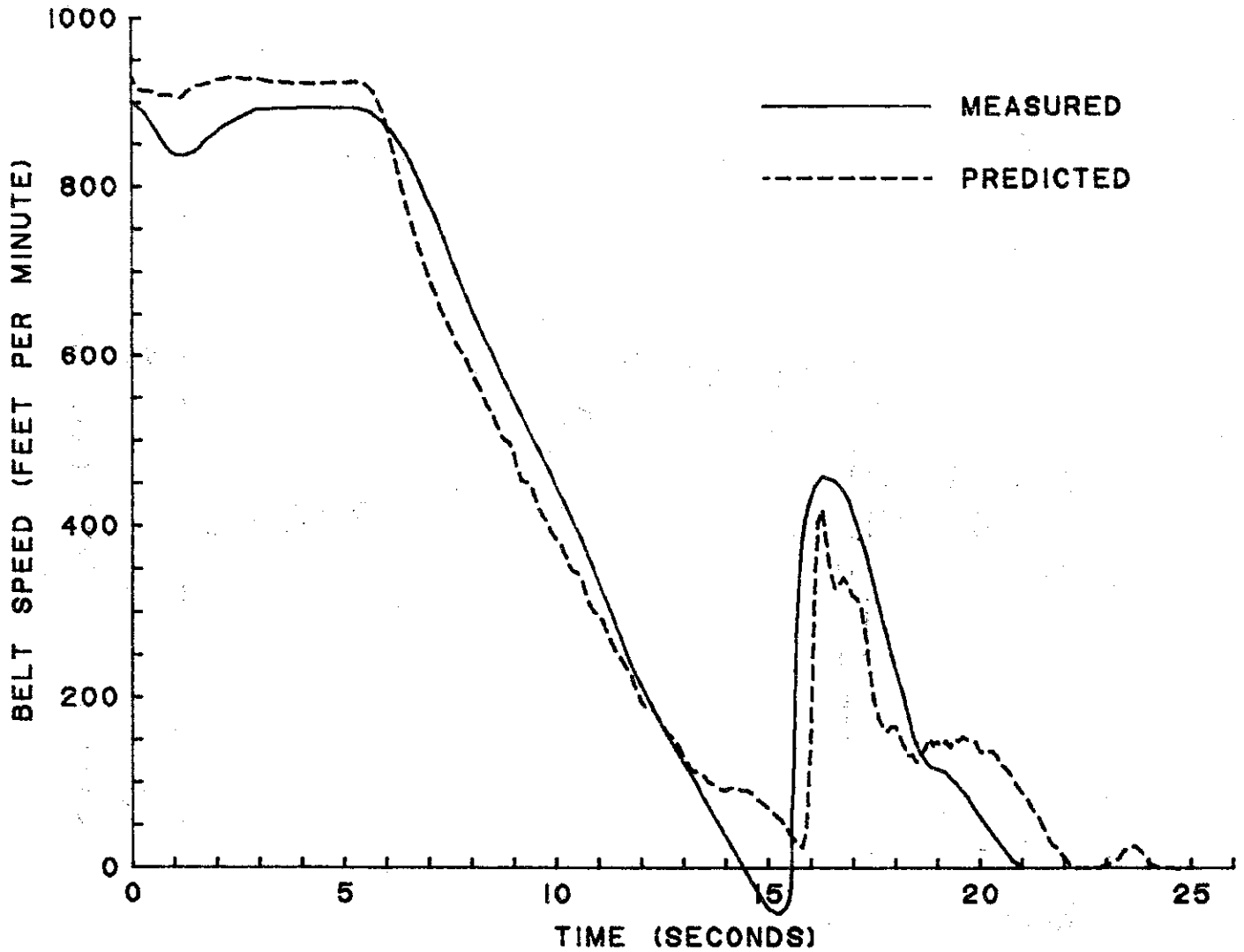

FIGURE 8 VELOCITY VS. TIME AT SHUTDOWN - POINT C

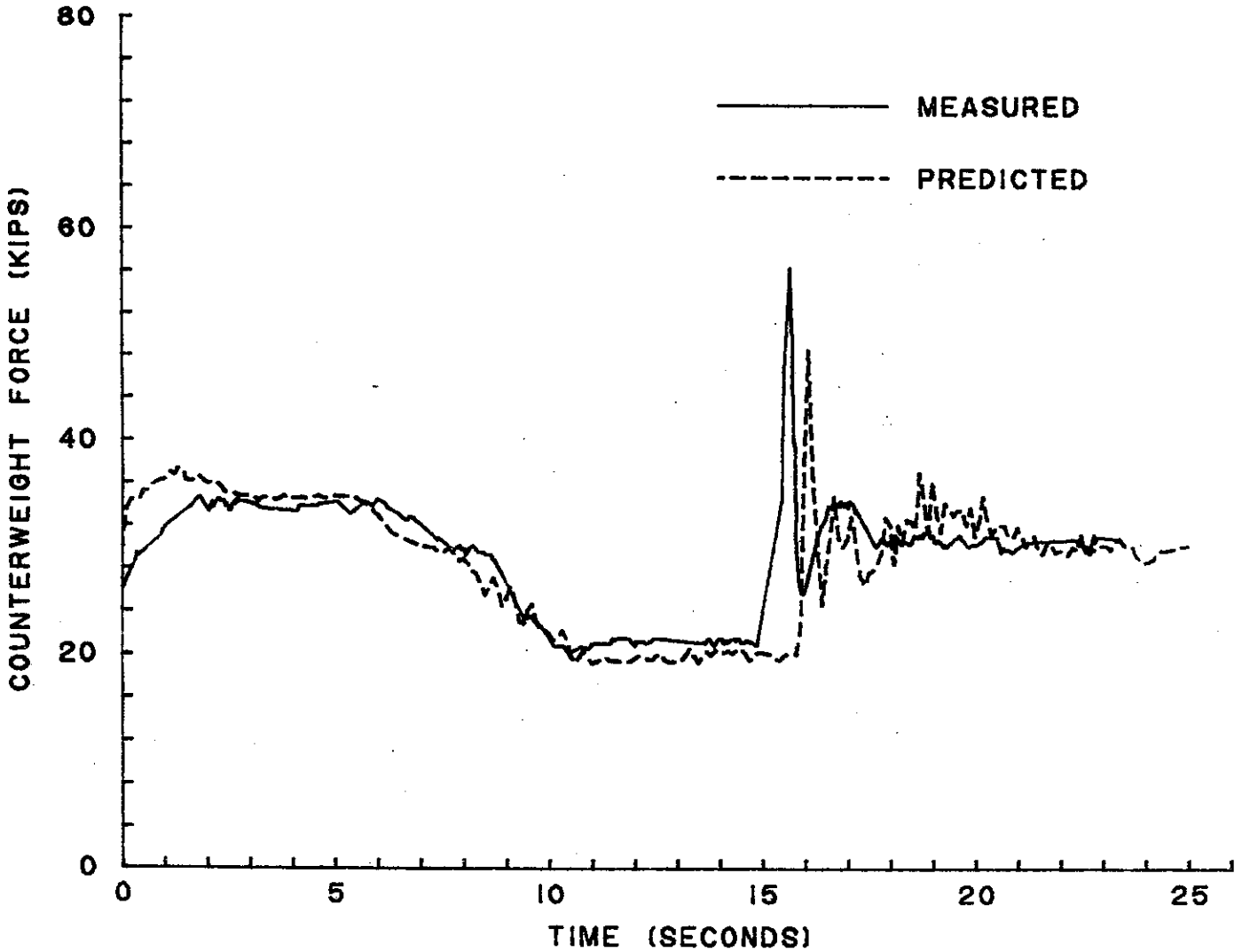

FIGURE 9 TAKEUP FORCE RESPONSE

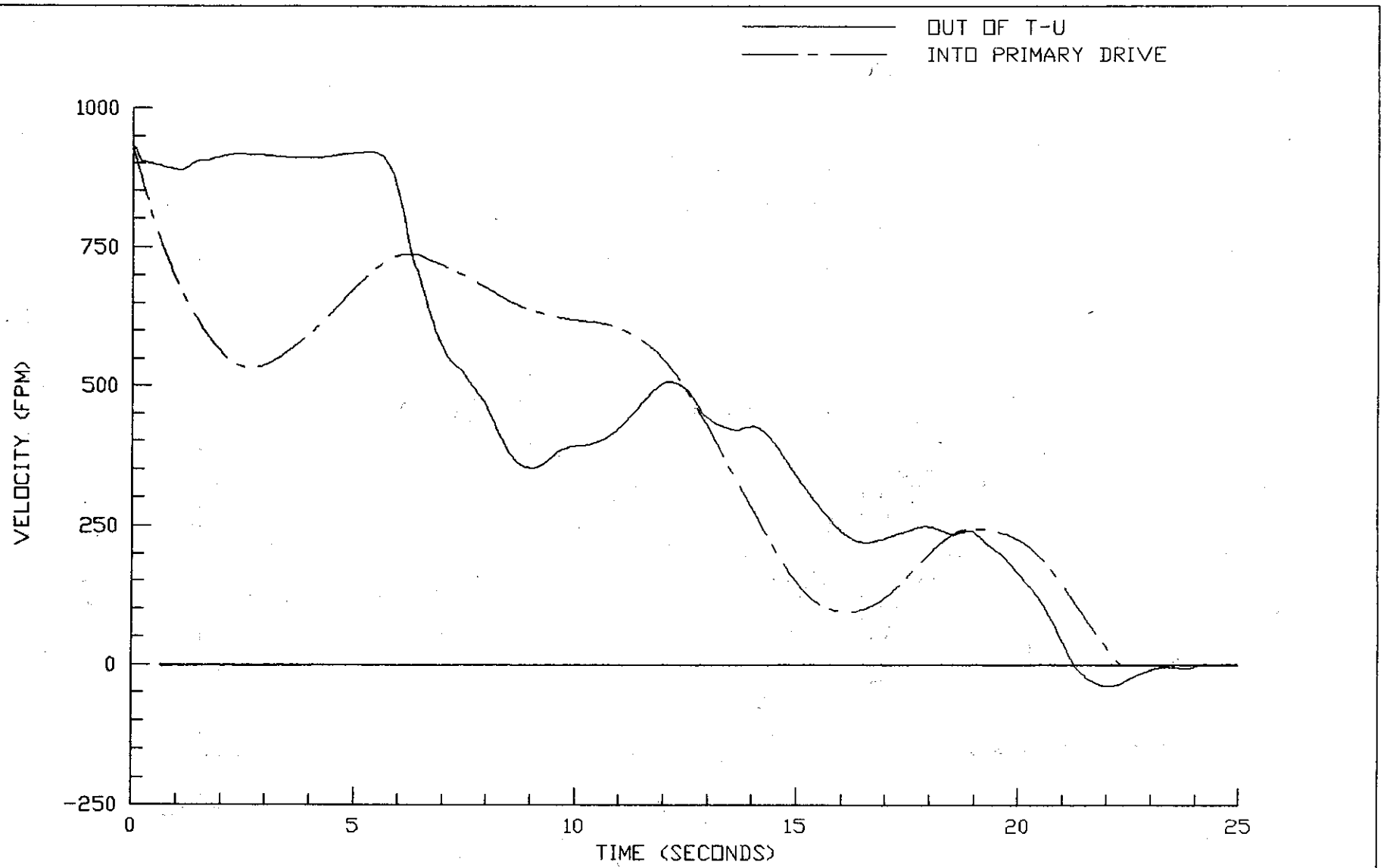

FIGURE 10A LINEAR SPRING

CLIENT: BELTCON CONFERENCE	CONV: 1		CONF1.V	BELTFLEX ANALYSIS
PROJECT: STUDY	DATE: 03-SEP-87	REV: 1	CONF1	CONVEYOR DYNAMICS, INC.

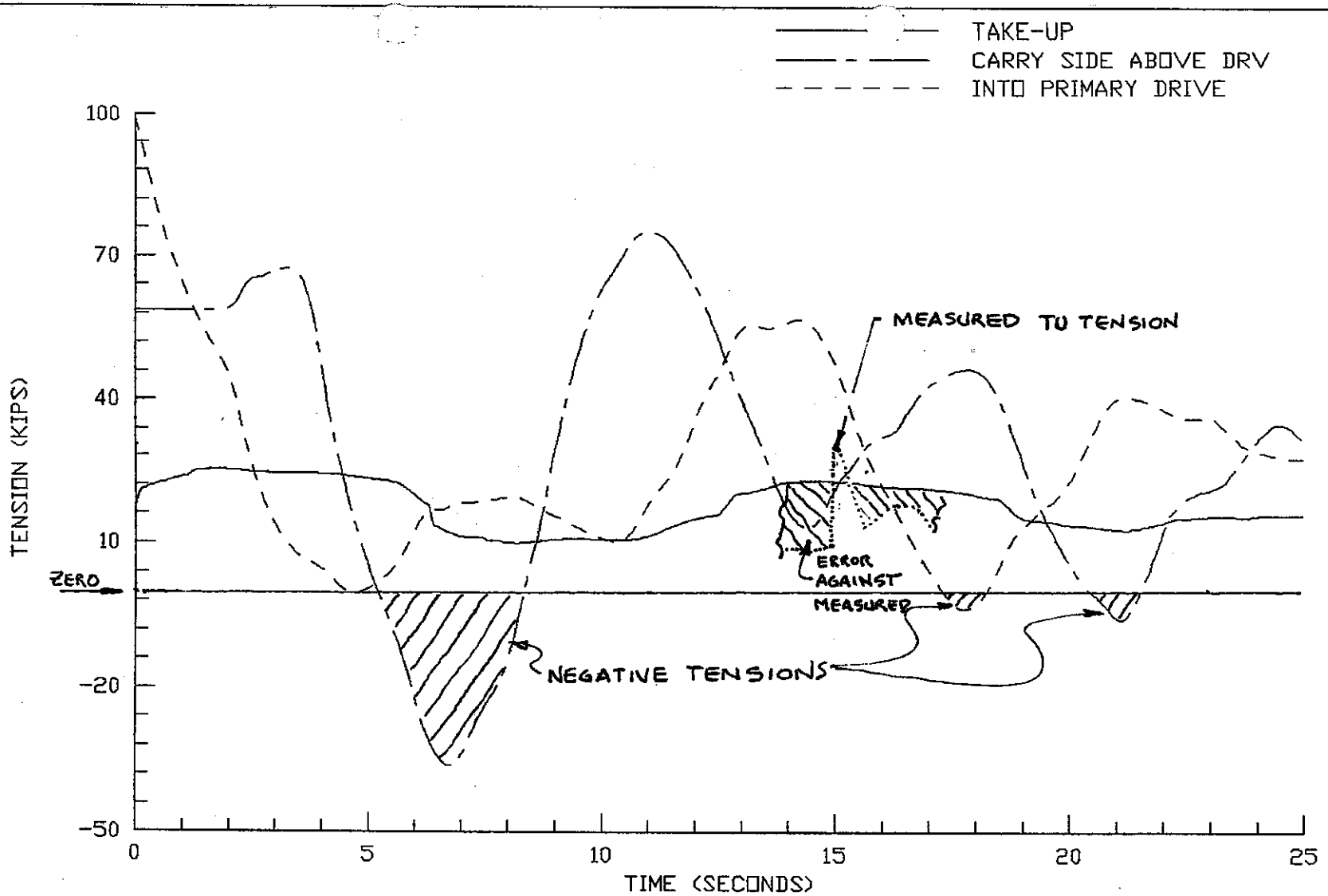

FIGURE 10B LINEAR SPRING

CLIENT: BELTCON CONFERENCE	CONV: 1		CONF1.V
PROJECT: STUDY	DATE: 03-SEP-87	REV: 1	CONF1

BELTFLEX ANALYSIS
CONVEYOR DYNAMICS, INC.

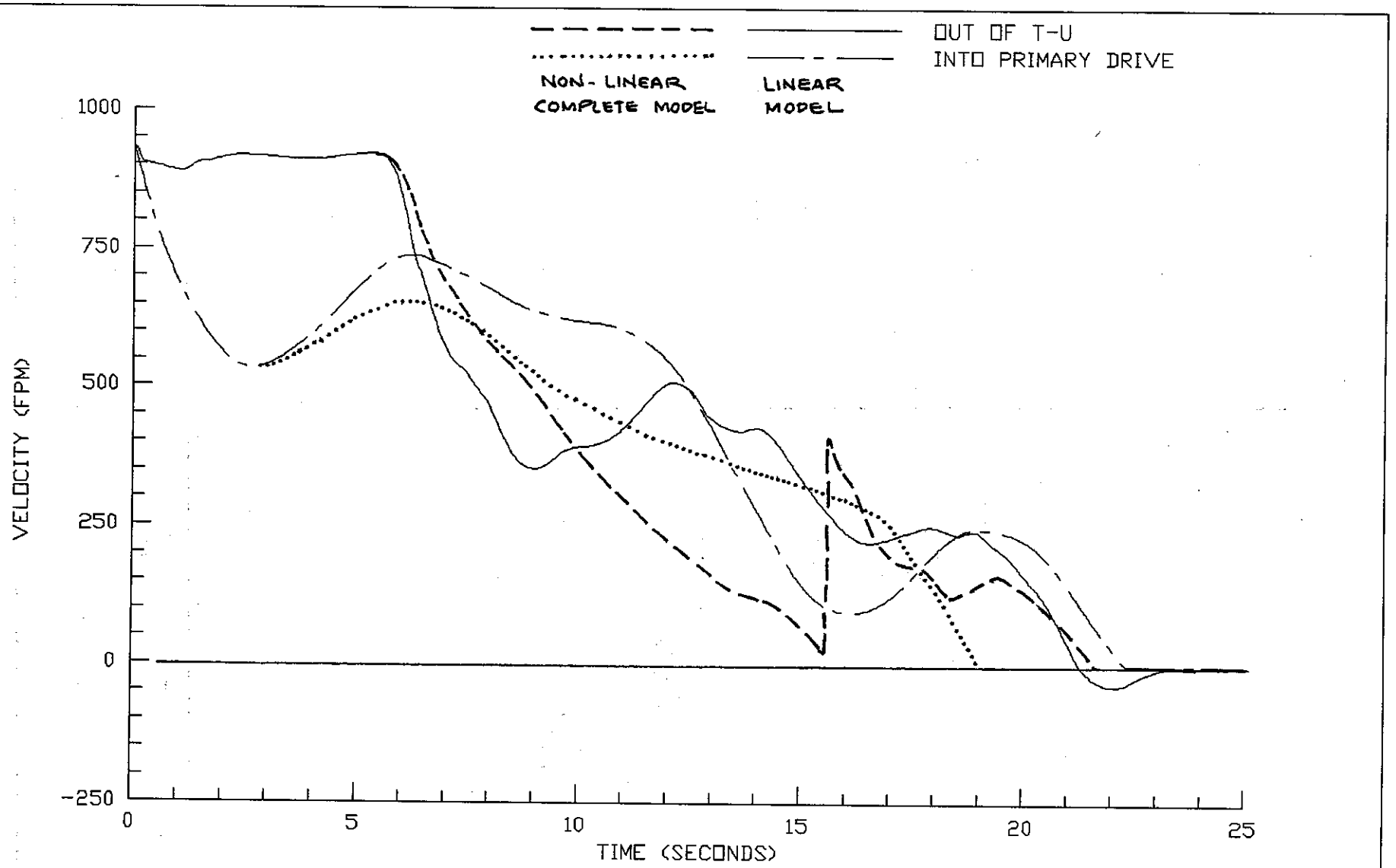

FIGURE 11 LINEAR VS NON-LINEAR SPRING

CLIENT: BELTCON CONFERENCE	CONV: 1		CONF1.V	BELTFLEX ANALYSIS
PROJECT: STUDY	DATE: 03-SEP-87	REV: 1	CONF1	CONVEYOR DYNAMICS, INC.

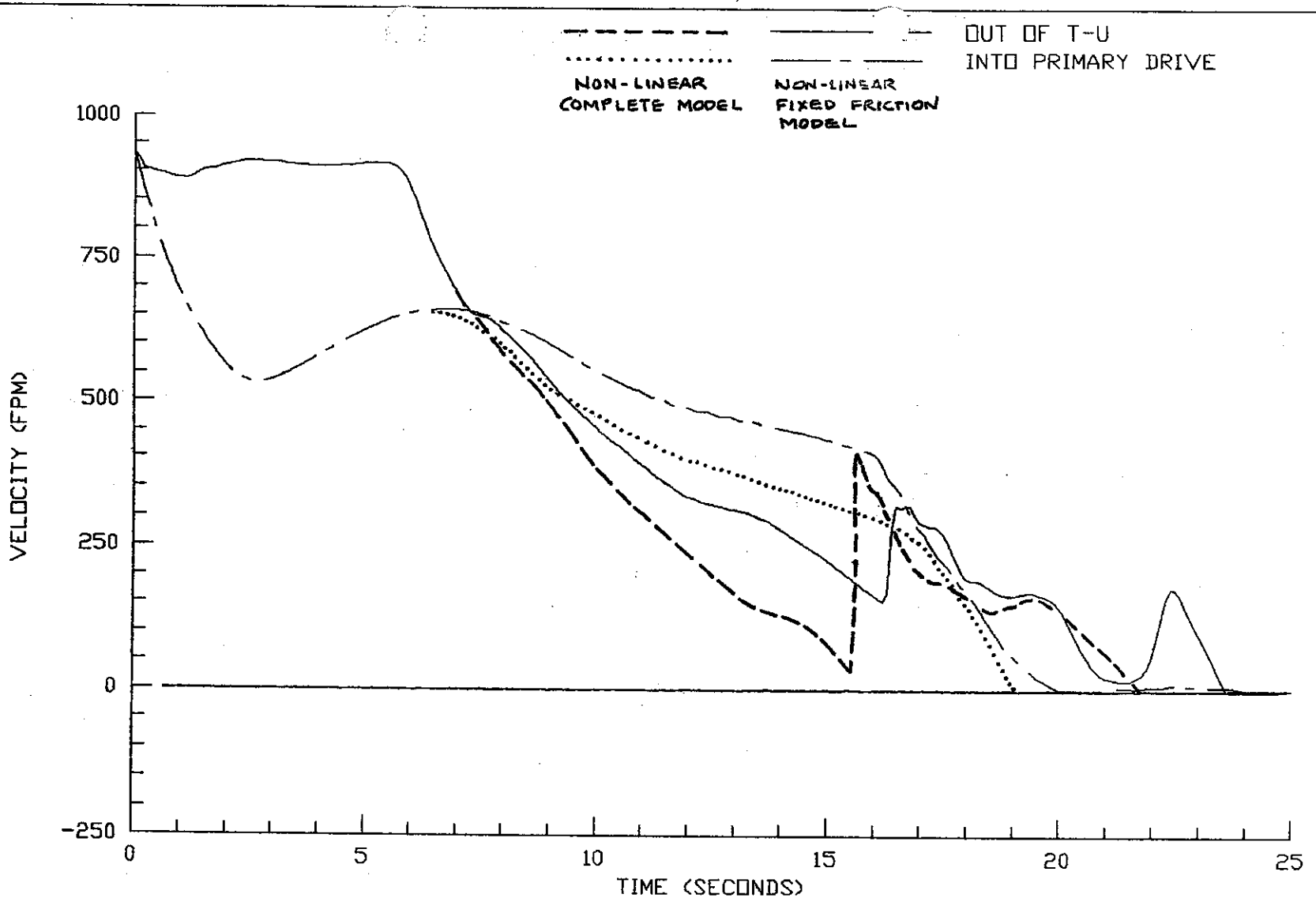

FIGURE 12A NON-LINEAR SPRING WITH FIXED FRICTION

CLIENT: BELTCON CONFERENCE	CONV: 1		VB6
PROJECT: STUDY	DATE: 03-SEP-87	REV: 1	CONF1

BELTFLEX ANALYSIS
CONVEYOR DYNAMICS, INC.

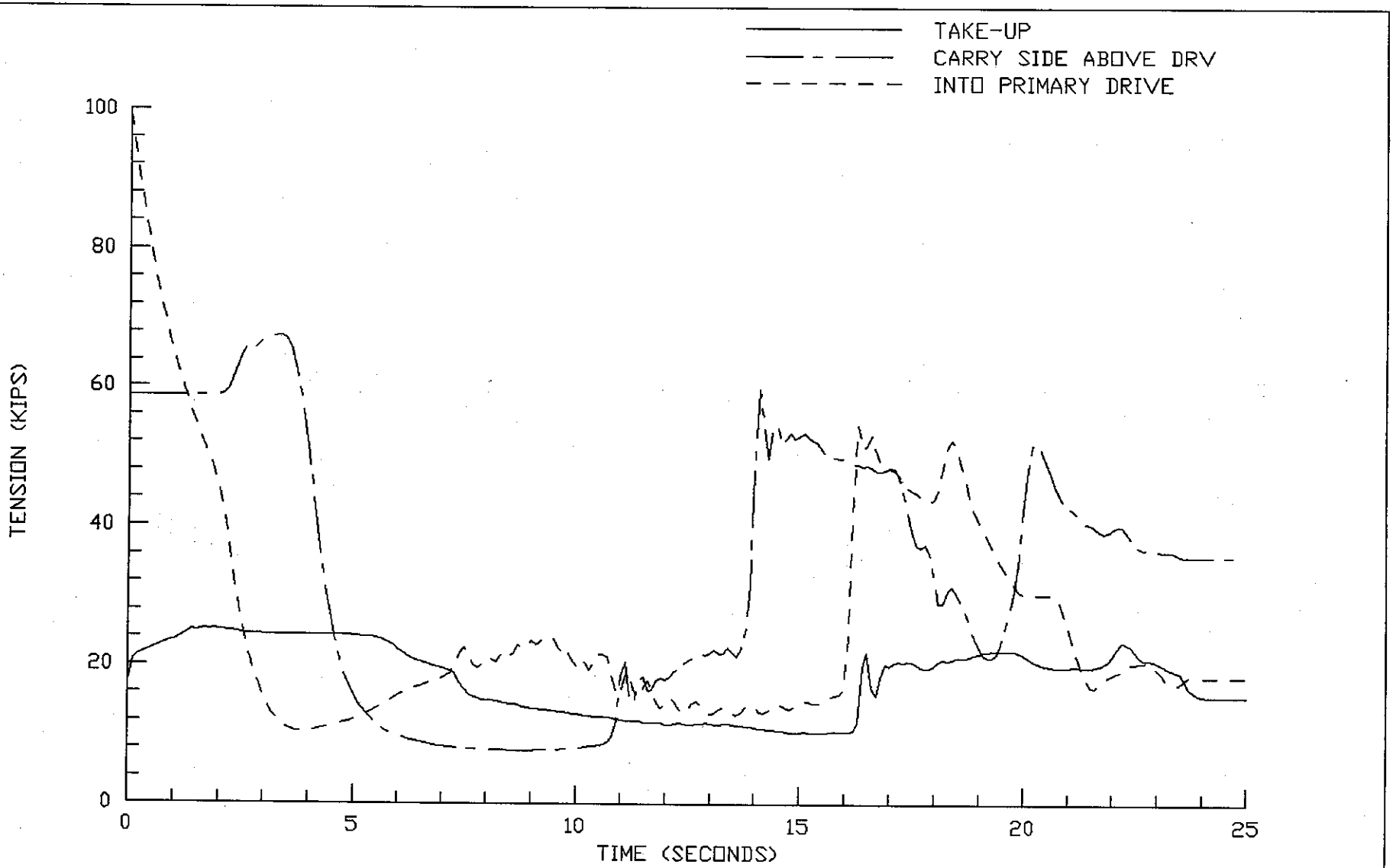

FIGURE 12 B NON-LINEAR SPRING WITH FIXED FRICTION

CLIENT: BELTCON CONFERENCE	CONV: 1		VB6	BELTFLEX ANALYSIS
PROJECT: STUDY	DATE: 03-SEP-87	REV: 1	CONF1	CONVEYOR DYNAMICS, INC.

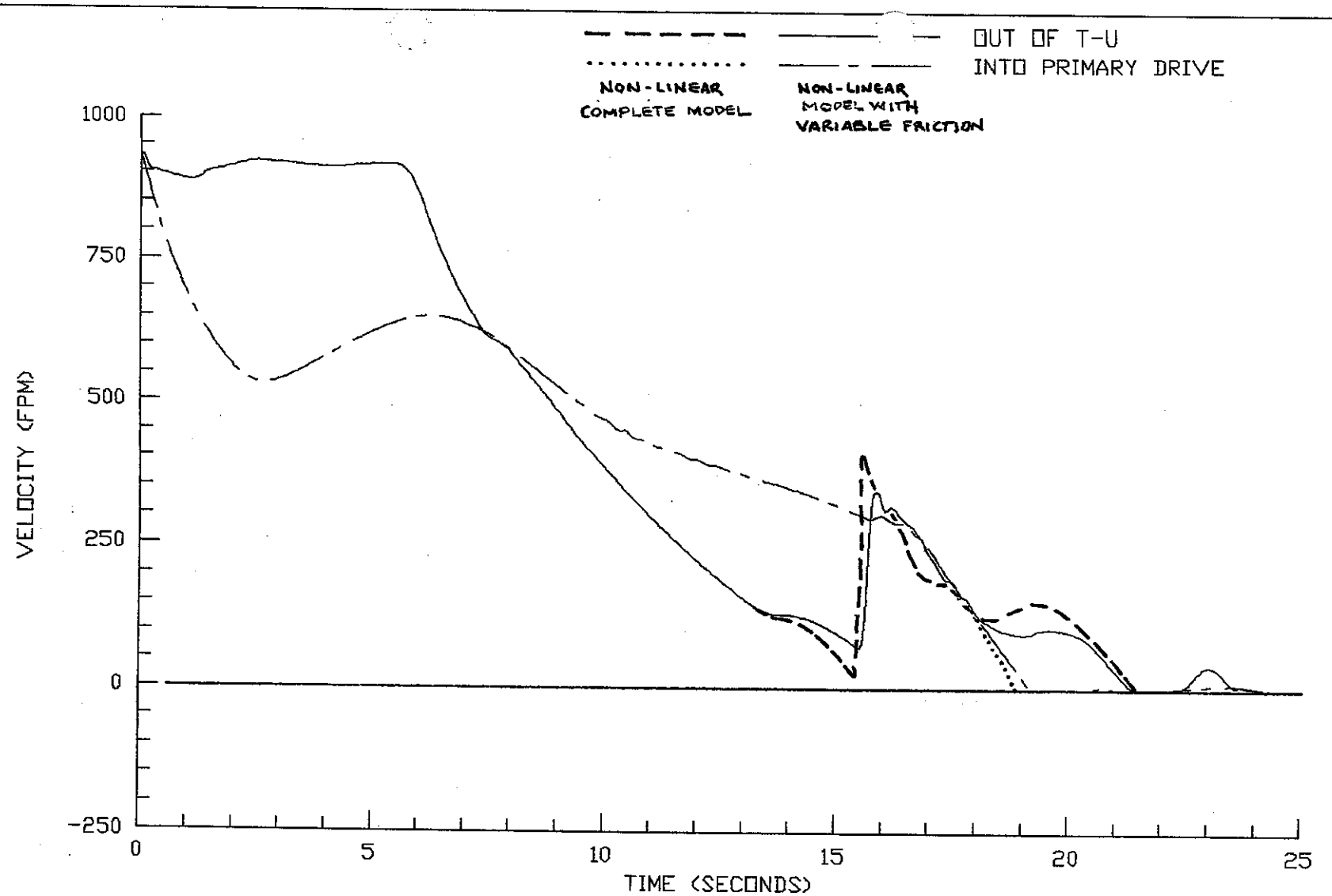

FIGURE 13A NON-LINEAR SPRING WITH VARIABLE FRICTION

CLIENT: BELTCON CONFERENCE	CONV: 1		VB8	BELTFLEX ANALYSIS CONVEYOR DYNAMICS, INC.
PROJECT: STUDY	DATE: 03-SEP-87	REV: 1	CONF1	

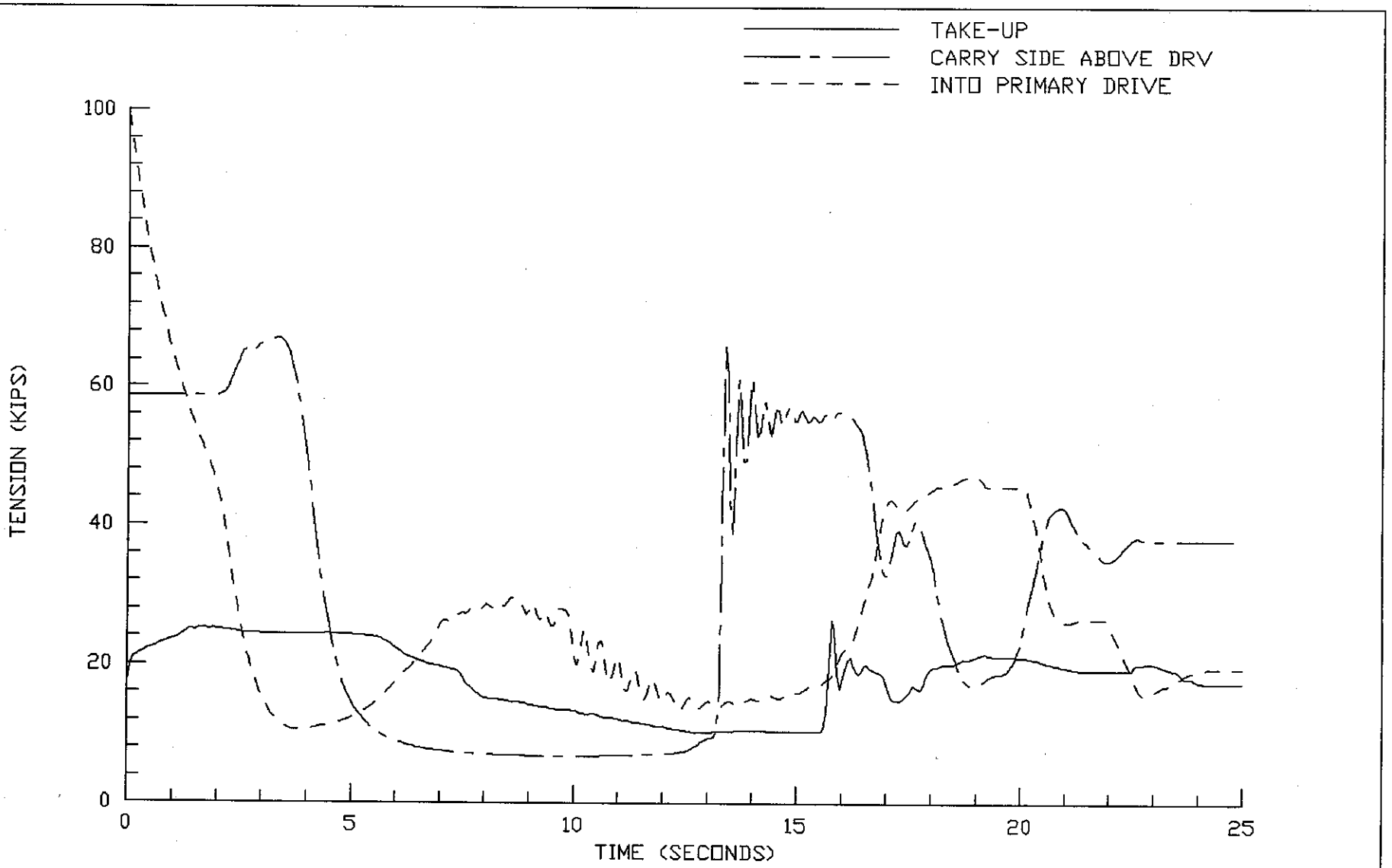

FIGURE 13B NON-LINEAR SPRING WITH VARIABLE FRICTION

CLIENT: BELTCON CONFERENCE	CONV: 1		VB8	BELTFLEX ANALYSIS
PROJECT: STUDY	DATE: 03-SEP-87	REV: 1	CONF1	CONVEYOR DYNAMICS, INC.

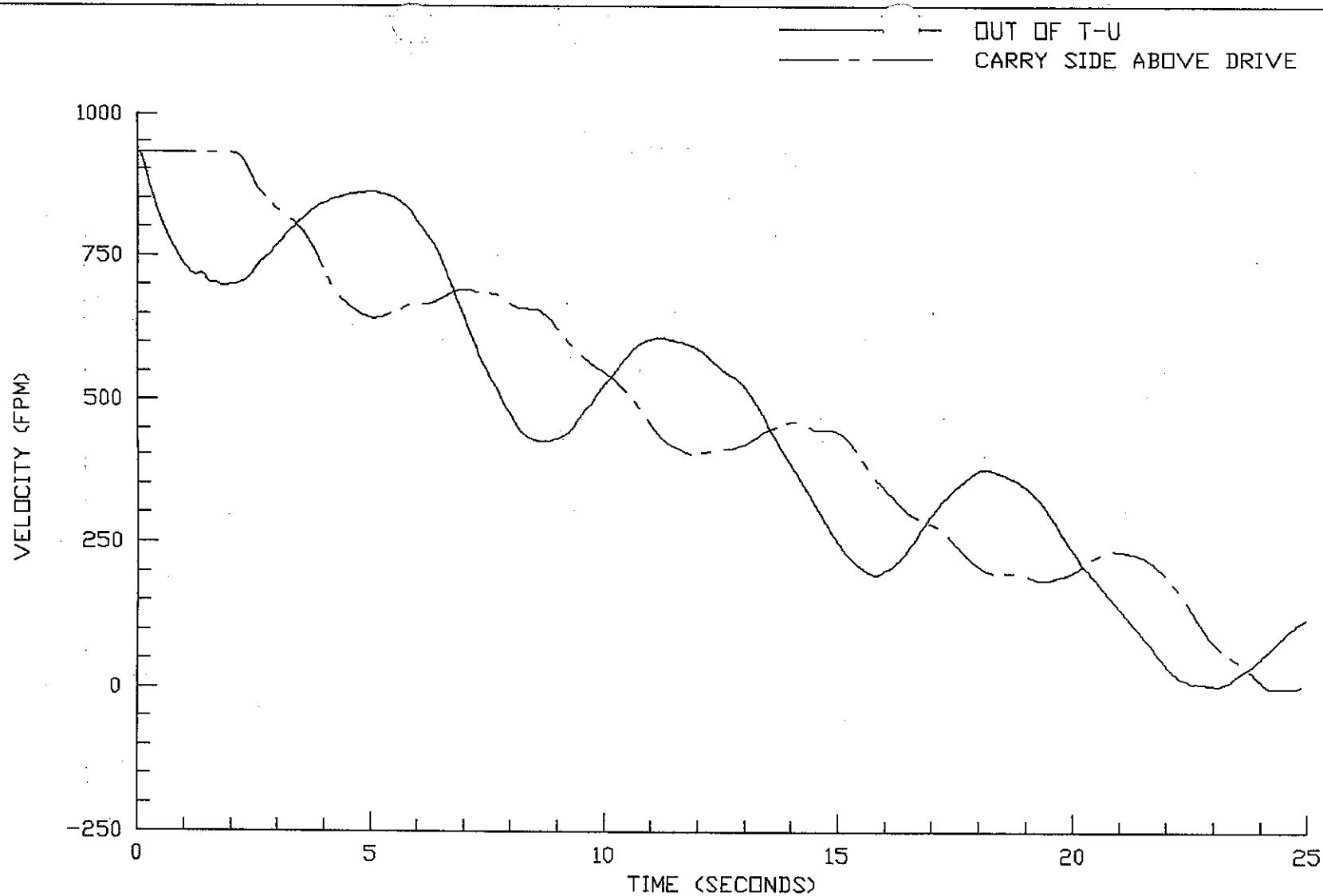

FIGURE 14A NON-LINEAR SPRING WITH FIXED TAKE-UP

CLIENT: BELTCON CONFERENCE	CONV: 1		VB4	BELTFLEX ANALYSIS
PROJECT: STUDY	DATE: 03-SEP-87	REV: 1	CONF1	CONVEYOR DYNAMICS, INC.

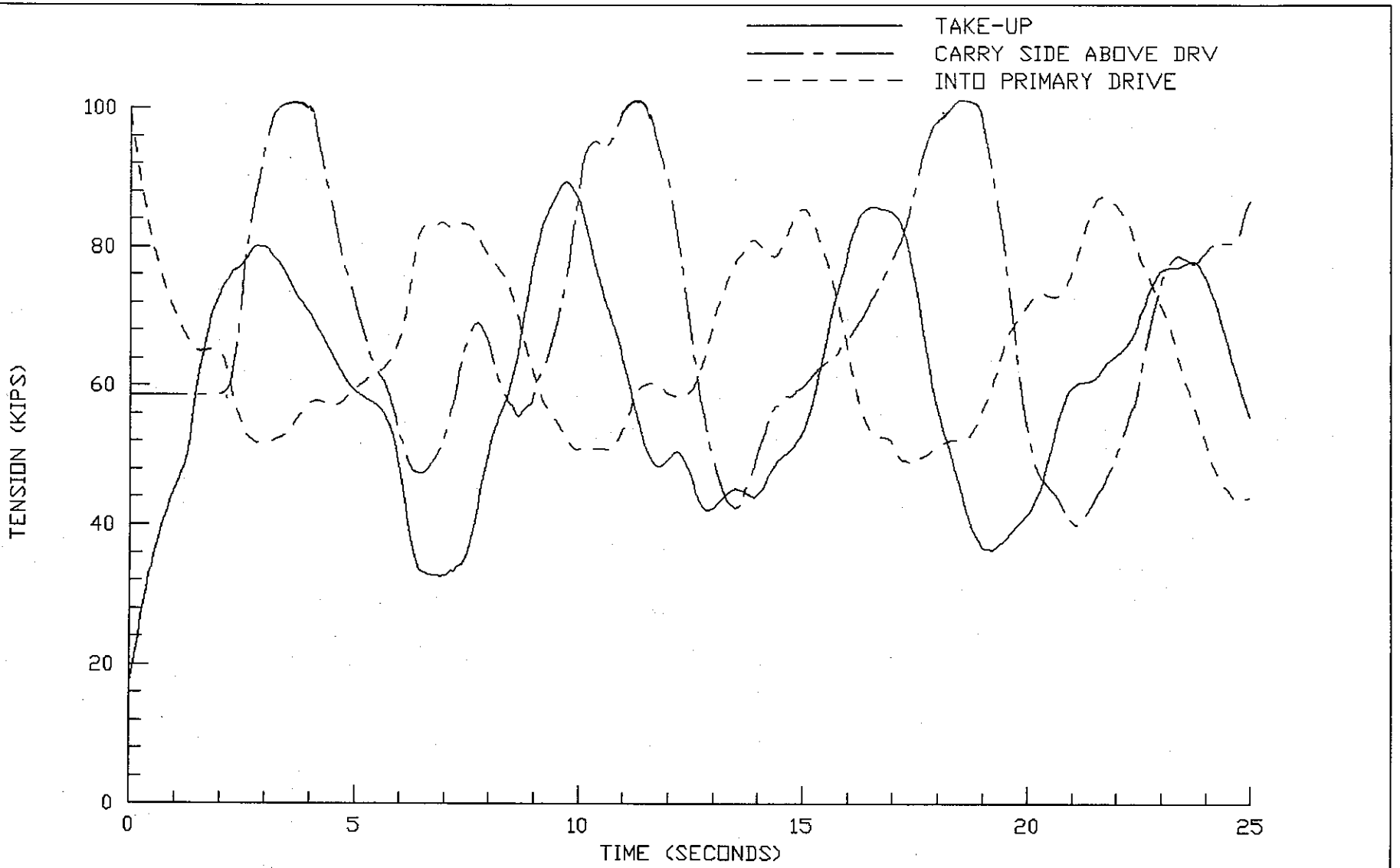

FIGURE 14B NON-LINEAR SPRING WITH FIXED TAKE-UP

CLIENT: BELTCON CONFERENCE	CONV: 1		VB4	BELTFLEX ANALYSIS
PROJECT: STUDY	DATE: 02-SEP-87	REV: 1	CONF1	CONVEYOR DYNAMICS, INC.

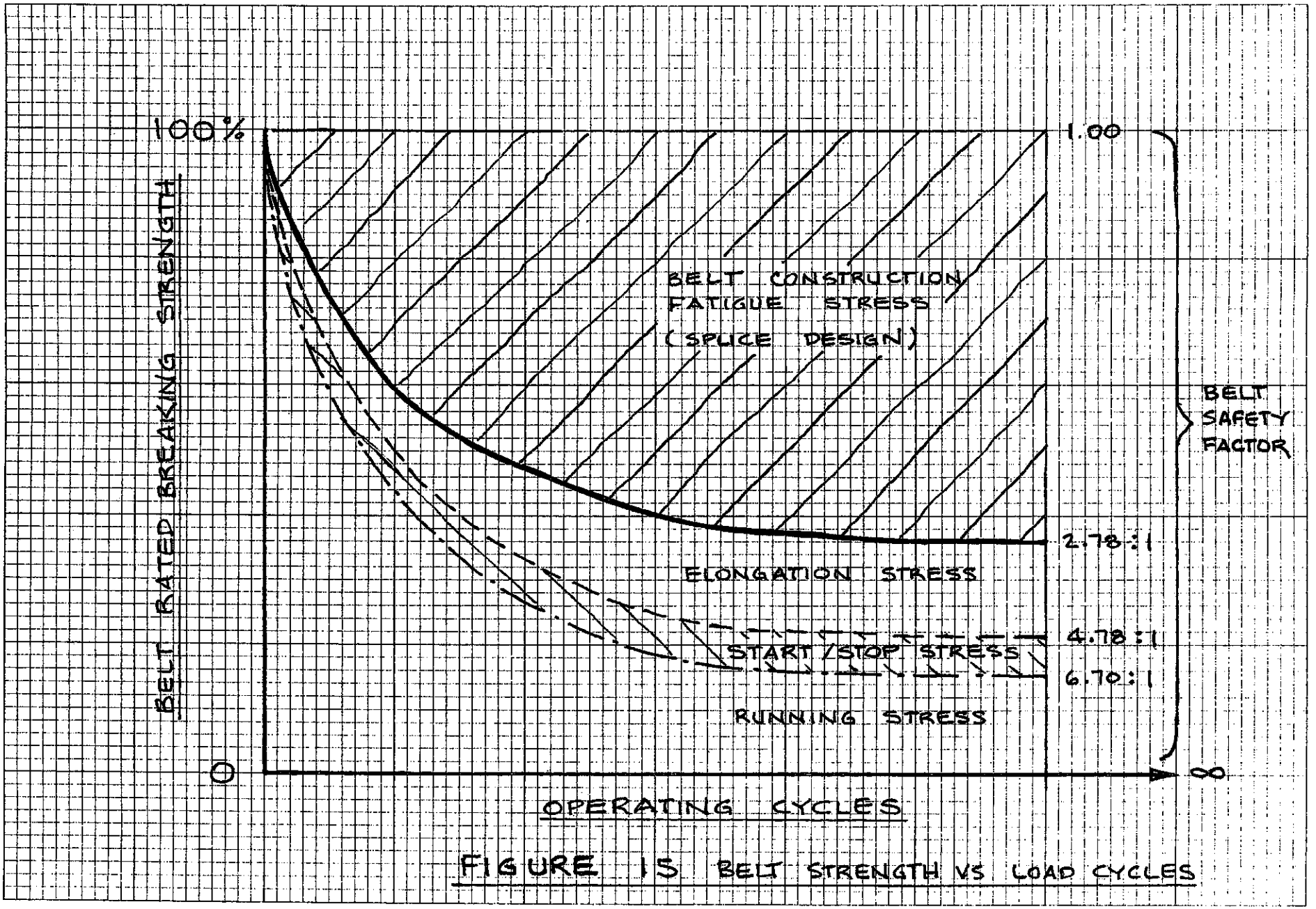

FIGURE 15 BELT STRENGTH VS LOAD CYCLES

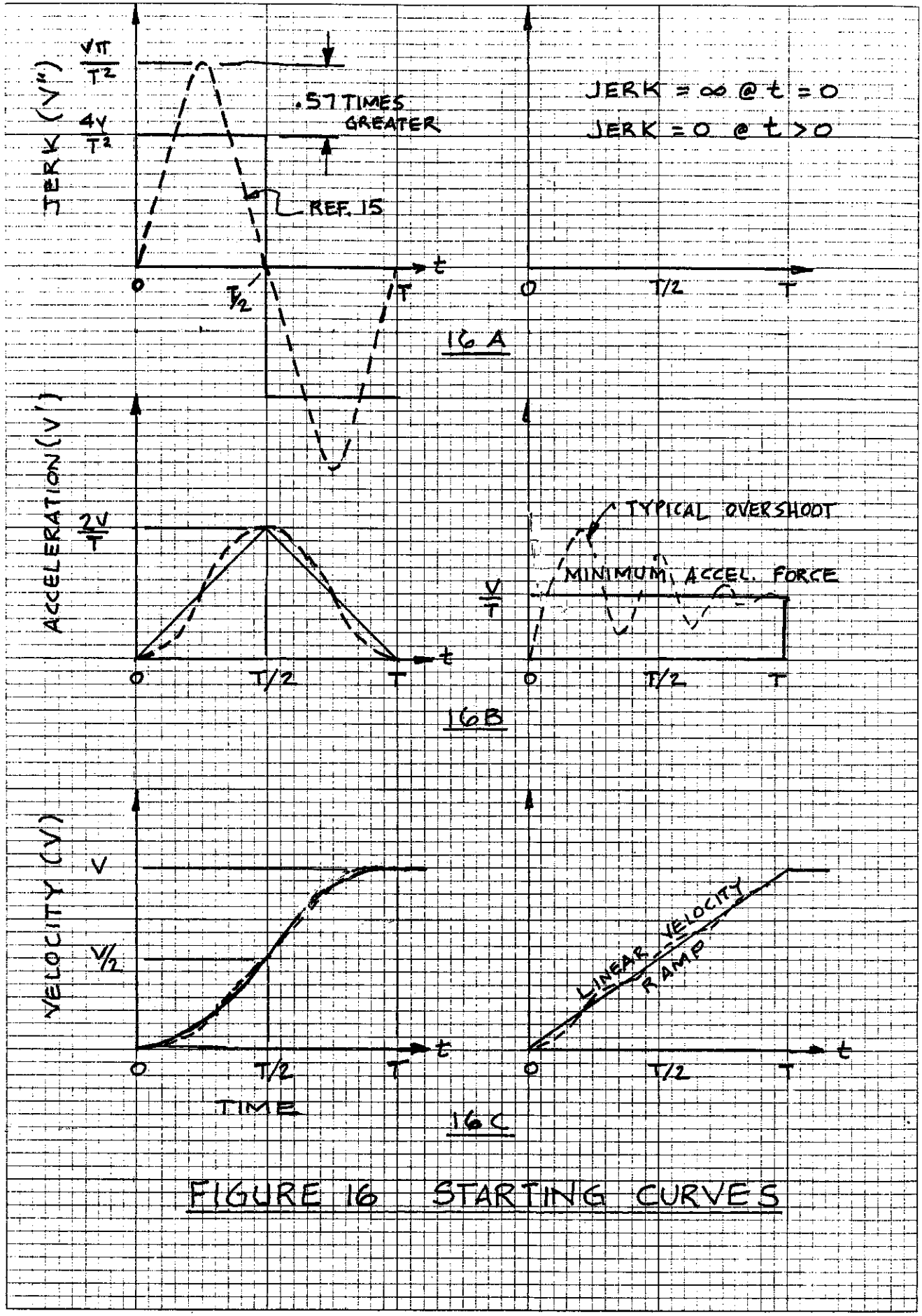

FIGURE 16 STARTING CURVES

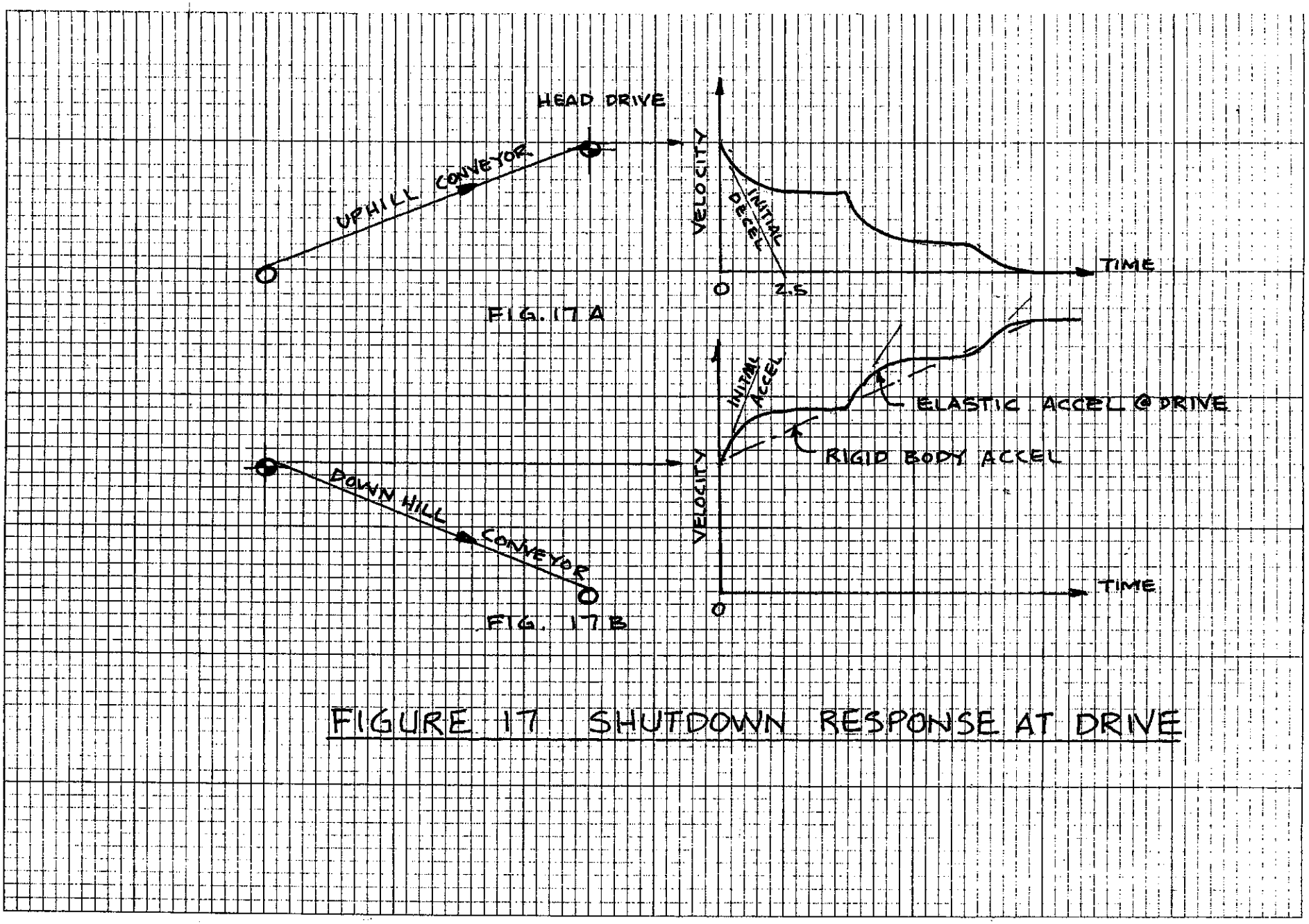

FIGURE 17 SHUTDOWN RESPONSE AT DRIVE

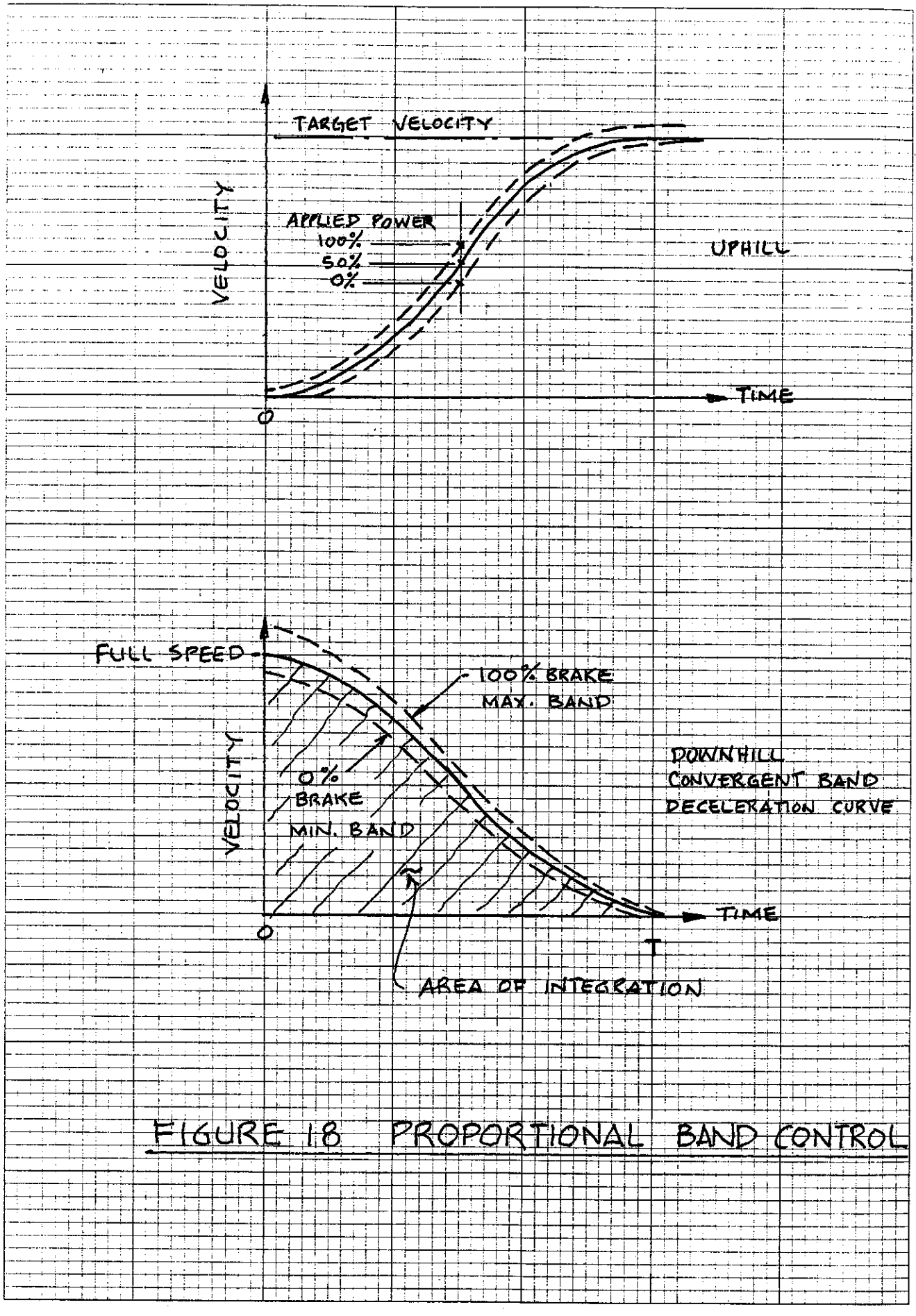

FIGURE 18 PROPORTIONAL BAND CONTROL

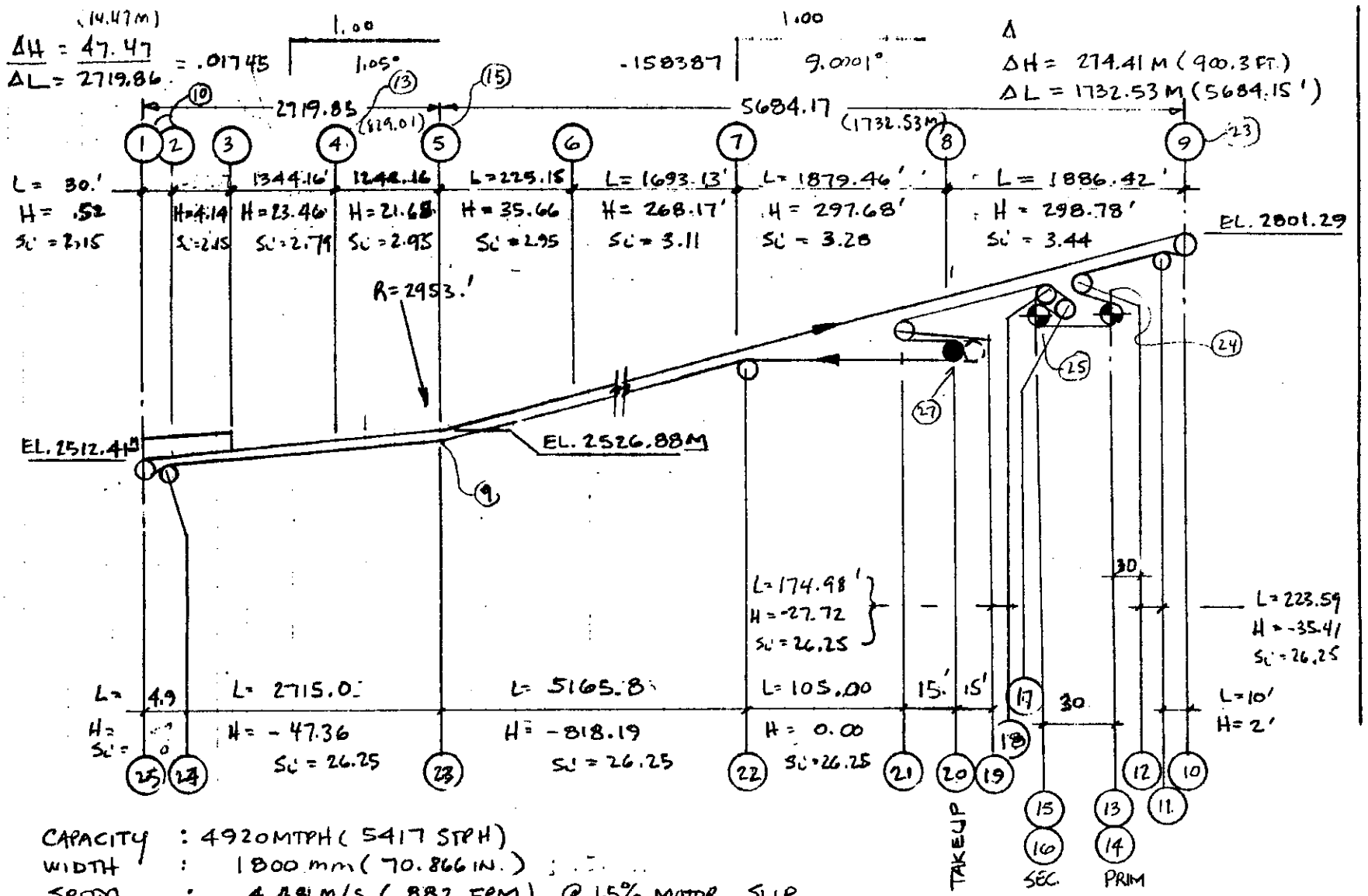

CUSTOMER:

ADDRESS:

S.O. NO.

DATE 10/20/84

CAPACITY : 4920MTPH (5417 STPH)
WIDTH : 1800 mm (70.866 IN.)
SPEED : 4.48 M/S (882 FPM) @ 1.5% MOTOR SLIP
DENSITY : 110 PCF
GEAR RATIO : 21.32:1
MATL : 8" x 0 COPPER ORE

FIGURE 19 PROFILE

FIGURE 20 TENSION vs TIME

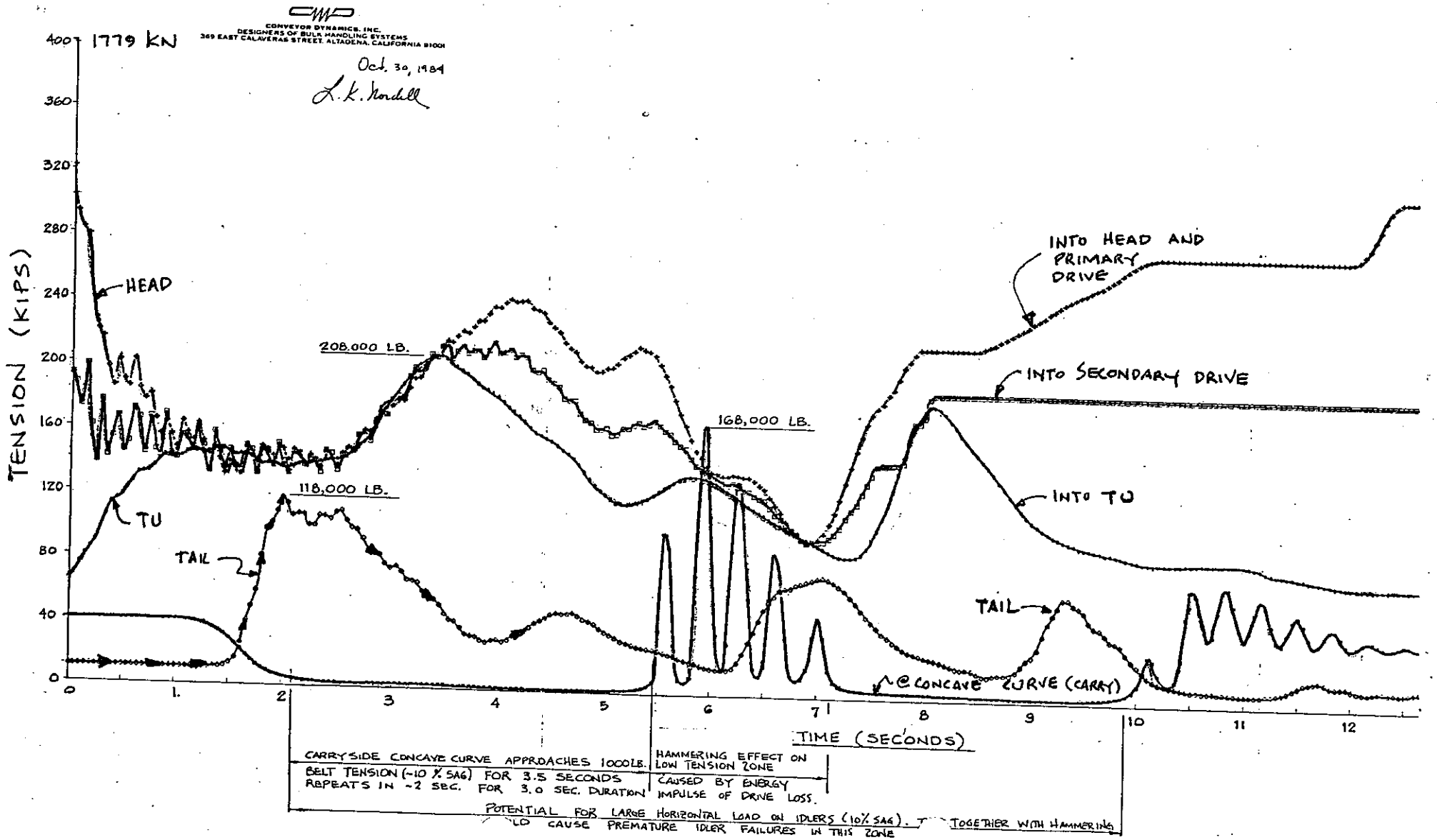

FIGURE 21 VELOCITY VS TIME

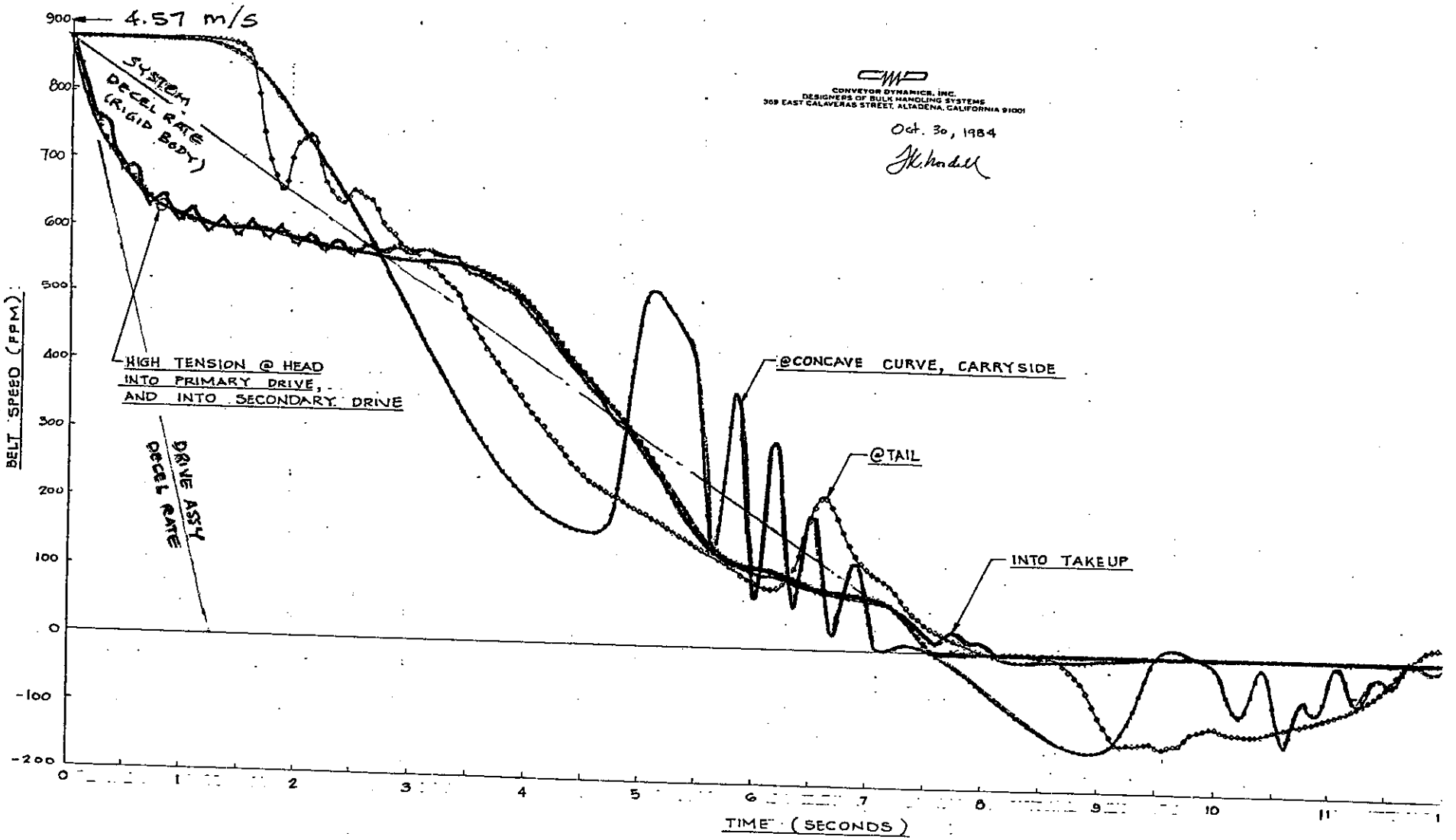

CONVEYOR DYNAMICS, INC.
DESIGNERS OF BULK HANDLING SYSTEMS
359 EAST CALAVERAS STREET, ALTADENA, CALIFORNIA 91001

Oct. 30, 1984

JK Nordell

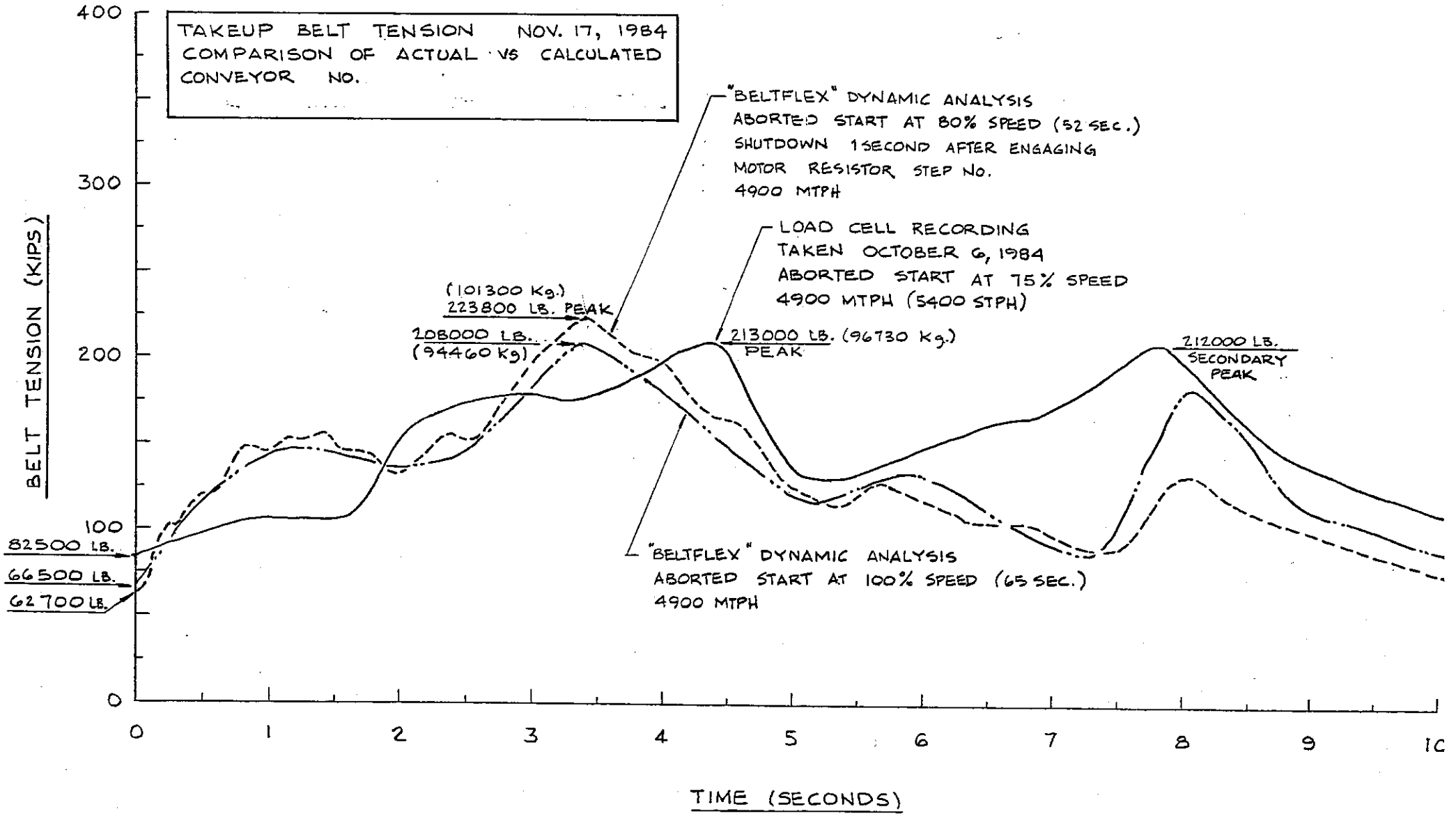

FIGURE 22 : TAKEUP TENSION VERSUS TIME CURVE

CONVEYOR DYNAMICS, INC.

TITLE _____ SHEET NO. _____ OF _____

JOB NO. BELTSTAR/BELTFLEX DEPARTMENT _____ AUTHOR Z. P. CIOZDA / NKOCH DATE NOV. 28, 84

REV	CHECKER	DATE	REV	CHECKER	DATE	REV	CHECKER	DATE

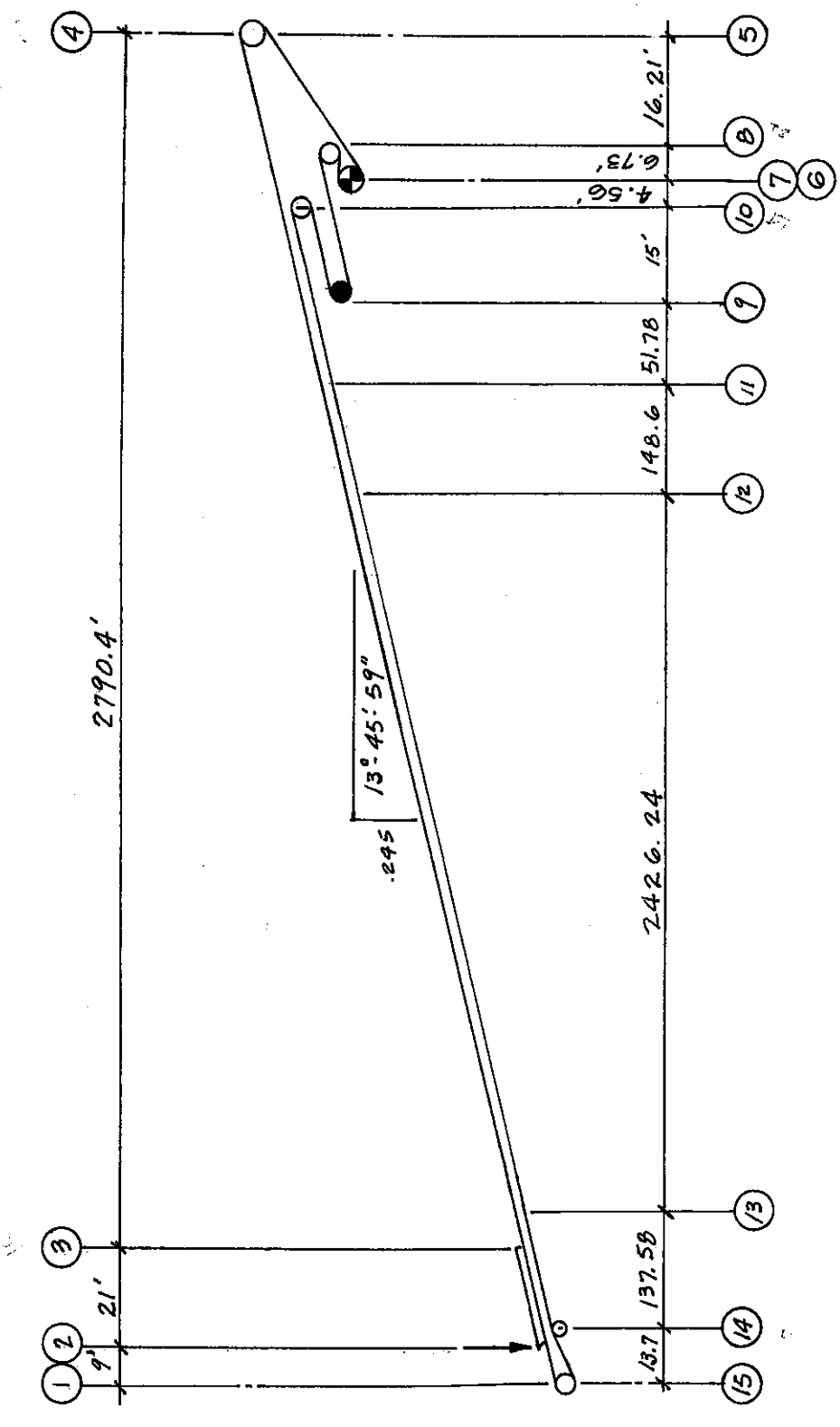

CAPACITY : 4000 STPH (3636 T/H)
BELT SPEED : 822 FPM (4.2 M/S)
MATERIAL : COPPER ORE
POWER : 4000 HP (3000 KW)

FIGURE 23 PROFILE STUDY NO. 2

REF: DWG # D-1258-040-1715, REV. B
D-1258-040-1714, REV. B

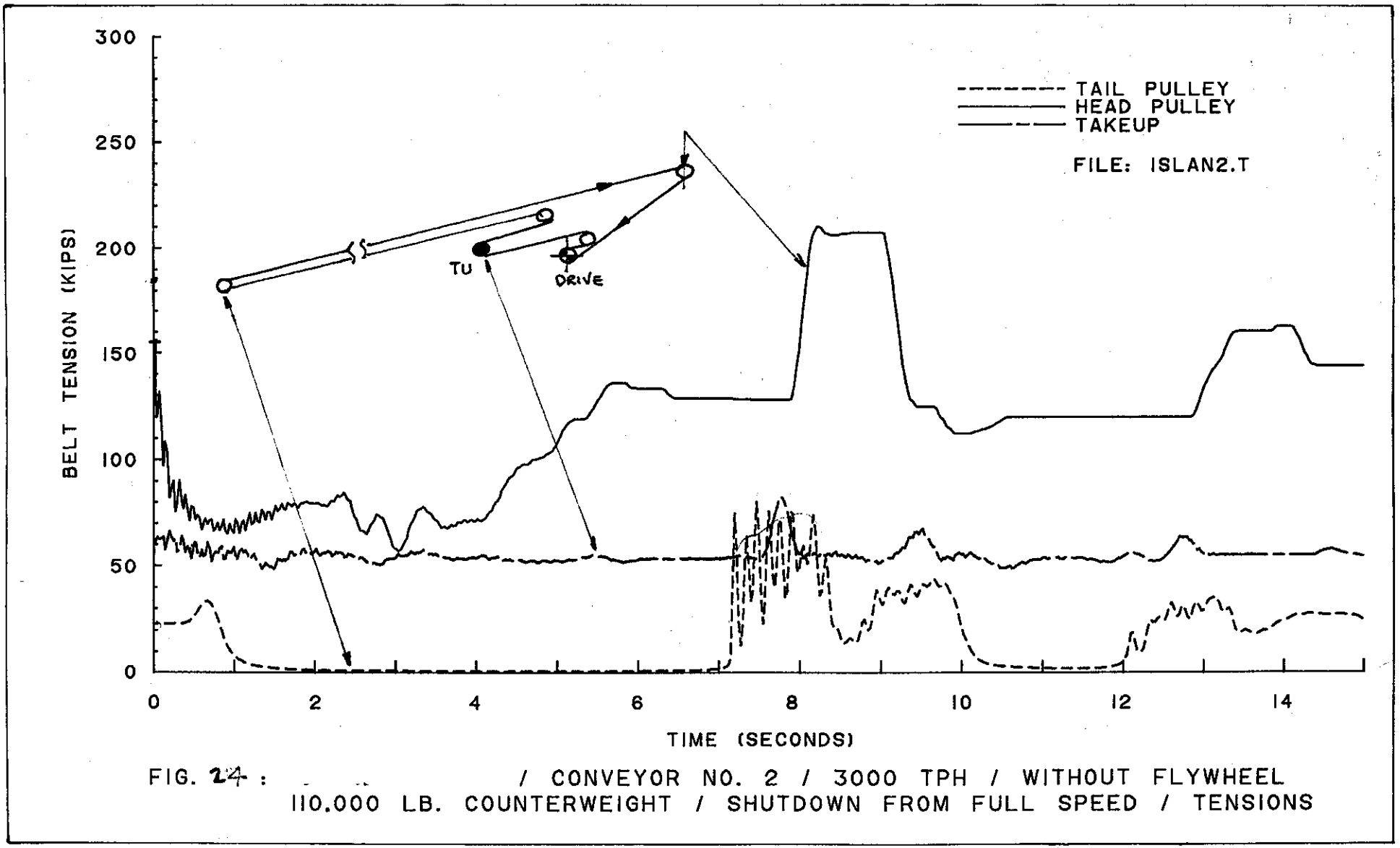

FIG. 24 : / CONVEYOR NO. 2 / 3000 TPH / WITHOUT FLYWHEEL
110.000 LB. COUNTERWEIGHT / SHUTDOWN FROM FULL SPEED / TENSIONS

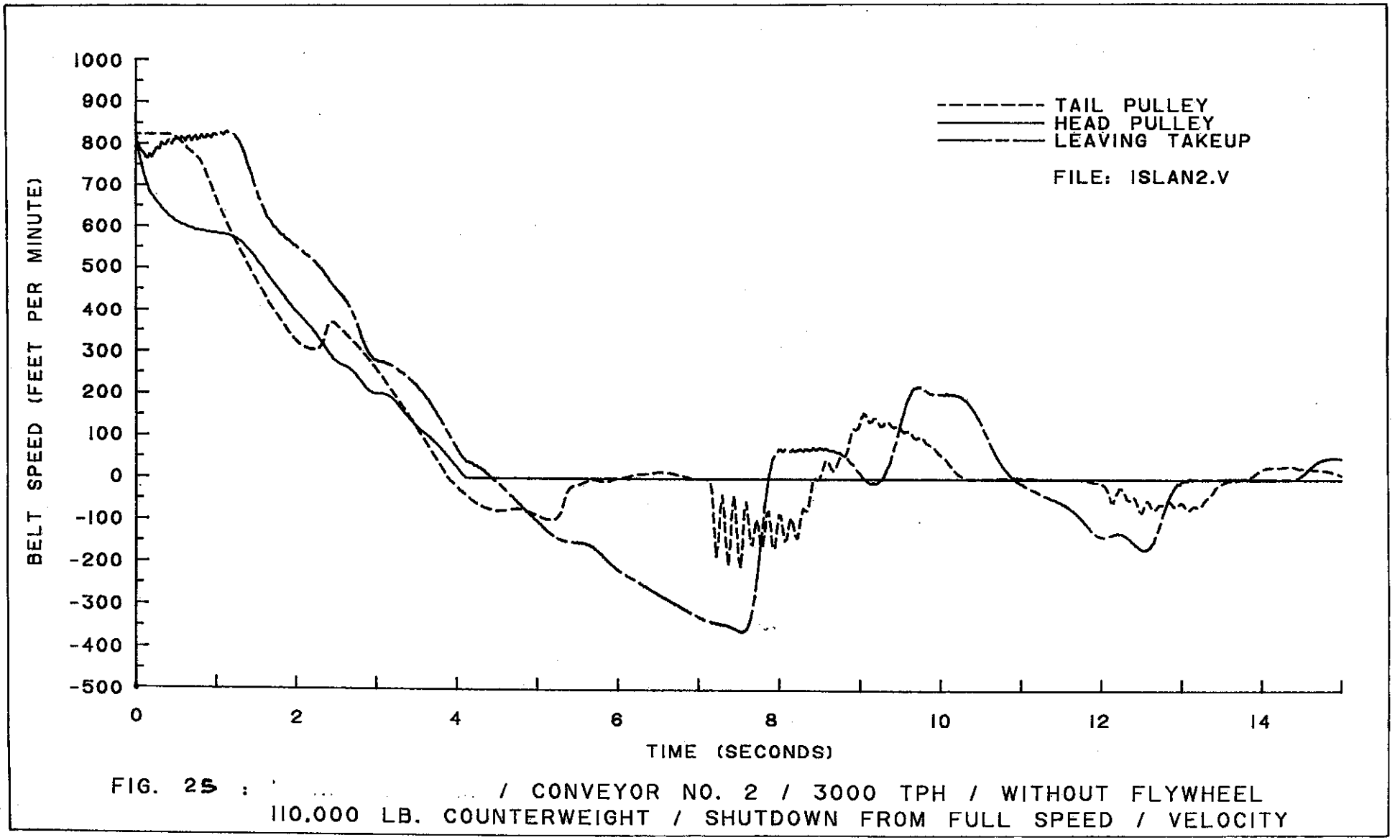

FIG. 25 : ... / CONVEYOR NO. 2 / 3000 TPH / WITHOUT FLYWHEEL
110.000 LB. COUNTERWEIGHT / SHUTDOWN FROM FULL SPEED / VELOCITY

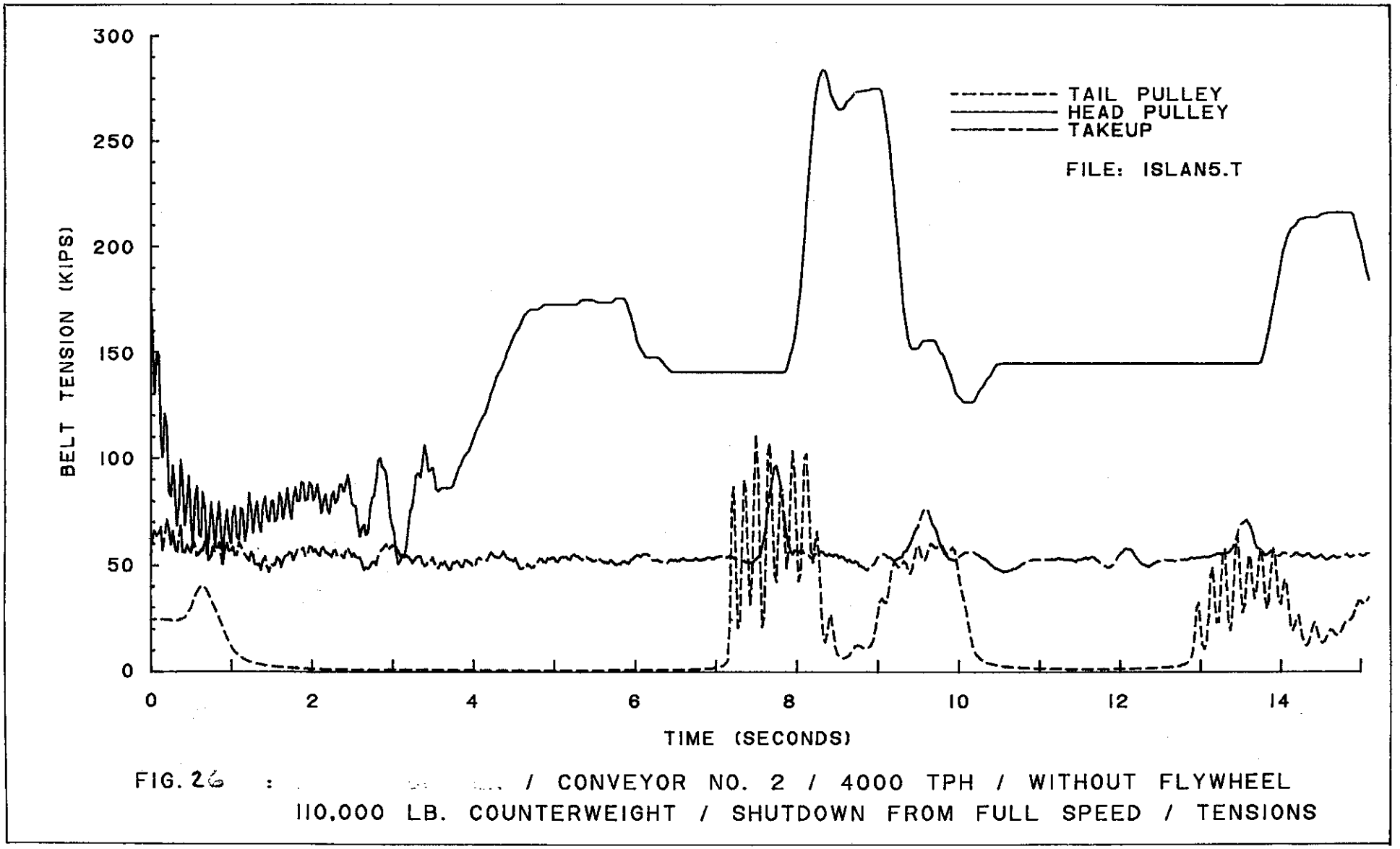

FIG. 26 : ... / CONVEYOR NO. 2 / 4000 TPH / WITHOUT FLYWHEEL
110,000 LB. COUNTERWEIGHT / SHUTDOWN FROM FULL SPEED / TENSIONS

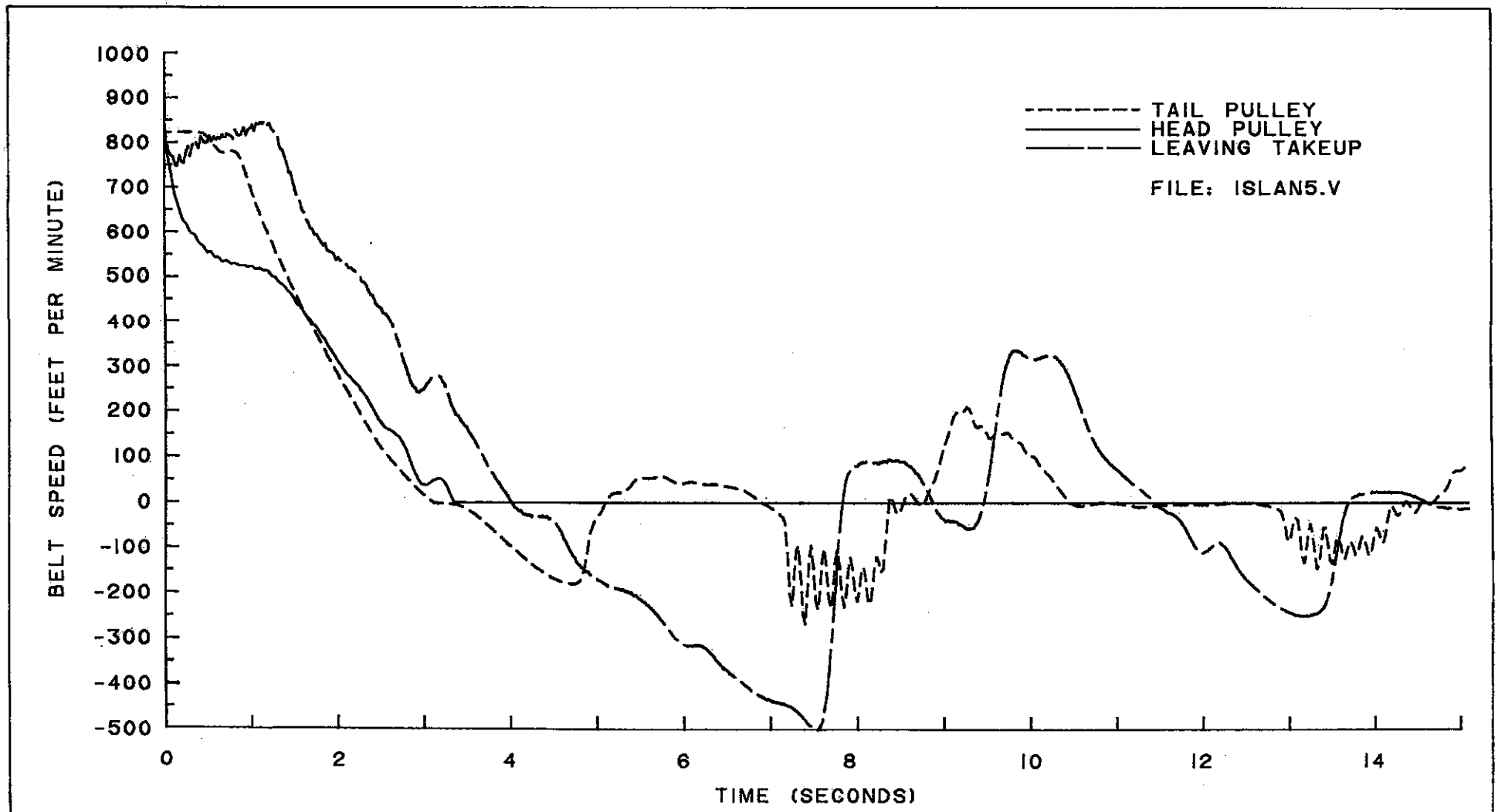

FIG. 27 : _____ / CONVEYOR NO. 2 / 4000 TPH / WITHOUT FLYWHEEL
110,000 LB. COUNTERWEIGHT / SHUTDOWN FROM FULL SPEED / VELOCITY

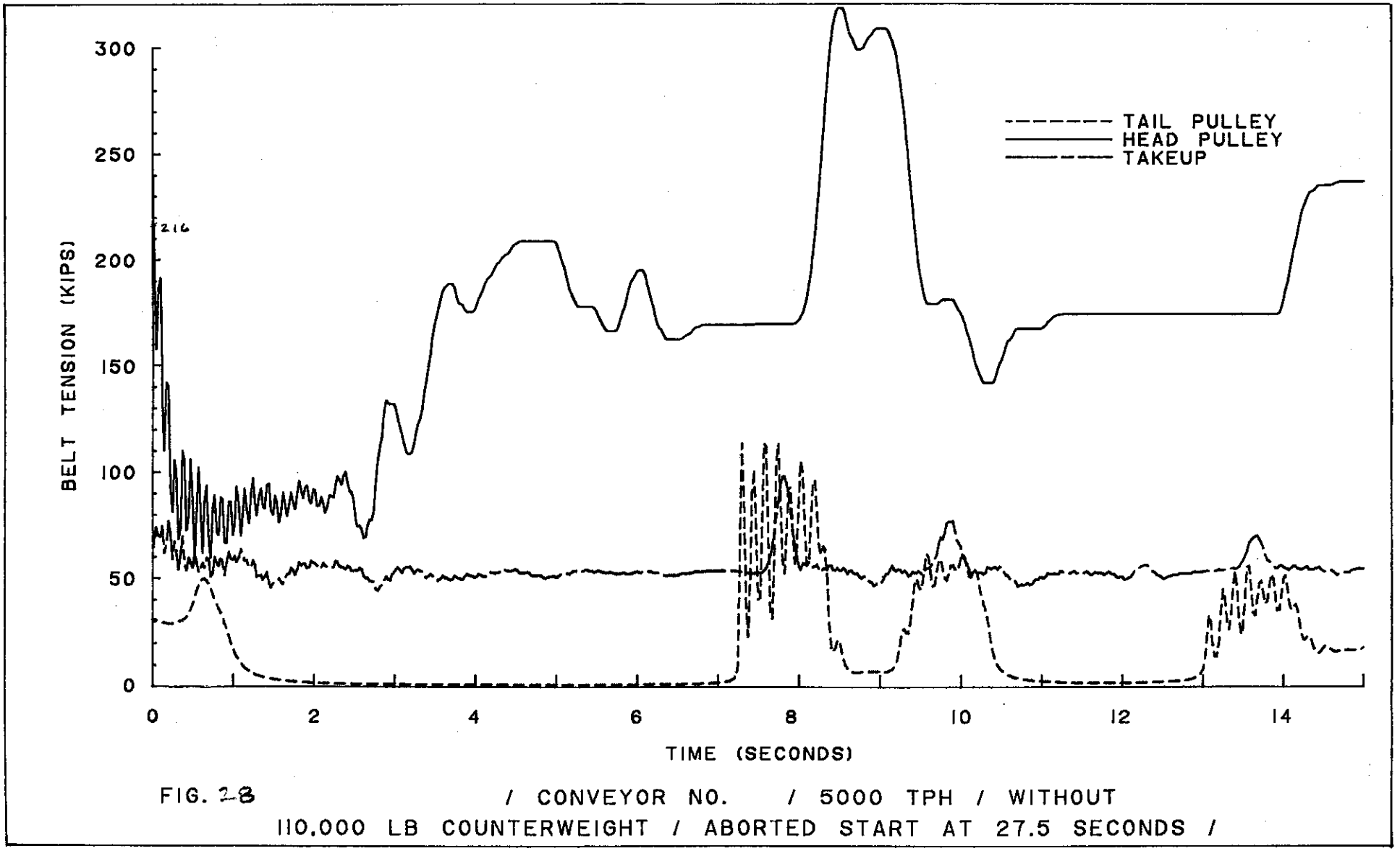

FIG. 2-8 / CONVEYOR NO. / 5000 TPH / WITHOUT 110,000 LB COUNTERWEIGHT / ABORTED START AT 27.5 SECONDS /

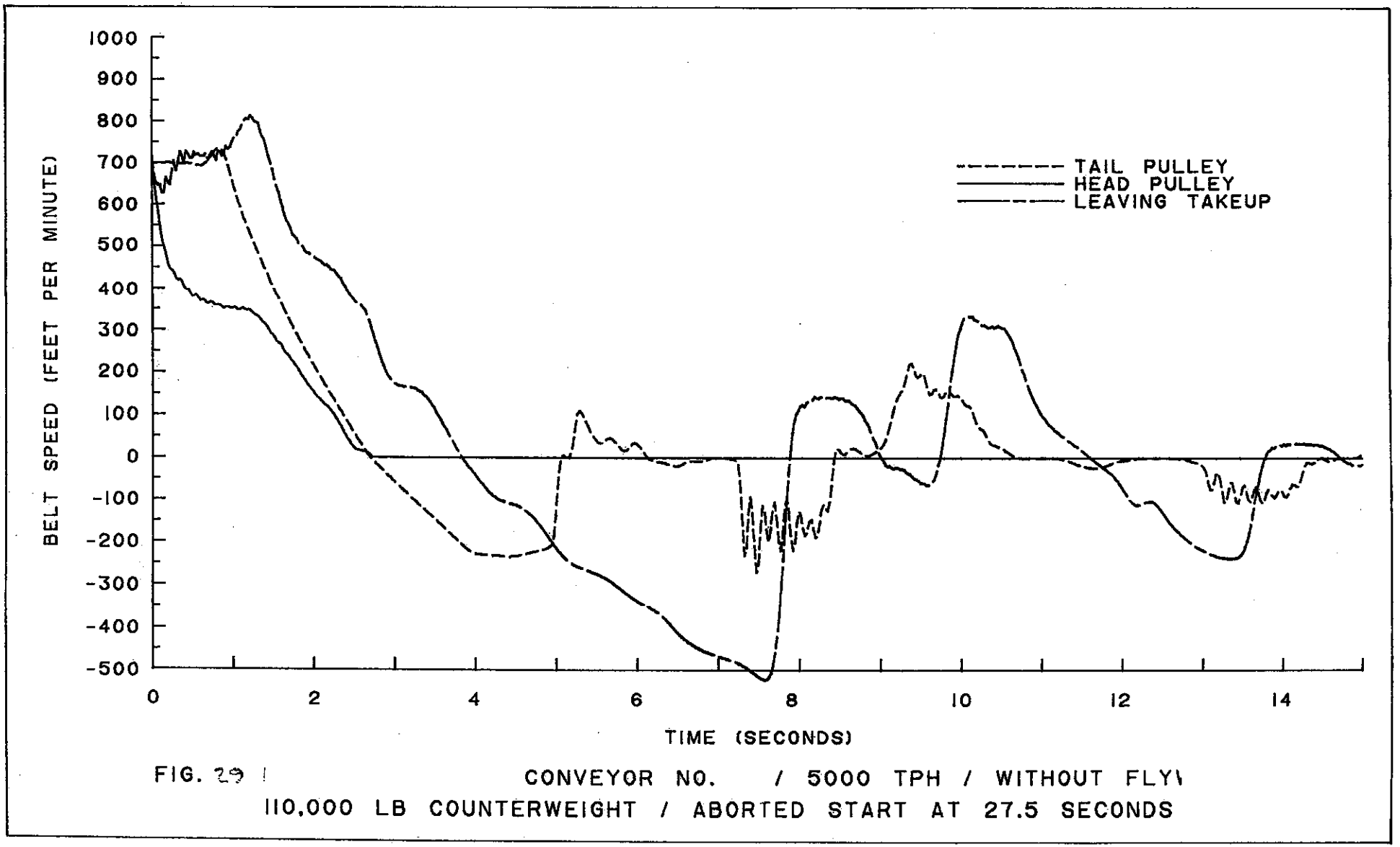

FIG. 29 | CONVEYOR NO. / 5000 TPH / WITHOUT FLY\
110,000 LB COUNTERWEIGHT / ABORTED START AT 27.5 SECONDS

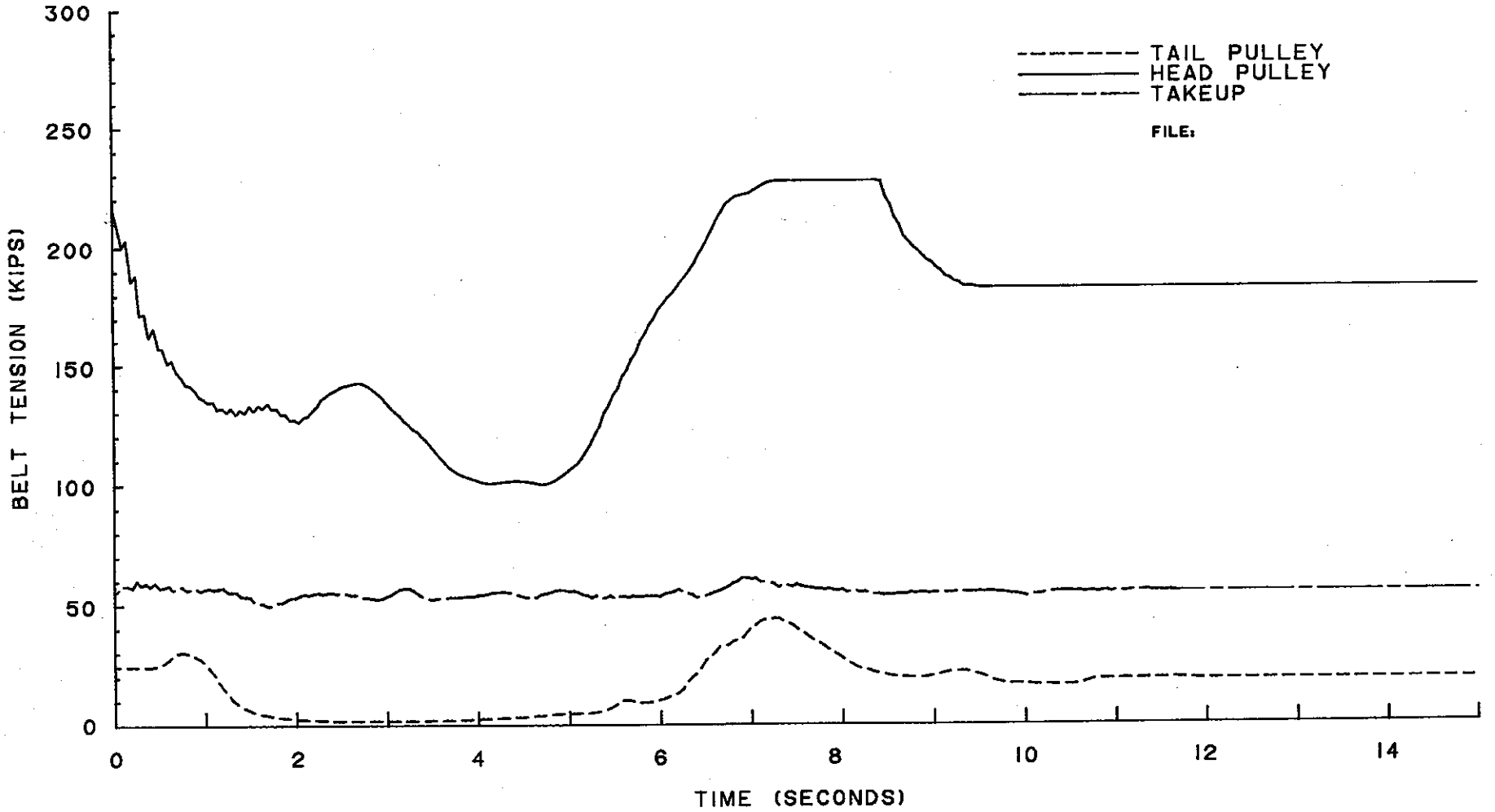

FIG. 30: / CONVEYOR NO. / WITH 110,000 LB. COUNTERWEIGHT / SHUTDOWN FROM FULL SPEED /

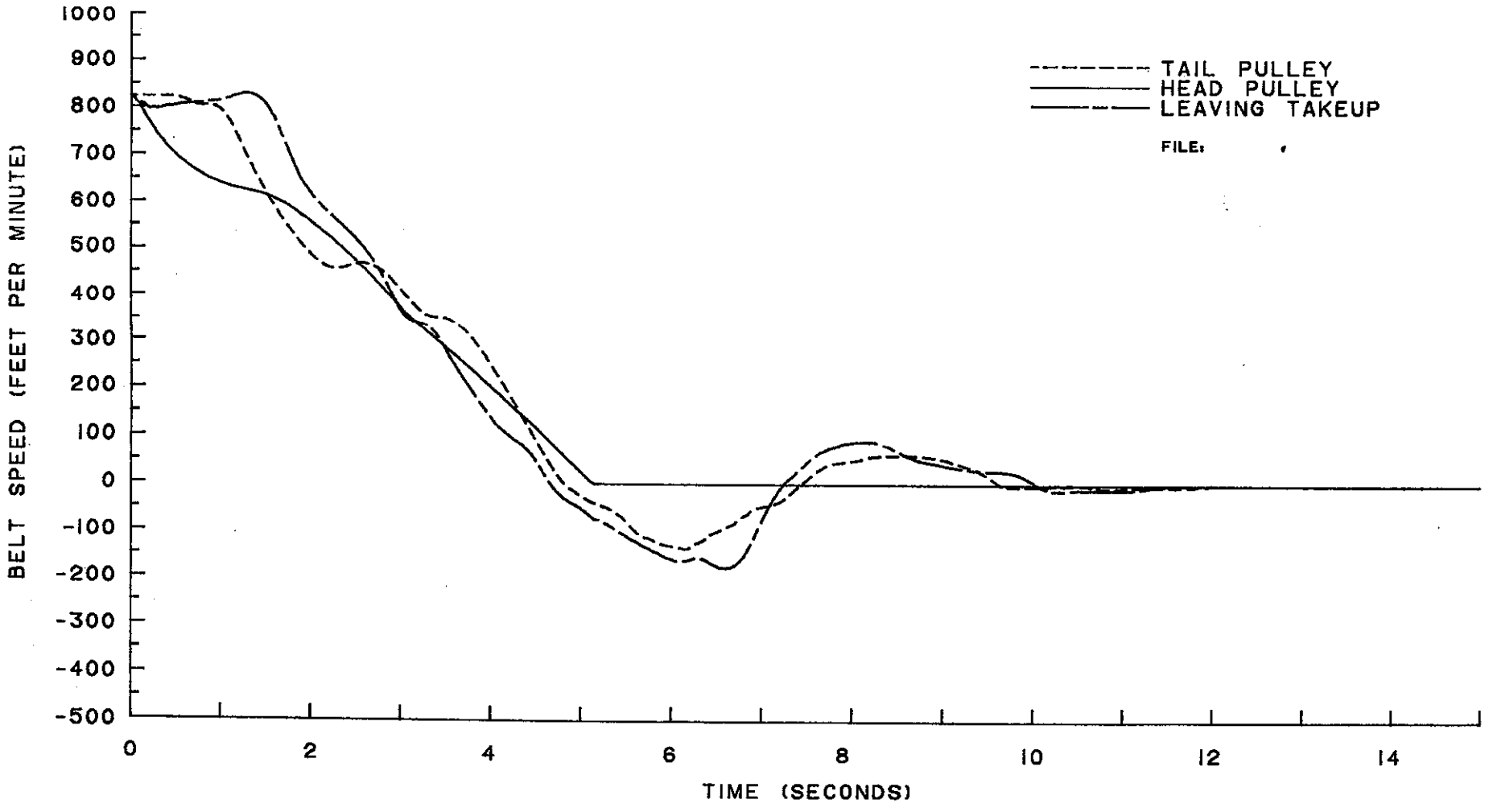

FIG. 31 : / CONVEYOR NO. / WITH
110,000 LB. COUNTERWEIGHT / SHUTDOWN FROM FULL SPEED /

CALCULATION SHEET

REV	DATE	BY	CK	TITLE	PAGE NUMBER
	AUG. 21 1986	LKN		CONVEYOR NO. 6	COST CENTER
				SHEET OF	JOB NUMBER

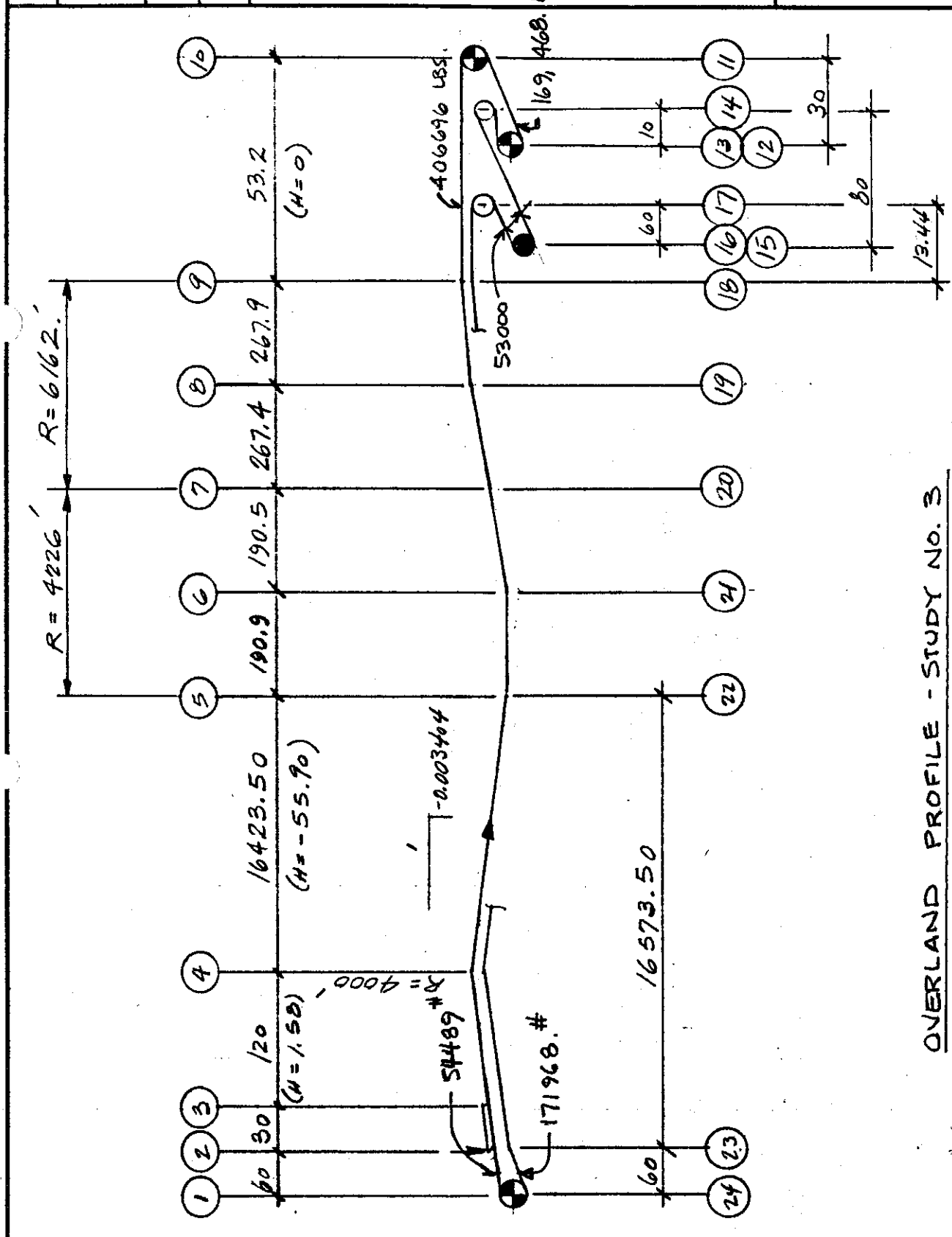

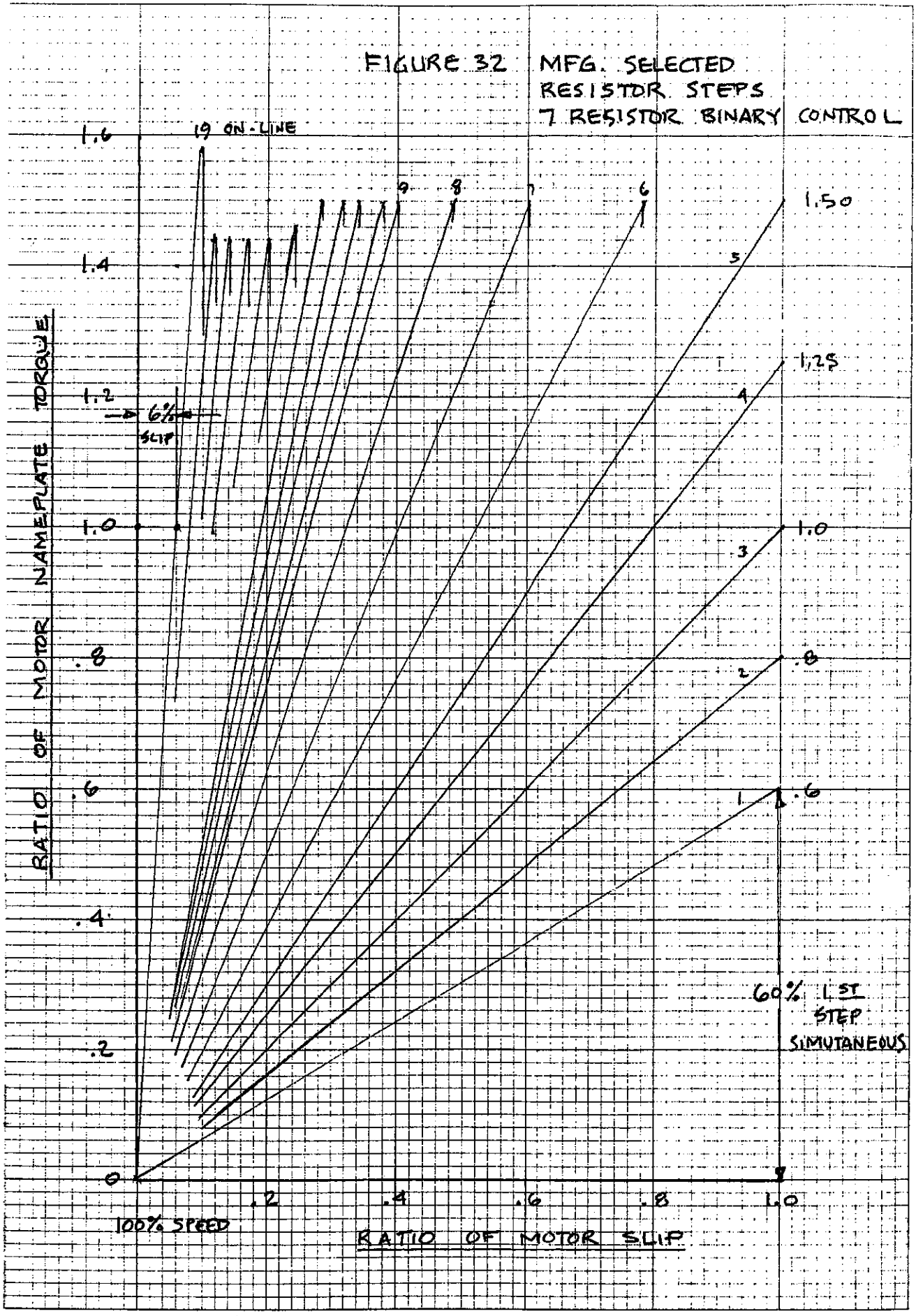

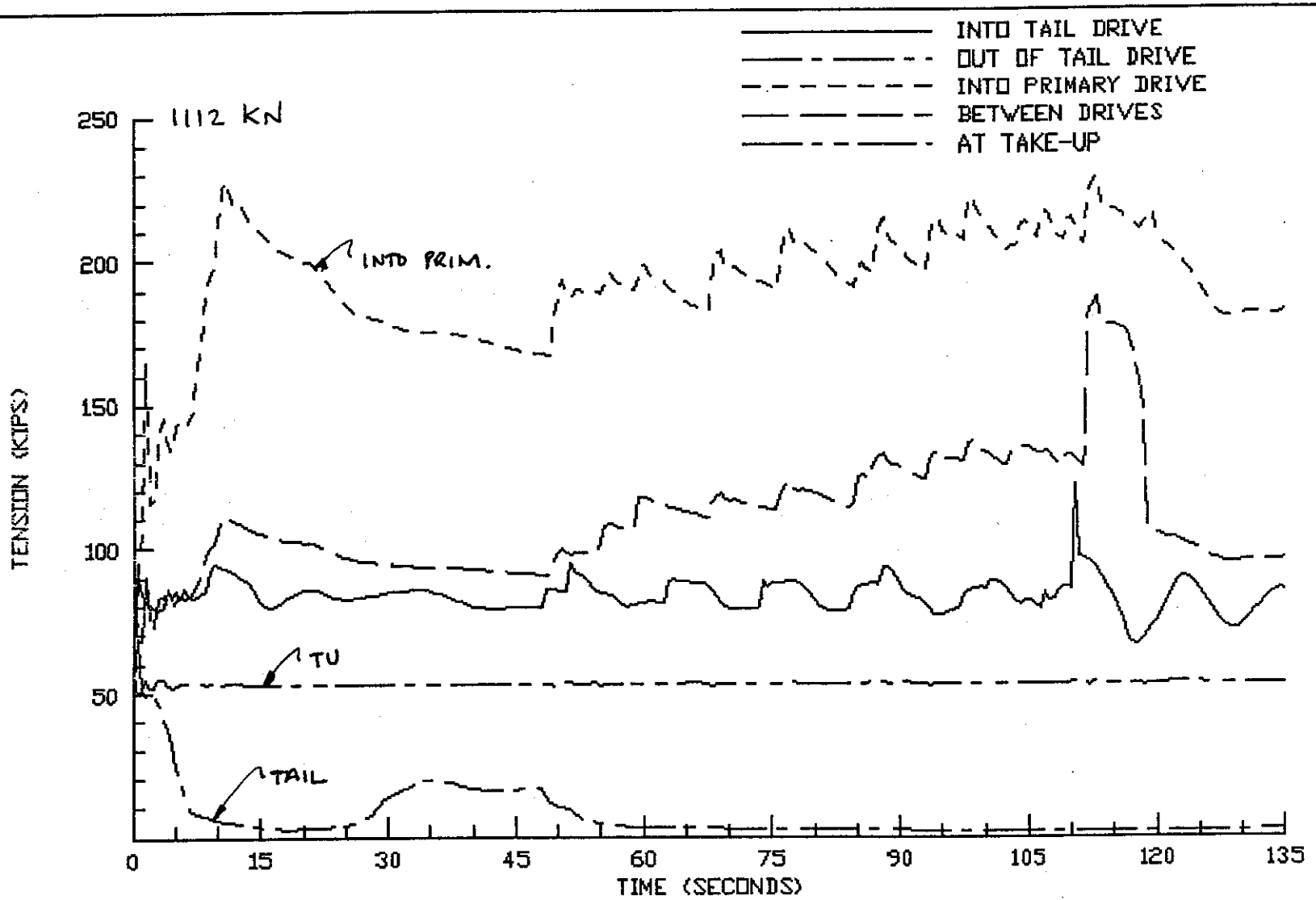

FIGURE 33 START-UP / FULLY LOADED / WINTER FRICTION
N° FLYWHEELS / 120 SECOND TIME RAMP ON ALL DRIVES
SELECTED RESISTOR STEPS & LOGIC

CLIENT:	CONV: 6		P6WF.VB2	BELTFLEX ANALYSIS
PROJECT:	DATE: 15-SEP-86	REV: 1	p6wft2.DXF	CONVEYOR DYNAMICS, INC.

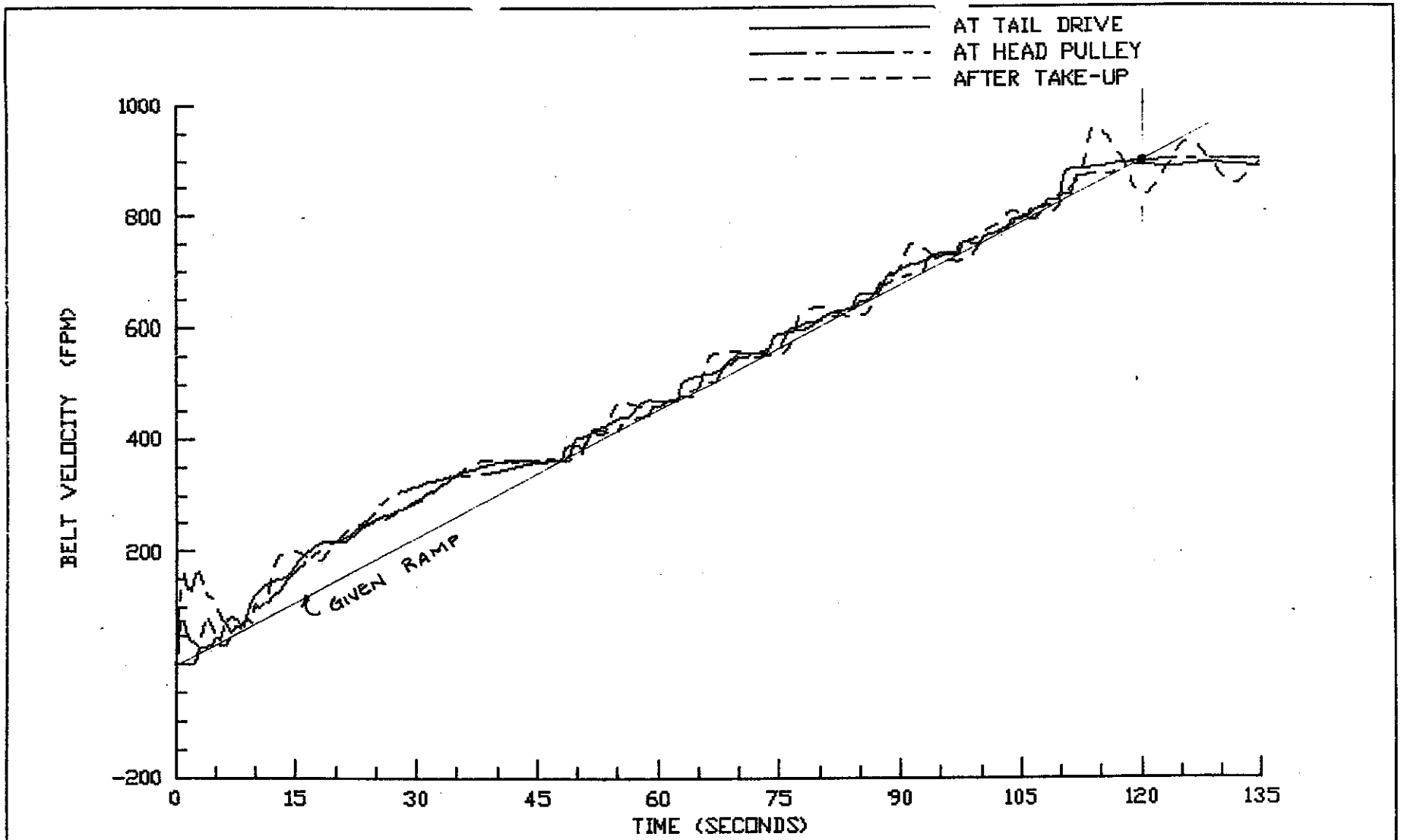

FIGURE 34 START-UP / FULLY LOADED / WINTER FRICTION
NO FLYWHEELS / 120 SECOND TIME RAMP ON ALL DRIVES
SELECTED RESISTOR STEPS & LOGIC

CLIENT:	CONV: 6		P6WF.VB2	BELTFLEX ANALYSIS
PROJECT:	DATE: 15-SEP-86	REV: 1	P6WFV2.DXF	CONVEYOR DYNAMICS, INC.

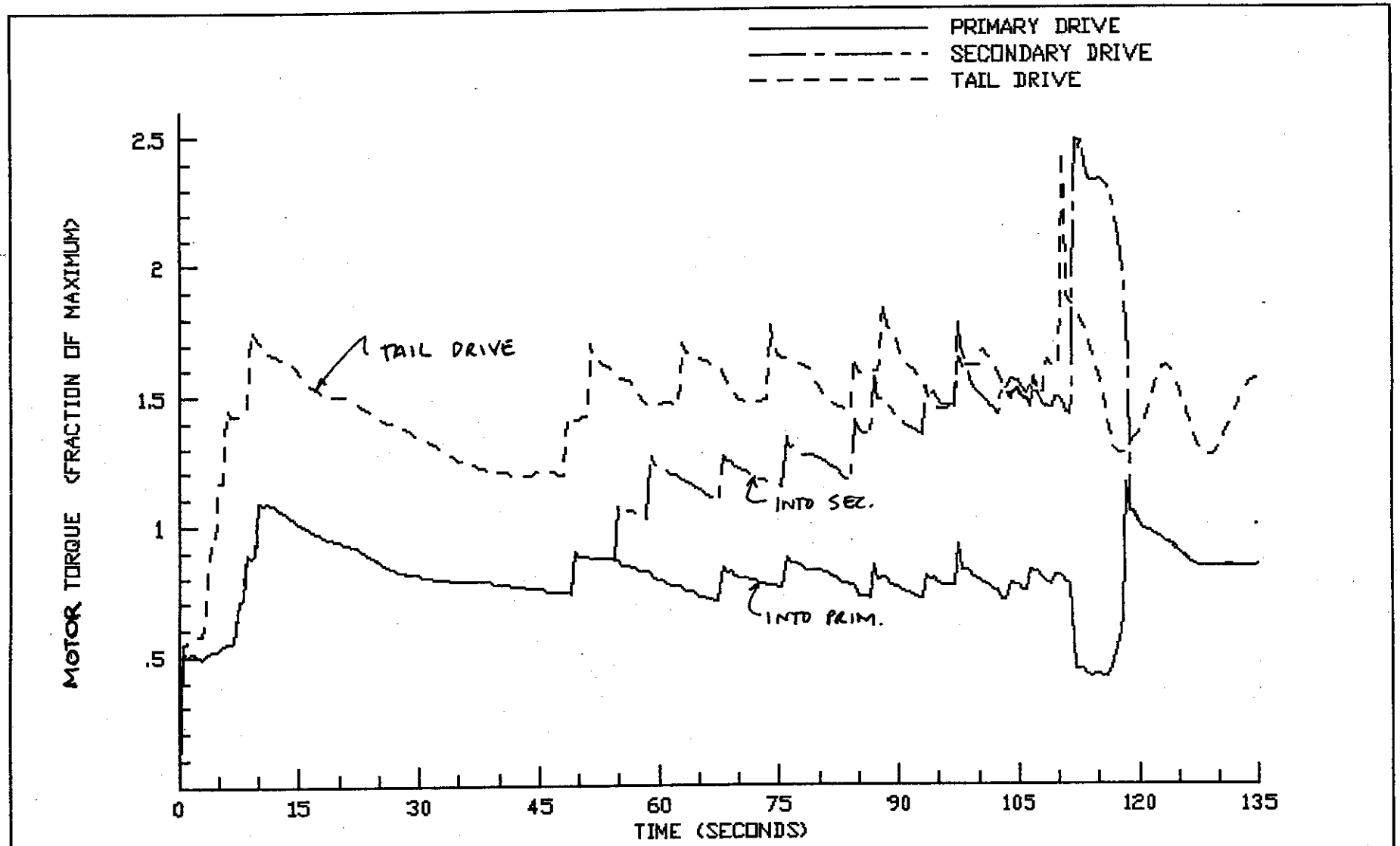

FIGURE 35: START-UP / FULLY LOADED / WINTER FRICTION
NO FLYWHEELS / 120 SECOND TIME RAMP ON ALL DRIVES
SELECTED RESISTOR STEPS & LOGIC

CLIENT:	CONV: 6		P6WF.VB2	BELTFLEX ANALYSIS
PROJECT:	DATE: 15-SEP-86	REV: 1	p6wfq2.DXF	CONVEYOR DYNAMICS, INC.

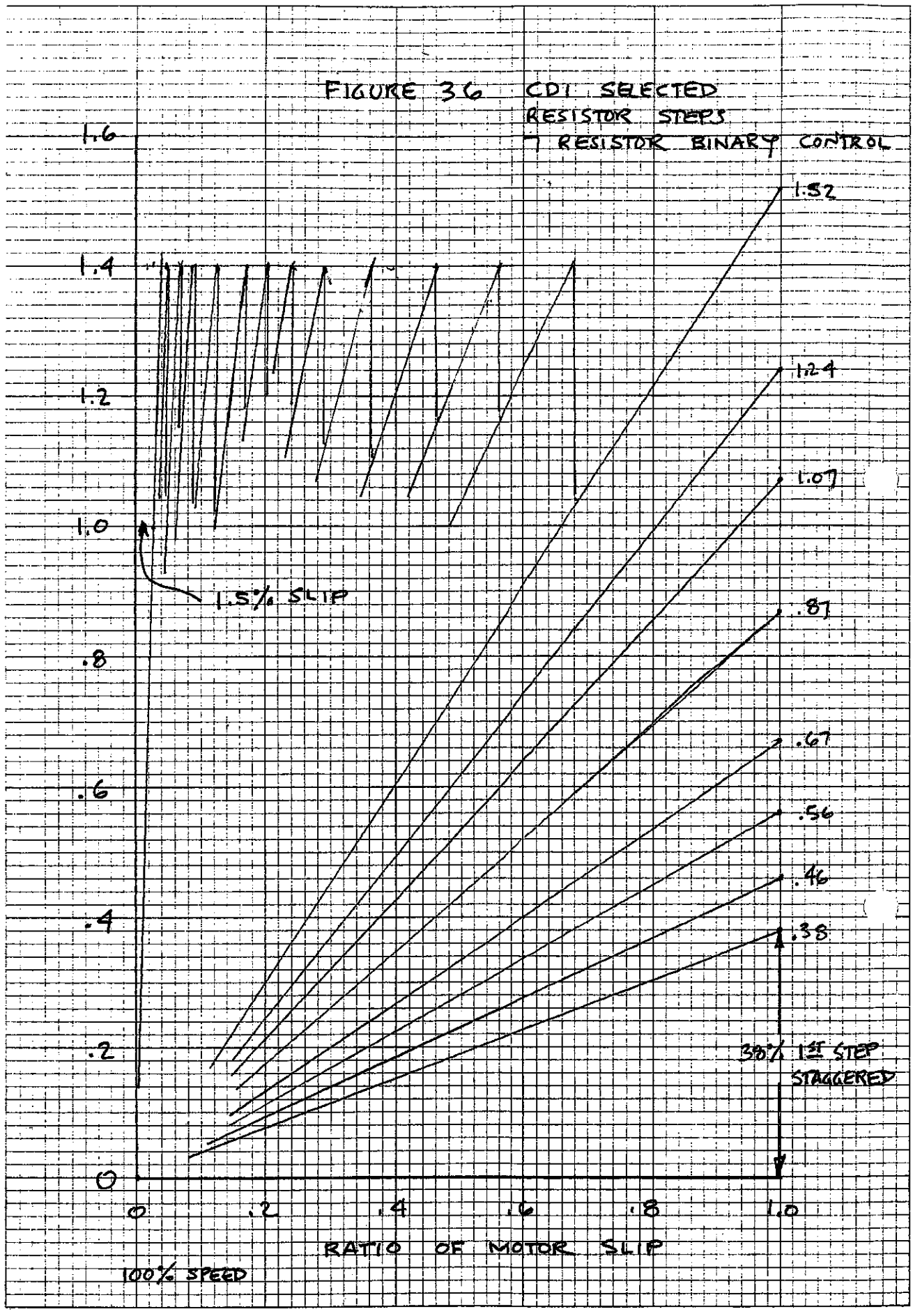

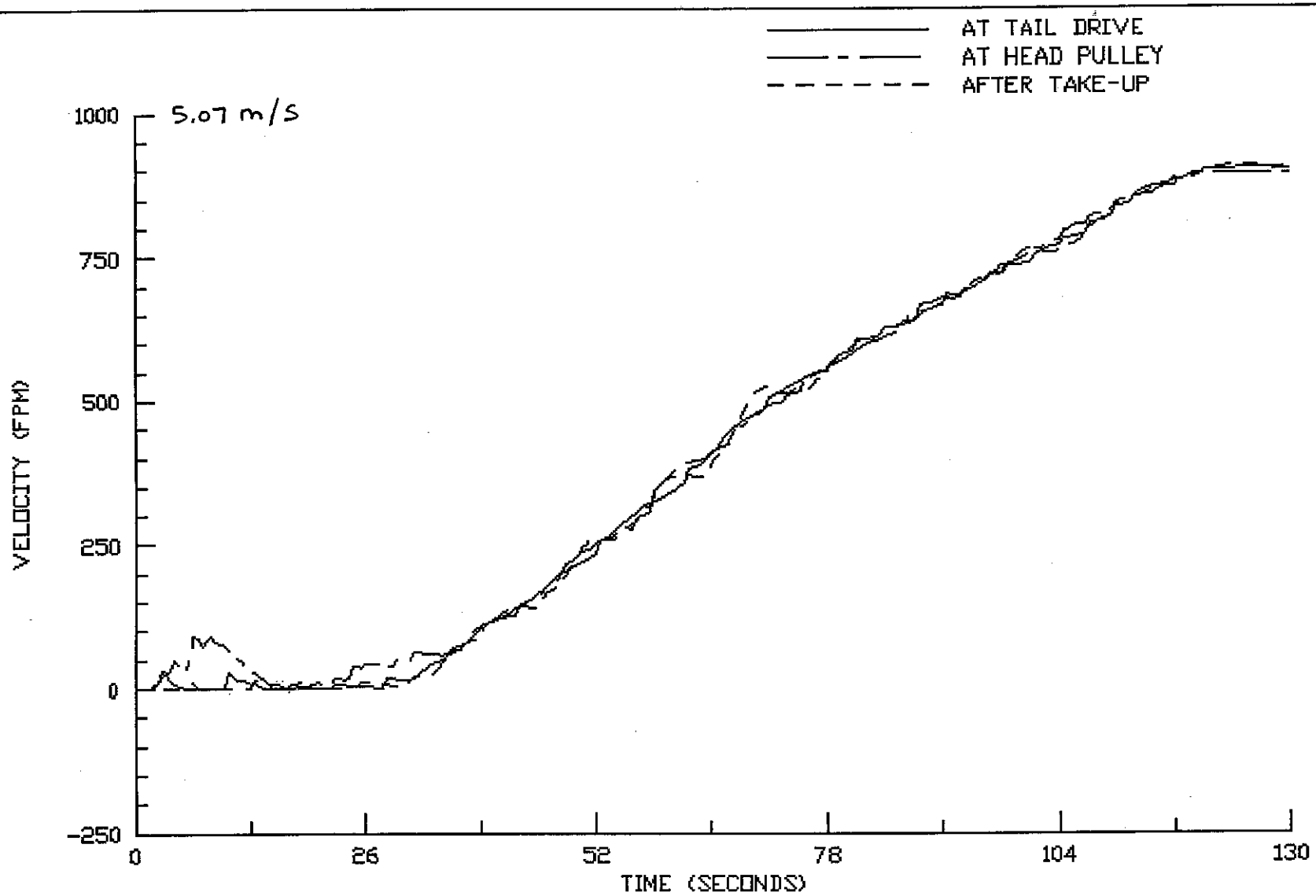

FIGURE 37: START-UP / FULLY LOADED / WINTER FRICTION
NO FLYWHEELS / 22 RESISTOR STEPS / CDI / 2.5% PERM SLIP
FIXED TIMING / TEST 5 / BRAKES RELEASED PRIOR TO START

CLIENT:	CONV: 6 (FROM : & :)		P6/1WF/2
PROJECT:	DATE: 01-DEC-87	REV: 8F	PF6WFC2

BELTFLEX ANALYSIS
CONVEYOR DYNAMICS, INC.

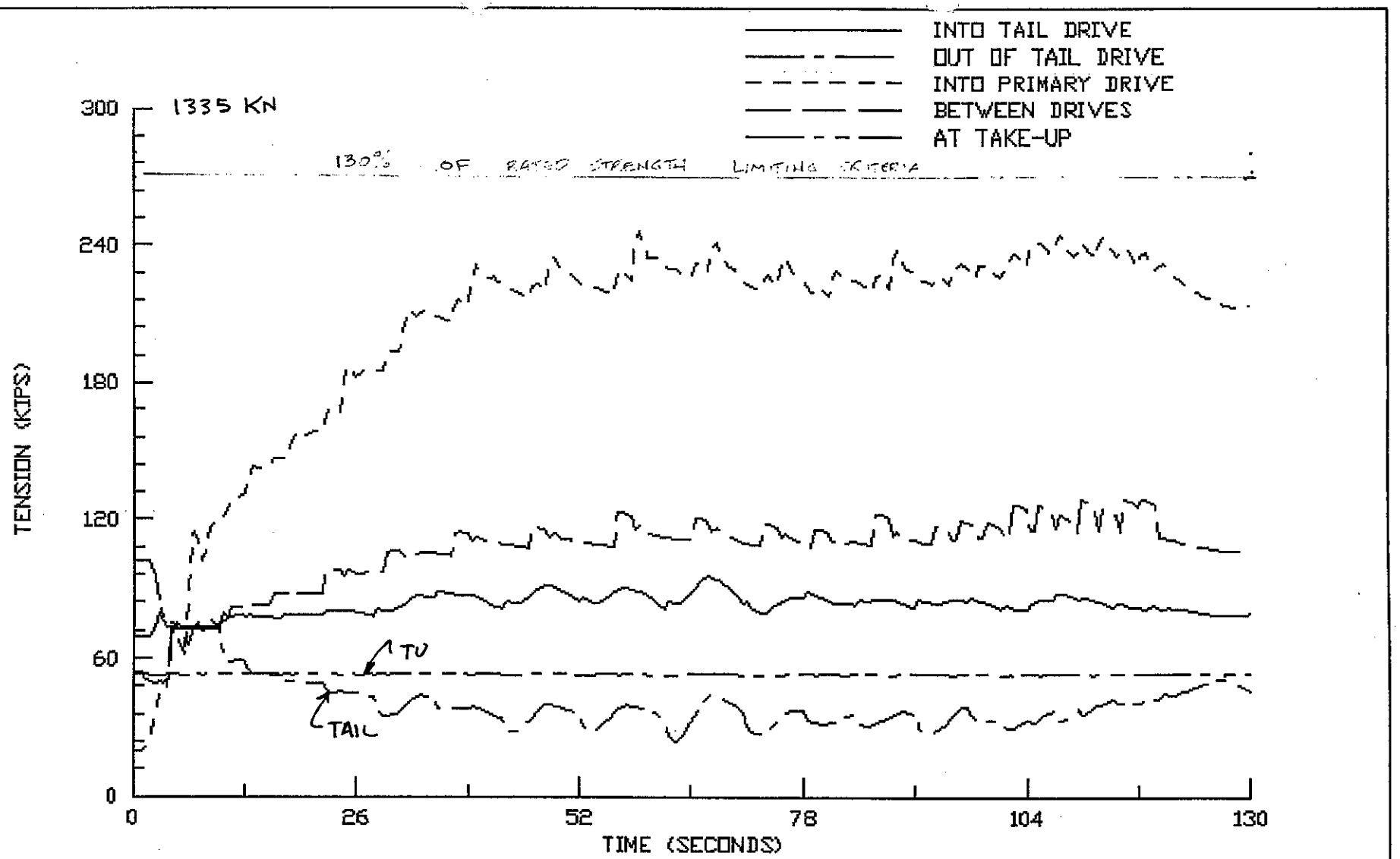

FIGURE 38: START-UP / FULLY LOADED / WINTER FRICTION
NO FLYWHEELS / 22 RESISTOR STEPS / CDI / 2.5% PERM SLIP
FIXED TIMING / TEST 5 / BRAKES RELEASED PRIOR TO START

CLIENT:	CONV: 6 (FROM &)		P6/1WF/2	BELTFLEX ANALYSIS
PROJECT:	DATE: 01-DEC-87	REV: 8F	PF6WFC2	CONVEYOR DYNAMICS, INC.

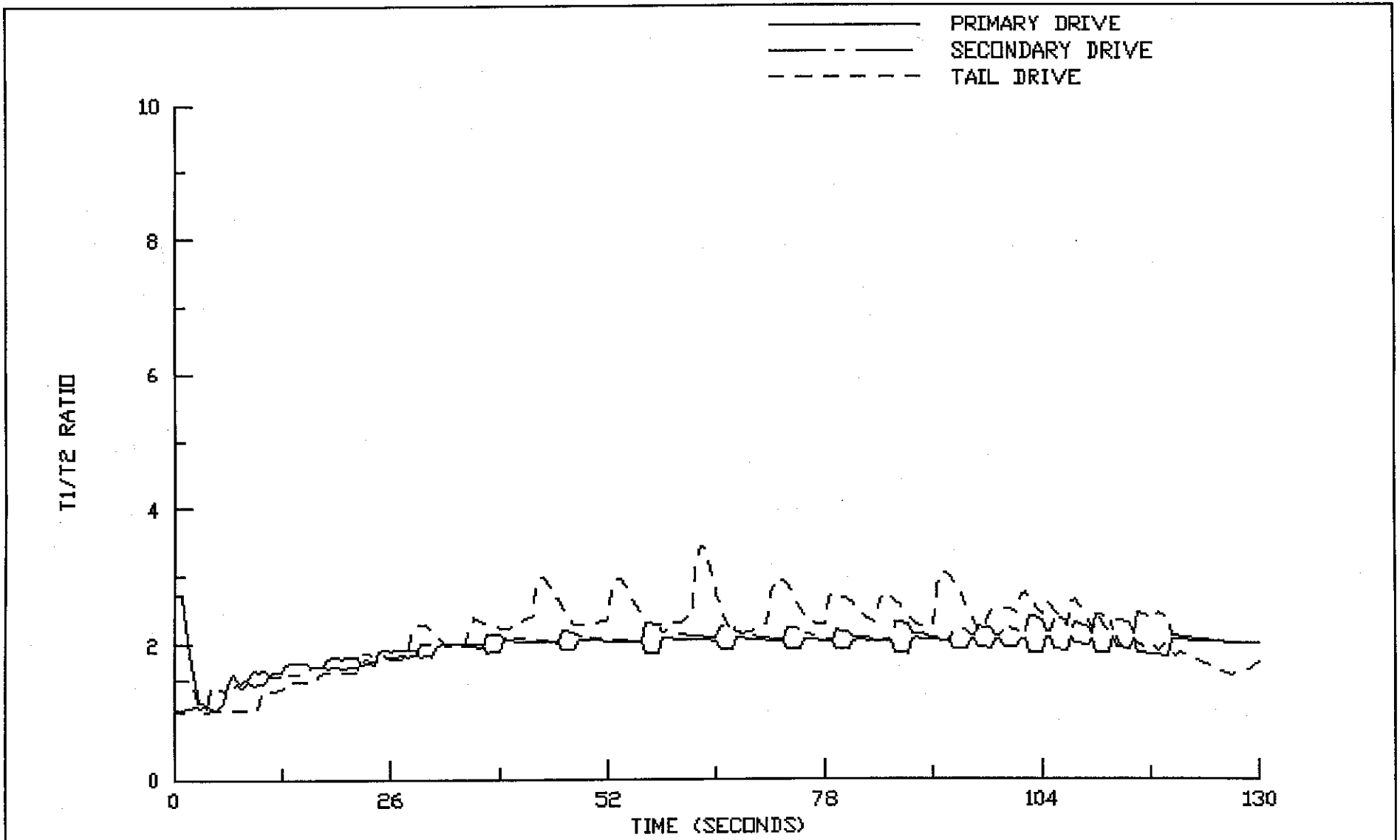

FIGURE 39: START-UP / FULLY LOADED / WINTER FRICTION
NO FLYWHEELS / 22 RESISTOR STEPS / CDI / 2.5% PERM SLIP
FIXED TIMING / TEST 5 / BRAKES RELEASED PRIOR TO START

CLIENT:	CONV: 6 (FROM M2 & M4)		P6/1WF/2
PROJECT:	DATE: 01-DEC-87	REV: 8F	PF6WFC2

BELTFLEX ANALYSIS
CONVEYOR DYNAMICS, INC.

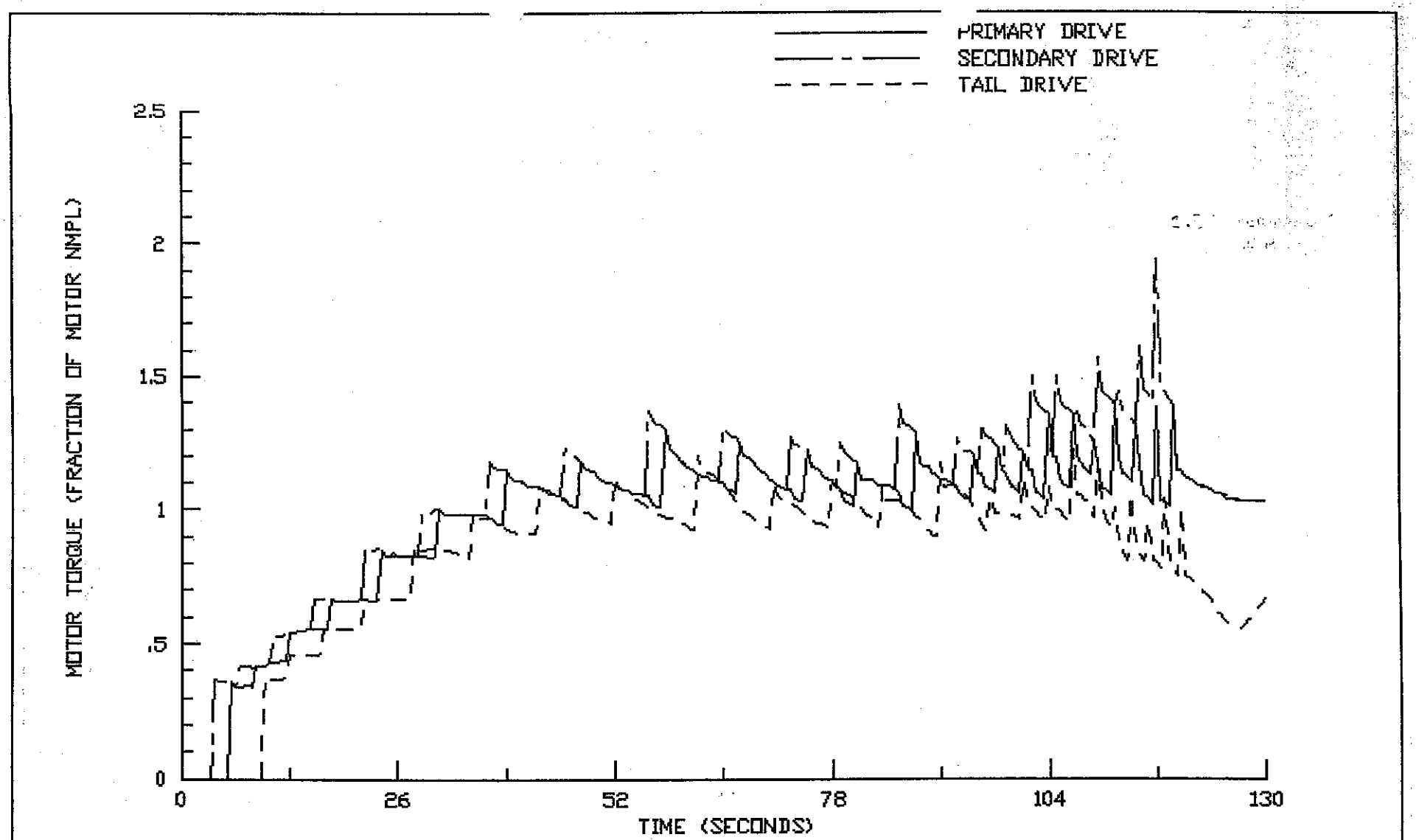

FIGURE 40: START-UP / FULLY LOADED / WINTER FRICTION
NO FLYWHEELS / 22 RESISTOR STEPS / CDI / 2.5% PERM SLIP
FIXED TIMING / TEST 5 / BRAKES RELEASED PRIOR TO START

CLIENT:	CONV: 6 (FROM M2 & M4)		P6/1WF/2
PROJECT:	DATE: 01-DEC-87	REV: 8F	PF6WFC2

BELTFLEX ANALYSIS
CONVEYOR DYNAMICS, INC.